One-pot synthesis of a white-light emissive bichromophore operated by aggregation-induced dual emission (AIDE) and partial energy transfer

Melanie Denißen,[a] Ricarda Hannen,[a] Dana Itskalov,[a] Lukas Biesen,[a] Nithiya Nirmalananthan-Budau,[b] Katrin Hoffmann,[b] Guido J. Reiss,[c] Ute Resch-Genger,*[b] and Thomas J. J. Müller*[a]

[a]Institut für Organische Chemie und Makromolekulare Chemie, Heinrich-Heine-Universität Düsseldorf, Universitätsstrasse 1, D-40225 Düsseldorf, Germany
Email: ThomasJJ.Mueller@hhu.de
[b]Division Biophotonics, Bundesanstalt für Materialforschung und -prüfung (BAM), Department 1, Richard-Willstätter-Straße 11, D-12489 Berlin, Germany
Email: ute.resch@bam.de
[c]Institut für Anorganische Chemie und Strukturchemie, Heinrich-Heine-Universität Düsseldorf, Universitätsstrasse 1, D-40225 Düsseldorf, Germany

Table of Contents

1 General considerations

All reactions were performed in flame-dried Schlenk tubes under a nitrogen atmosphere. Reaction progress was qualitatively monitored by thin layer chromatography using silica gel layered aluminium foil (60 F254 Merck, Darmstadt). For detection, UV light of wavelengths 254 and 366 was employed. Column chromatography was performed using silica gel 60 (Macherey Nagel), mesh 230–400. All commercially available chemicals were purchased from Sigma Aldrich, Alfa Aesar, Fluorochem, and ACROS and were used as received without any further purification. ^{1}H and ^{13}C NMR spectra were measured on a Bruker Avance III-300 or Bruker Avance III-600 spectrometer. Chemical shifts are given in ppm (δ) and were referenced to the internal solvent signal: $CDCl_3$ (1H δ 7.26, 13C δ 77.2), $(CD_3)_2SO$ (^{1}H δ 2.05, ^{13}C δ 29.92, 206.26) or CD_2Cl_2 (^{1}H δ 5.32, ^{13}C δ 54.0). Multiplicities are stated as: s (singlet), d (doublet), t (triplet), q (quartet), dd (doublet of doublet), ddd (doublet of doublet of doublet), m (multiplet). Broad signals are assigned as br. Coupling constants (*J*) are given in Hz. The assignment of primary (CH_3), secondary (CH_2), tertiary (CH) and quaternary carbon nuclei (Cquat) was made using DEPT-135 spectra. Mass-spectrometric investigations were carried out in the Department of Mass Spectrometry of the Institute of Inorganic and Structural Chemistry, Heinrich-Heine-Universität Düsseldorf. IR spectra were recorded using a Shimadzu IRAffinity-1. The intensities of the IR bands are abbreviated as w (weak), m (medium), s (strong). Absorption spectra were recorded in various spectroscopy grade solvents at *T* = 293 K on a PerkinElmer UV/VIS/NIR Lambda 19 spectrometer. Emission spectra of drop-casted films were recorded at *T* = 293 K on a Perkin Elmer LS55 spectrometer. Emission spectra in solution were recorded at *T* = 293 K on a Hitachi F7000 spectrometer. The molar extinction coefficients were carried out in a multipoint setup. Melting points (uncorrected) were measured using a Büchi Melting Point B-540. Combustion analyses were measured on a Perkin Elmer Series II Analyser 2400 in the Institute of Pharmaceutical and Medicinal Chemistry, Heinrich-Heine University, Düsseldorf.

Photoluminescence quantum yield (Φ) values were determined absolutely with an integrating sphere setup from Hamamatsu (Quantaurus-QY C11347-11). All Φ measurements were performed at 25 °C using special 10 mm × 10 mm long neck quartz cuvettes from Hamamatsu. With this setup, Φ values ≥ 0.01 can be reliably measured.

Fluorescence decay kinetics providing the fluorescence lifetimes (τ) of the dyes and aggregates were recorded with the fluorometer Edinburgh Instruments (FLS 920) equipped with an EPLED (ex 330 ± 10 nm, 375 ± 10 nm and 485 ± 10 nm) and a fast multi-channel plate photomultiplier (MCP-PMT) as detector. With this setup, τ values ≥ 0.2 ns can be reliably measured. All decay kinetics were detected at the respective emission maximum with a spectral bandwidth of the emission monochromator of 10 nm, a 4096-channel setting, and time

ranges of 20 and 50 ns. The measured fluorescence decay kinetics were evaluated using the reconvolution procedure of the FAST program (Edinburgh Instruments). This procedure considers the measured instrument response function which can influence the fluorescence decays. All photoluminescence decay profiles could be analyzed satisfactorily with mono-, bi- or tri-exponential fits. From the multiexponential decays, subsequently, the intensity-weighted average lifetimes were calculated.

For confocal laser scanning microscopy (CLSM) of the samples in solid state, the crystals formed in suspension were transferred onto a 24 x 65 mm coverslip and analyzed with an FluoView 1000 system (Olympus GmbH, Hamburg, Germany). A DPSS Cobolt Zouk® (355 nm; 10 mW) and a multiline argon ion laser (488 nm; 30 mW) were applied as excitation sources, which were reflected by a beam splitter (BS) 20/80 and focused onto the sample through an Olympus objective UPLSAPO 10x (numerical aperture N.A. 0.4). The fluorescence emission was collected by the same objective and focused into the photomultiplier tube (PMT).

2 Synthesis of Starting Materials

2.1 Synthesis of 3-Aryl propynoyl *ortho*-Bromo Anilides 1

2.1.1 Synthesis of *N*-(2-Bromophenyl)-3-phenylpropiolamide[1]

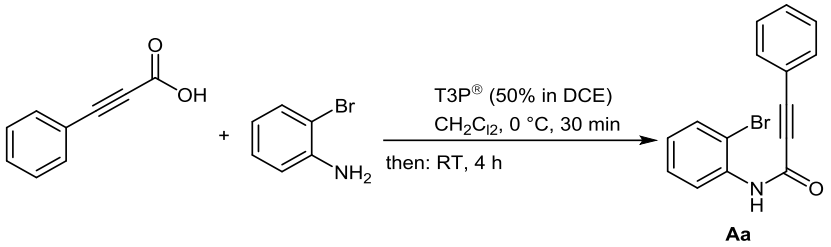

Aa

In a dry screw-cap Schlenk tube with a magnetic stir bar under nitrogen were placed the 3-phenylpropiolic acid[2] (3.65g, 25.0 mmol) and dry dichloromethane (0.6 mL/mmol) and the solution was cooled to 0 °C (ice-salt bath). Then 4.73g (27.5 mmol) 2-bromo aniline was added to reaction mixture before T3P® (50 weight% in 1,2-dichloroethane, 1.00 equiv) was slowly added dropwise at 0 °C. After complete addition the mixture was stirred at 0 °C for 30 min and then allowed to come to room temp where stirring was continued for 4 h. Then dichloromethane (20 mL) was added the organic phase was washed with 2 M aqueous hydrochloric acid (2 x 10 mL). The organic phase was washed with saturated aqueous sodium carbonate solution and dried (anhydrous magnesium sulfate). After removal of the solvents in vacuo the crude product was adsorbed on celite® and chromatographed on silica gel (*n*-hexane-ethyl/acetate 7:1) to give 6.45g (86%) pure *N*-(2-bromophenyl)-3-phenylpropiolamide **Aa** as a colorless liquid, Mp 120 °C. R_f (*n*-hexane:EtOAc, 5:1): 0.41. ^{1}H NMR (300 MHz, $CDCl_3$): δ 7.02 (t, J = 7.5 Hz, 1 H), 7.28-7.51 (m, 4 H), 7.51-7.68 (m, 3 H), 8.00 (s, 1 H), 8.37 (d, J = 8.0 Hz, 1 H). ^{13}C NMR (75 MHz, $CDCl_3$): δ 83.4 (C_{quat}), 86.5 (C_{quat}), 113.2 (C_{quat}), 119.9 (C_{quat}), 122.4, 125.9, 128.7, 128.8, 130.7, 132.5, 132.9, 135.4 (C_{quat}), 151.0 (C_{quat}). IR (ATR): $\tilde{\nu}$ 3177 (w), 3146 (w), 3100 (w), 3019 (w), 2982 (w), 2959 (w), 2216 (m), 1622 (m), 1582 (m), 1530 (s), 1489 (m), 1470 (m), 1435 (s), 1412 (w), 1306 (s), 1273 (m), 1240 (m), 1188 (m), 1177 (m), 1157 (w), 1121 (w), 1047 (m), 1030 (m), 964 (m), 920 (w), 868 (m), 854 (w), 789 (w), 758 (m), 743 (s), 716 (m), 704 (m), 687 (s), 665 (s), 619 (m). GC-MS: *m/z* (%) 301 (M^+(^{81}Br), 2), 299 (M^+(^{79}Br), 2), 220 ($C_{15}H_{10}NO^+$, 33), 130 (10), 129 ($C_9H_5O^+$, 100), 101 ($C_8H_5^+$, 11), 75 (20). Anal. calcd. for $C_{15}H_{10}BrNO$ (299.0): C 60.02, H 3.36, N 4.67; Found: C 59.75, H 3.34, N 4.61.

2.1.2 General Procedure 1 (GP 1) for the Preparation of *N*-Substituted *N*-(2-Bromophenyl)-3 arylpropiolamides 1[3]

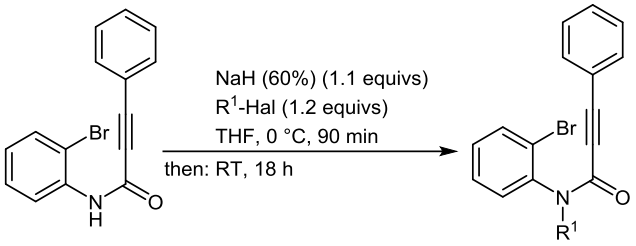

In a dry screw-cap Schlenk tube with a magnetic stir bar under nitrogen were placed sodium hydride (60% dispersion in petroleum, 1.1 equivs) and dry THF (2.7 mL/mmol) and the suspension was cooled to 0 °C (ice-salt bath). Then the corresponding secondary propiolamide (1.0 equiv) dissolved in dry THF (2.0 mL/mmol) was slowly added dropwise to the sodium hydride suspension (for experimental details, see Table SI-1). After complete addition the mixture was stirred at 0 °C for 1 h. Then the electrophile R^1-Hal (1.2 equivs) was added and the mixture was stirred at 0 °C for 30 min and then allowed to come to room temp where stirring was continued for 18 h. Then the solvent was removed in vacuo and to the residue was added dichloromethane (20 mL/mmol). The organic layer was then washed with deionized water (2 x 20 mL/mmol) and saturated brine (2 x 20 mL/mmol) and dried (anhydrous magnesium sulfate). After removal of the solvents in vacuo the crude product was adsorbed on celite® and chromatographed on silica gel (*n*-hexane-ethyl acetate) to give the pure *N*-substituted *N*-(2-bromophenyl)-3-arylpropiolamides **1**.

Table SI-1. Experimental details of the preparation of *N*-substituted N-(2-bromophenyl)-3-arylpropiolamides **1a** and **b** according GP 1.

Entry	propiolamide [g] (mmol)	electrophile R^1-Hal [g] (mmol)	*N*-substituted *N*-(2-bromophenyl)-3-arylpropiolamides **1** [g] (%)	*n*-hexane:EtOAc
1	0.30 (1.00)	0.18 (1.10) of methyliodide (R^1 = Me, Hal = I)	0.29 (93) of **1a**	5:1
2	2.98 (9.90)	2.28 (11.9) of *p*-tosylchloride (R^1 = Tos, Hal = Cl)	4.05 (90) of **1b**	6:1

N-(2-Bromophenyl)-*N*-methyl-3-phenylpropiolamide (1a)

According to GP 1 compound **1a** was obtained as a colorless amorphous solid, Mp 88 °C. R_f (*n*-hexane:EtOAc, 10:1): 0.17. ^{1}H NMR (300 MHz, $CDCl_3$): δ 3.32 (s, 3 H), 7.08 (dd, *J* = 8.4, 1.4 Hz, 2 H), 7.17-7.25 (m, 2 H), 7.27-7.37 (m, 2 H), 7.39-7.44 (m, 2 H), 7.67-7.77 (m, 1 H). ^{13}C NMR (75 MHz, $CDCl_3$): δ 35.2 (CH_3), 82.3 (C_{quat}), 90.5 (C_{quat}), 120.3 (C_{quat}), 124.0 (C_{quat}), 128.4, 128.6, 130.1, 130.2, 130.7, 132.6, 133.7, 142.2 (C_{quat}), 154.5 (C_{quat}). IR (ATR): $\tilde{\nu}$ 2980

(m), 2972 (w), 2932 (w), 2889 (w), 2212 (m), 1630 (s), 1582 (m), 1530 (w), 1491 (m), 1474 (m), 1433 (m), 1420 (m), 1360 (s), 1314 (m), 1242 (m), 1188 (w), 1159 (m), 1132 (m), 1115 (m), 1063 (m), 1026 (m), 964 (w), 935 (w), 914 (w), 802 (w), 772 (s), 754 (s), 723 (s), 708 (m), 681 (s), 650 (m), 604 (m). EI-MS (70 eV): *m/z* (%) 315 (M^+(^{81}Br), 0.3), 313 (M^+(^{79}Br), 0.3), 235 (17), 234 ($C_{16}H_{12}NO^+$, 100), 129 ($C_9H_5O^+$, 59), 77 ($C_6H_5^+$, 4). Anal. calcd. for $C_{16}H_{12}BrNO$ (313.0): C 61.17, H 3.85, N 4.46; Found: C 61.11, H 3.81, N 4.38.

N-(2-Bromophenyl)-3-phenyl-*N*-tosylpropiolamide (1b)

According to GP 1 compound **1b** was obtained as a colorless amorphous solid, Mp 142 °C. R_f (*n*-hexane:EtOAc, 5:1): 0.24. ^{1}H NMR (300 MHz, $CDCl_3$): δ 2.43 (s, 3 H), 7.01 (dd, *J* = 8.3, 1.3 Hz, 2 H), 7.20 (t, *J* = 7.6 Hz, 2 H), 7.27-7.41 (m, 4 H), 7.42-7.49 (m, 2 H), 7.73 (dd, *J* = 7.4, 1.3 Hz, 1 H), 8.04 (d, *J* = 8.4 Hz, 2 H). ^{13}C NMR (75 MHz, $CDCl_3$): δ 21.9 (CH_3), 81.7 (C_{quat}), 93.2 (C_{quat}), 119.2 (C_{quat}), 126.3 (C_{quat}), 128.55, 128.61, 129.5, 130.0, 131.1, 131.6, 132.8, 133.0, 133.9, 135.6 (C_{quat}), 136.0 (C_{quat}), 145.8 (C_{quat}), 152.1 (C_{quat}). IR (ATR): $\tilde{\nu}$ 3063 (w), 2222 (m), 1682 (s), 1468 (m), 1377 (m), 1362 (m), 1288 (m), 1281 (m), 1242 (w), 1157 (s), 1086 (m), 1055 (m), 1028 (m), 976 (m), 917 (m), 845 (w), 820 (m), 779 (m), 758 (m), 723 (m), 704 (s), 660 (s), 646 (m). EI-MS (70 eV): *m/z* (%) 374 (M^+-Br, 2), 284 (C_9H_4(^{81}Br)NO_3S^+, 17), 282 (C_9H_4(^{79}Br)NO_3S^+, 17), 220 ($C_6H_8NO_3S^+$, 15), 130 (10), 129 ($C_9H_5O^+$, 100), 91 ($C_7H_7^+$, 8). Anal. calcd. for $C_{22}H_{16}BrNO_3S$ (453.0): C 58.16, H 3.55, N 3.08, S 7.06; Found: C 58.12, H 3.51, N 2.91, S 7.13.

2.2 Synthesis of *tert*-Butyl Piperazine-1-carboxylate[4]

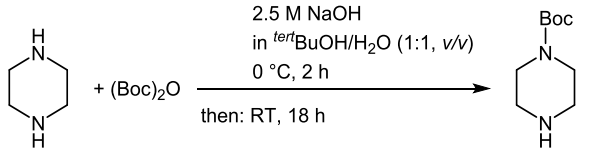

Ba
$C_9H_{18}N_2O_2$
186.26

Piperazine (24.5 g, 284 mmol) was dissolved in a mixture of *tert*-BuOH (300 mL) and deionized water (300 mL) in a 1 L two-neck roundbottom flask with a dropping funnel under nitrogen and cooled to 0 °C (ice-salt bath). After stirring for 10 min an aqueous solution of 2.5 M sodium hydroxide (63.0 mL, 158 mmol) was added dropwise over 30 min. After the addition the reaction mixture was stirred at 0 °C for 30 min before di-*tert*-butyldicarbonate (24.9 g, 114 mmol) was added. After the addition the mixture was stirred at 0 °C for 2 h and allowed to come to room temperature, where stirring was continued for 18 h. The reaction mixture was transferred to a 1 L roundbottom flask and *tert*-butanol was removed in vacuo. The remaining

suspension was filtered and the filtrate was extracted with dichloromethane (4 x 150 mL). The combined organic phases were washed with brine and dried (anhydrous sodium sulfate). After filtration the solvents were removed in vacuo to give after drying in vacuo *tert*-Butyl piperazine-1-carboxylate (14.0 g, 33 %) as a crystalline colorless solid, Mp 46 °C. ^{1}H NMR (300 MHz, $CDCl_3$): δ 1.42 (s, 9 H), 1.74 (s, 1 H), 2.72-2.83 (m, 4 H), 3.30-3.40 (m, 4 H). ^{13}C NMR (75 MHz, $CDCl_3$): δ 28.5 (CH_3), 46.0 (CH_2), 79.6 (C_{quat}), 154.9 (C_{quat}). IR (ATR): $\tilde{\nu}$ 3323 (w), 2976 (w), 2928 (w), 2860 (w), 2814 (w), 2737 (w), 1688 (s), 1476 (m), 1454 (m), 1418 (s), 1393 (m), 1364 (m), 1341 (w), 1317 (m), 1290 (m), 1242 (s), 1167 (s), 1121 (s), 1090 (m), 1053 (m), 1005 (m), 926 (w), 903 (w), 862 (m), 847 (m), 808 (m), 768 (m). EI-MS (70 eV): *m/z* (%) 186 (M^+, 19), 143 ($C_7H_{13}NO_2^+$, 63), 130 ($C_5H_{10}N_2O_2^+$, 47), 113 (32), 88 (16), 85 ($C_4H_9N_2^+$, 23), 57 ($C_4H_9^+$, 100), 56 (57), 55 (15), 44 (65), 43 ($C_2H_5N^+$, 17), 42 (15), 41 (28).

2.3 4-Bromo-*N,N*-bis(4-methoxyphenyl)aniline

2.3.1 Via Buchwald-Hartwig Coupling[5]

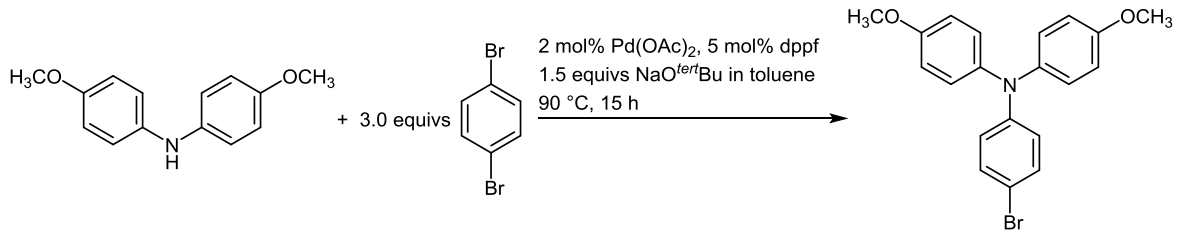

Ca
$C_{20}H_{18}BrNO_2$
384.27

In a dry screw-cap Schlenk tube with a magnetic stir bar under nitrogen 2-mol% $Pd(OAc)_2$ (60.4 mg, 0.27 mmol), 5-mol% 1,1‘-bis(diphenylphosphan)ferrocen (368 mg, 0.66 mmol), 4,4‘-dimethoxydiphenylamine (3.04 g, 13.0 mmol) and 1,4-dibromobenzene (9.40 g, 40 mmol) were dissolved in 53 mL toluene and stirred at room temperature for 15 min. Then, *tert*-BuONa (1.91 g, 20.0 mmol) was added. The reaction mixture was heated to 90 °C (oil bath) for 15 h. After cooling to room temperature 100 mL deionized water were added. The reaction mixture was extracted with ethyl acetate (4 x 100 mL). The combined organic layers were dried (anhydrous magnesium sulfate) and after removal of the solvents in vacuo the residue was chromatographed on silica gel (*n*-hexane) to give 4-bromo-*N,N*-bis(4-methoxyphenyl)aniline (**Ca**) (3.21 g, 64 %) as a colorless to light grey amorphous solid.

2.3.2 Via Bromination of 4-Methoxy-*N*-(4-methoxyphenyl)-*N*-phenylaniline

2.3.2.1 4-Methoxy-*N*-(4-methoxyphenyl)-*N*-phenylaniline

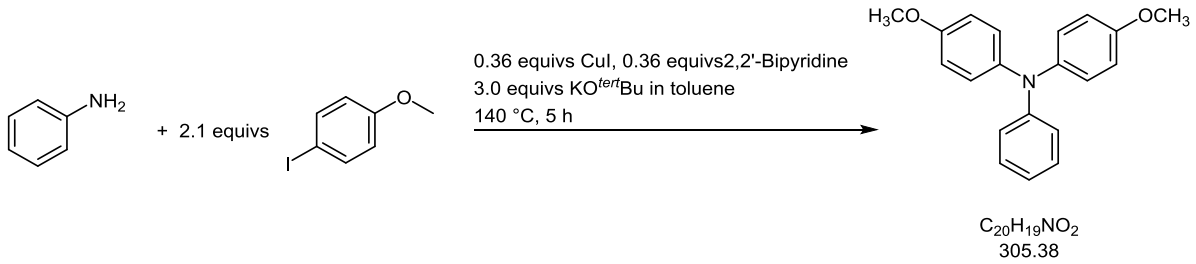

$C_{20}H_{19}NO_2$
305.38

In a dry screw-cap Schlenk tube with a magnetic stir bar under nitrogen 4-iodoanisol (5.89 g, 25.1 mmol) and aniline (1.1 mL, 12.1 mmol) were dissolved in 35 mL toluene. Then, 0.82 g (4.31 mmol) CuI and 0.68 g 2,2‘-bipydridine were added successively. After addition of 4.04 g (36.0 mmol) *tert*-BuOK the reaction mixture was heated to 140 °C (oil bath) and stirred for 5 h. After cooling to room temperature the reaction mixture was filtered. After removal of toluene (filtrate) in vacuo the residue was diluted in dichloromethane. After removal of the solvents in vacuo the crude product was adsorbed on celite® and chromatographed on silica gel (gradient *n*-hexane to n-hexane/ethyl acetate 80:1) to give 2.72 g (8.91 mmol, 74 %) 4-methoxy-*N*-(4-methoxyphenyl)-*N*-phenylaniline as yellow to colorless viscous oil, R_f (*n*-hexane:EtOAc, 10:1): 0.45. ^{1}H NMR (300 MHz, $CDCl_3$): δ 3.79 (s, 6 H), 6.79-6.85 (m, 4 H), 6.85-6.90 (m, 1 H), 6.91-6.96 (m, 2 H), 7.00-7.08 (m, 4 H), 7.12-7.21 (m, 2 H). ^{13}C NMR (75 MHz, $CDCl_3$): δ 55.6 (CH_3), 114.8, 120.7, 121.1, 126.5, 129.1, 141.3 (C_{quat}), 148.9 (C_{quat}), 155.8 (C_{quat}). GC-MS: *m/z* (%) 306 (20), 305 (M^+, 100), 291 ($C_{19}H_{17}NO_2^+$, 18), 290 ($C_{19}H_{16}NO_2^+$, 92).

2.3.2.2 4-Bromo-*N*,*N*-bis(4-methoxyphenyl)aniline[6]

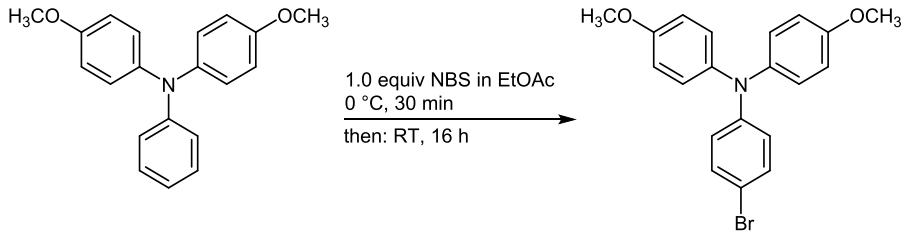

$C_{20}H_{18}BrNO_2$
384.27

In a dry screw-cap Schlenk tube with a magnetic stir bar under nitrogen 4-methoxy-*N*-(4-methoxy-phenyl)-*N*-phenylaniline (917 mg, 3.00 mmol) was dissolved in 15 mL ethyl acetate. Then, the reaction mixture was packed light-tight and cooled to 0 °C. After 10 min NBS (536 mg, 3.01 mmol) was added and stirred at 0 °C for 30 min. Afterwards the ice bath was removed and the reaction mixture was stirred at room temperature for 16 h. The reaction mixture was diluted in ethyl acetate and washed with deionized water (3 x 100 mL) and brine (1 x 100 mL). The combined organic layers were dried (anhydrous magnesium sulfate) and

after removal of the solvents in vacuo the residue was chromatographed on silica gel (*n*-hexane) to give 4-bromo-*N,N*-bis(4-methoxyphenyl)aniline (1.02 g, 88 %) as a colorless crystalline solid, Mp 95 °C. R_f (*n*-hexane): 0.17. ^{1}H NMR (300 MHz, $CDCl_3$): δ 3.79 (s, 6 H), 6.75-6.87 (m, 6 H), 6.99-7.07 (m, 4 H), 7.24 (dd, *J* = 9.1, 2.3 Hz, 2 H). ^{13}C NMR (75 MHz, $CDCl_3$): δ 55.6 (CH_3), 112.5 (C_{quat}), 114.9, 122.1, 126.7, 131.9, 140.7 (C_{quat}), 148.1 (C_{quat}), 156.2 (C_{quat}). IR (ATR): $\tilde{\nu}$ 3038 (w), 2999 (w), 2953 (w), 2932 (w), 2905 (w), 2832 (w), 1602 (w), 1585 (m), 1501 (s), 1483 (s), 1464 (m), 1452 (m), 1437 (m), 1402 (w), 1315 (m), 1285 (m), 1271 (m), 1238 (s), 1177 (s), 1161 (m), 1115 (w), 1101 (m), 1072 (m), 1030 (s), 1007 (m), 829 (s), 822 (s), 800 (m), 779 (m), 729 (m), 696 (m), 602 (m). EI-MS (70 eV): *m/z* (%) 386 (20), 385 (M^+(^{81}Br), 98), 384 (22), 383 (M^+(^{79}Br), 100), 371 (18), 370 (M^+(^{81}Br)-CH_3, 89), 369 (18), 368 (M^+(^{79}Br)-CH_3, 94), 260 (10), 217 (10), 152 (12), 144 (11), 128 (14). Anal. calcd. for $C_{20}H_{18}BrNO_2$ (383.1): C 62.51, H 4.72, N 3.65; Found: C 62.63, H 4.75, N 3.50.

2.4 9-(4-Bromophenyl)-3,6-dimethoxy-9*H*-carbazole

2.4.1 3,6-Dibromo-9H-carbazole[6]

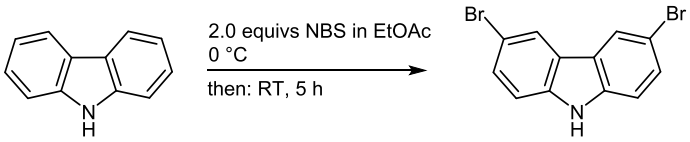

$C_{12}H_7Br_2N$
325.00

In a dry screw-cap Schlenk tube with a magnetic stir bar under nitrogen carbazole (3.37 g, 20.2 mmol) was dissolved in 150 mL ethyl acetate. Then, the reaction mixture was packed light-tight and cooled to 0 °C. After 10 min NBS (7.16 g, 40.2 mmol) was added . Afterwards the ice bath was removed and the reaction mixture was stirred at room temperature for 5 h. The reaction mixture was diluted in ethyl acetate and washed with deionized water and brine. The combined organic layers were dried (anhydrous magnesium sulfate) and after removal of the solvents in vacuo the residue was absorbed on celite® and chromatographed on silica gel (*n*-hexane/ethyl acetate 6:1) to give 3,6-dibromo-9*H*-carbazole (6.18 g, 95 %) as a light yellow crystalline solid. Mp 222 °C. R_f (*n*-hexane:EtOAc, 5:1): 0.30. ^{1}H NMR (300 MHz, $(CD_3)_2SO$): δ 7.47 (dd, *J* = 8.6, 0.6 Hz, 2 H), 7.53 (dd, *J* = 8.6, 1.9 Hz, 2 H), 8.43 (dt, *J* = 2.0, 0.6 Hz, 2 H), 11.59 (s, 1 H). ^{13}C NMR (75 MHz, $(CD_3)_2SO$): δ 111.0 (C_{quat}), 113.2, 123.3, 123.4 (C_{quat}), 128.7, 138.8 (C_{quat}). IR (ATR): $\tilde{\nu}$ 3404 (s), 3071 (w), 3051 (w), 2855 (w), 2196 (w), 1738 (w), 1645 (m), 1597 (m), 1518 (m), 1472 (s), 1458 (s), 1431 (s), 1371 (w), 1344 (w), 1301 (w), 1285 (s), 1234 (m), 1204 (m), 1173 (w), 1120 (m), 1107 (w), 1051 (s), 1006 (m), 907 (m), 870 (s), 804 (s), 789 (m), 760 (m), 706 (m), 687 (s), 640 (s), 631 (m). EI-MS (70 eV): *m/z* (%) 327 (M^+(^{81}Br^{81}Br), 49), 326 (15), 325 (M^+(^{81}Br^{79}Br), 100), 323 (M^+(^{79}Br^{79}Br), 50), 246 ($C_{12}H_7$(^{81}Br)N^+,

24), 244 ($C_{12}H_7(^{79}Br)N^+$, 26), 165 ($C_{12}H_7N^+$, 24), 164 (19), 162 (13), 149 (17), 83 (18), 43 (11). Anal. calcd. for $C_{12}H_7Br_2N$ (322.9): C 44.35, H 2.17, N 4.31; Found: C 44.38, H 2.22, N 4.23.

2.4.2 3,6-Dimethoxy-9*H*-carbazole[7]

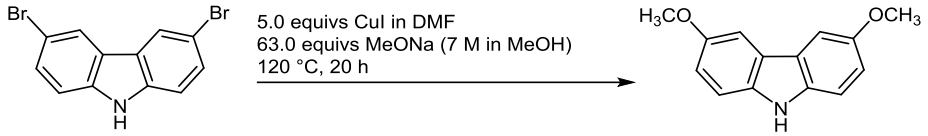

$C_{14}H_{13}NO_2$
227.26

In a dry screw-cap Schlenk tube with a magnetic stir bar under nitrogen 3,6-dibromo-9*H*-carbazole (3.03 g, 9.37 mmol) was dissolved in 10 mL DMF. Then, copper iodide (8.80 g, 46.2 mmol) and 20 mL DMF were added. After addition 81 mL of a sodium methanolate (7 M in methanol) the reaction mixture turned violet. The reaction mixture was stirred at 120 °C for 20 h. After cooling to room temperature the suspension was diluted with dichloromethane, filtered with silica gel and dried (anhydrous magnesium sulfate). The brown crude product was chromatographed on silica gel (*n*-hexane/ethyl acetate 6:1) to give 3,6-dibromo-9*H*-carbazol (6.18 g, 95 %) as a light yellow crystalline solid. Then, the reaction mixture was packed light-tight and cooled to 0 °C. After 10 min 7.16 g (40.2 mmol) NBS were added. Afterwards the ice bath was removed and the reaction mixture was stirred at room temperature for 5 h. The reaction mixture was diluted in ethyl acetate and washed with deionized water and brine. The combined organic layers were dried (anhydrous magnesium sulfate) and after removal of the solvents in vacuo the residue was absorbed on celite® and chromatographed on silica gel (*n*-hexane/ethyl acetate 5:1) to give 3,6-dimethoxy-9*H*-carbazole (1.11 g, 52 %) as a light brown amorphous solid, Mp 117 °C. R_f (*n*-hexane:EtOAc, 3:1): 0.43. ^{1}H NMR (600 MHz, $CDCl_3$): δ 3.94 (s, 6 H), 7.06 (dd, *J* = 8.7, 2.5 Hz, 2 H), 7.29 (d, *J* = 8.8 Hz, 2 H), 7.51 (d, *J* = 2.5 Hz, 2 H), 7.77 (s, 1 H). ^{13}C NMR (151 MHz, $CDCl_3$): δ 56.2 (CH_3), 103.0, 111.7, 115.4, 123.8 (C_{quat}), 135.4 (C_{quat}), 153.7 (C_{quat}). IR (ATR): $\tilde{\nu}$ 3375 (m), 3352 (w), 3063 (w), 2953 (w), 2909 (w), 2830 (w), 1611 (m), 1576 (m), 1491 (s), 1472 (s), 1458 (s), 1435 (m), 1337 (m), 1304 (m), 1265 (m), 1227 (w), 1200 (s), 1155 (s), 1109 (m), 1070 (w), 1028 (s), 968 (w), 934 (w), 889 (w), 826 (m), 806 (s), 779 (s), 752 (w), 727 (w), 602 (m). GC-MS: *m/z* (%) 228 (14), 227 (M^+, 100), 226 (10), 213 (15), 212 ($C_{13}H_{10}NO_2^+$, 99), 184 (20), 141 (13), 114 (10). Anal. calcd. for $C_{14}H_{13}NO_2$ (227.1): C 73.99, H 5.77, N 6.16; Found: C 73.89, H 5.70, N 6.09.

2.4.3 9-(4-Bromophenyl)-3,6-dimethoxy-9*H*-carbazole

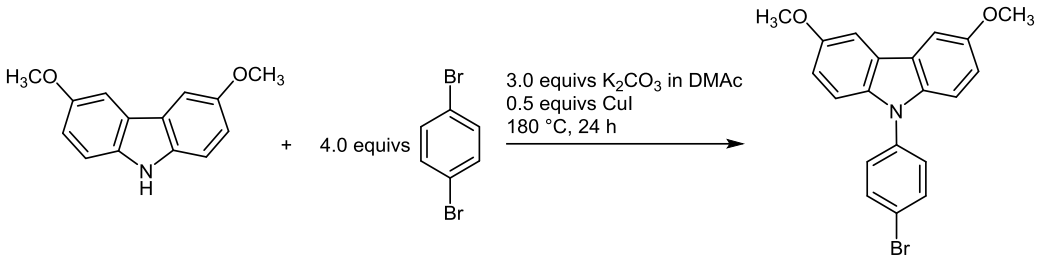

$C_{20}H_{16}BrNO_2$
382.26

In a dry screw-cap Schlenk tube with a magnetic stir bar under nitrogen 3,6-dimethoxy-9*H*-carbazole (0.92 g, 4.04 mmol) and 1,4-dibromobenzene (3.76 g, 16.0 mmol) were dissolved in *N*,*N*-dimethylacetamide (DMAc) (25 mL). After a solution had formed potassium carbonate (1.60 g, 11.6 mmol) and copper iodide (403 mg; 2.12 mmol) were added and the screw-cap tube was sealed. The reaction mixture was heated to 180 °C (oil bath) for 24 h. After cooling to room temp 100 mL deionized water were added to the reaction mixture. The reaction mixture was diluted with dichloromethane (80 mL) and the aqueous layer was extracted with dichloromethane (3 x 50 mL). The combined organic layers were washed with saturated ammonium cloride (50 mL) and dried (anhydrous magnesium sulfate). The residue was chromatographed on silica gel (*n*-hexane/dichloromethane 20:1) to give 9-(4-bromophenyl)-3,6-dimethoxy-9*H*-carbazole (1.01 g, 66 %) as a colorless crystalline solid, Mp >250°C. R_f (*n*-hexane:EtOAc, 2:1): 0.75. ^{1}H NMR (300 MHz, $CDCl_3$): δ 3.95 (s, 6 H), 7.04 (dd, J = 8.9, 2.5 Hz, 2 H), 7.30 (d, J = 9.0 Hz, 2 H), 7.42 (d, J = 8.7 Hz, 2 H), 7.55 (d, J = 2.4 Hz, 2 H), 7.70 (d, J = 8.7 Hz, 2 H). ^{13}C NMR (75 MHz, $CDCl_3$): δ 56.3 (CH_3), 103.1, 110.6, 115.4, 120.3 (C_{quat}), 123.9 (C_{quat}), 128.3, 133.1, 136.1 (C_{quat}), 137.4 (C_{quat}), 154.3 (C_{quat}). MALDI-TOF: *m/z* 383 (M^+(^{81}Br)), 381 (M^+(^{79}Br)). Anal. calcd. for $C_{20}H_{16}BrNO_2$ (381.0): C 62.84, H 4.22, N 3.66; Found: C 62.55, H 4.33, N 3.48.

2.5 9-(4-Bromophenyl)-9*H*-carbazole[8]

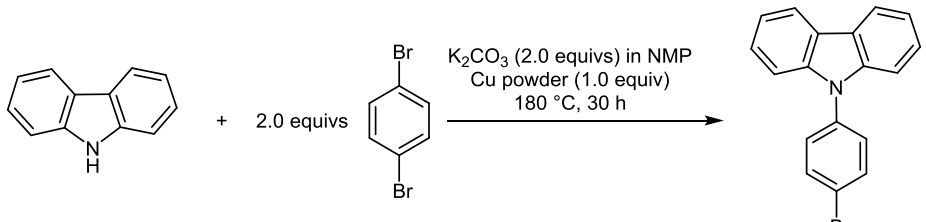

$C_{18}H_{12}BrN$
322.21

In a dry screw-cap Schlenk tube with a magnetic stir bar under nitrogen carbazole (3.36 g, 20.1 mmol) and 1,4-dibromobenzene (9.45 g, 40.1 mmol) were dissolved in *N*-methyl-2-

pyrrolidone (NMP) (20 mL). After a solution had formed potassium carbonate (5.58 g, 40.4 mmol) and copper powder (1.54 g; 24.3 mmol) were added an the screw-cap tube was sealed. The reaction mixture was heated to 180 °C (oil bath) for 30 h. After cooling to room temp the copper powder was filtered off and the residue was washed several times with small amounts of ethyl acetate. The filtrate was diluted with ethyl acetate and the combined organic layer was extracted with deionized water (4 x 30 mL) and finally with saturated brine (50 mL). The combined organic layers were dried (anhydrous magnesium sulfate) and after removal of the solvents in vacuo the residue was chromatographed on silica gel (*n*-hexane/dichloromethane 6:1) to give 9-(4-bromophenyl)-9*H*-carbazole (3.65 g, 56 %) as a colorless solid, Mp 149 °C. R_f (*n*-hexane:CH_2Cl_2, 2:1): 0.69. ^{1}H NMR (600 MHz, $CDCl_3$): δ 7.32 (ddd, *J* = 8.1, 6.6, 1.6 Hz, 2 H), 7.37-7.51 (m, 6 H), 7.74 (d, *J* = 8.7 Hz, 2 H), 8.16 (d, *J* = 7.7 Hz, 2 H). ^{13}C NMR (151 MHz, $CDCl_3$): δ 109.7, 120.4, 120.5, 121.0 (C_{quat}), 123.6 (C_{quat}), 126.2, 128.8, 133.2, 136.9 (C_{quat}), 140.7 (C_{quat}). IR (ATR): $\tilde{\nu}$ 3046 (w), 2928 (w), 1946 (w), 1906 (w), 1873 (w), 1829 (w), 1784 (w), 1597 (w), 1585 (m), 1497 (s), 1479 (s), 1452 (s), 1404 (w), 1364 (m), 1337 (m), 1315 (m), 1292 (w), 1229 (s), 1182 (m), 1167 (m), 1152 (w), 1123 (m), 1101 (m), 1067 (m), 1022 (w), 1011 (m), 999 (m), 935 (w), 912 (m), 854 (w), 826 (s), 748 (s), 725 (s), 708 (m), 637 (m), 617 (m). EI-MS (70 eV): *m/z* (%) 324 (19), 323 (M^+(^{81}Br), 100), 322 (22), 321 (M^+(^{79}Br), 99), 242 (24), 241 (55), 240 (12), 121 (52). Anal. calcd. for $C_{18}H_{12}BrN$ (321.0): C 67.10, H 3.75, N 4.35; Found: C 67.31, H 3.78, N 4.37.

2.6 General Procedure (GP2) for the Syntheses of Pinacolyl *p*-(Diaryl)aminophenylboronates 5

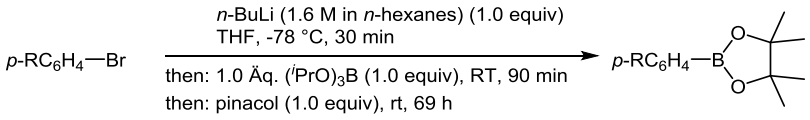

5a-d

In a dry screw-cap Schlenk tube with a magnetic stir bar the corresponding *p*-(diaryl)aminophenylbromide (1.0 equiv) and dry THF (1.5 mmol/mL) were dissolved under nitrogen (for experimental details, see Table SI-2). The solution was cooled to -78 °C (dry ice/acetone bath) and stirred for 10 min. Then *n*-BuLi (1.6 M in *n*-hexanes) (1.0 equiv) was added dropwise to the solution. The solution changed its color from yellow to brown. After stirring at this temperature for 30 min tris(isopropyl)borate (1.0 equiv) was added dropwise to the solution and stirring was continued for 10 min. The reaction mixture was allowed to come to room temp and stirred for 30 min before pinacol (1.2 equivs) was added dropwise to the reaction mixture. Then the suspension was stirred at room temp for 69 h. The reaction was stopped by addition of acetic acid (1.0 equiv) and stirring at room temp was continued for 1 h.

The reaction mixture was poured in dichloromethane and extracted with dichloromethane (3 x 10 mL). The combined organic layers were washed with brine and dried (anhydrous magnesium sulfate). The residue was absorbed on Celite® and chromatographed on silica gel (*n*-hexane/ethyl acetate) to give pinacolyl *p*-(diaryl)aminophenylboronates **5**.

Table SI-2. Experimental details of the synthesis of pinacolyl *p*-(diaryl)aminophenylboronates **5**.

Entry	*p*-(diaryl)amino-phenylbromide	THF	*n*-BuLi (1.6 M)	$(^{i}PrO)_3B$	pinacol	acetic acid	pinacolyl *p*-(diaryl)amino-phenylboronates **5**
1	2.88 g (7.49 mmol) of 4-bromo-*N*,*N*-bis(4-methoxy-phenyl)aniline	5 mL	4.70 mL (7.52 mmol)	1.75 mL (7.58 mmol)	1.07 g (9.05 mmol)	0.45 mL (7.5 mmol)	2.68 g (83%) of **5a**
2[a]	0.90 g (2.35 mmol) of 9-(4-bromo-phenyl)-3,6-dimethoxy-9*H*-carbazole	1.5 mL	1.50 mL (2.40 mmol)	0.55 mL (2.38 mmol)	0.34 g (2.88 mmol)	0.15 mL (2.4 mmol)	0.52 g (52%) of **5b**
3	2.44 g (7.57 mmol) of 9-(4-bromo-phenyl)-9*H*-carbazole	5 mL	4.75 mL (7.60 mmol)	1.75 mL (7.58 mmol)	1.08 g (9.14 mmol)	0.45 mL (7.5 mmol)	1.87 g (67%) of **5c**
4	1.75 g (5.40 mmol) of 4-bromo-*N*,*N*-diphenylaniline	3.6 mL	3.4 mL (5.4 mmol)	1.0 mL (5.4)	0.83 mL (6.5 mmol)	0.32 mL (5.4 mmol)	1.00 g (54%) of **5d**

2.6.1 4-Methoxy-*N*-(4-methoxyphenyl)-*N*-(4-(4,4,5,5-tetramethyl-1,3,2-dioxaborolan-2-yl)-phenyl)aniline (5a)

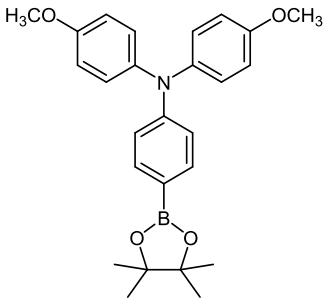

$C_{26}H_{30}BNO_4$ (431.34)

According to the GP 2 and after chromatography on silica gel (*n*-hexane/ethyl acetate 10:1 to 2:1) compound **5a** (2.68 g, 83%) was obtained as a colorless amorphous solid, Mp 128 °C, R_f (*n*-hexane/ethyl acetate 20:1 to 2:1): 0.16. ^{1}H NMR (300 MHz, $CDCl_3$): δ 11.32 (s, 12 H), 3.80 (s, 6 H), 6.83 (d, *J* = 9.0 Hz, 4 H), 6.87 (d, *J* = 8.7 Hz, 2 H), 7.07 (d, *J* = 9.0 Hz, 4 H), 7.60 (d, *J* = 8.7 Hz, 2 H). ^{13}C NMR (75 MHz, $CDCl_3$): δ 25.0 (CH_3), 55.6 (CH_3), 83.5 (C_{quat}), 114.8, 118.8,

127.3, 135.9, 140.5 (C_{quat}), 151.5 (C_{quat}), 156.3 (C_{quat}).[1] IR (ATR): $\tilde{\nu}$ 3100 (w), 2997 (w), 2957 (w), 2934 (w), 2837 (w), 1610 (m), 1597 (m), 1504 (s), 1464 (m), 1439 (w), 1422 (w), 1389 (m), 1360 (s), 1327 (s), 1315 (s), 1287 (s), 1273 (m), 1244 (s), 1233 (s), 1198 (m), 1197 (m), 1178 (w), 1167 (m), 1142 (s), 1092 (s), 961 (m), 947 (w), 916 (w), 860 (m), 831 (s), 816 (m), 779 (m), 733 (m), 718 (w), 658 (s). EI-MS (70 eV): *m/z* (%) 432 (25), 431 (M^+, 100), 430 (23), 417 (16), 416 ($C_{25}H_{27}BNO_4^+$, 62), 415 (15), 316 ($C_{18}H_{11}BNO_4^+$, 23). Anal. calcd. for $C_{26}H_{30}BNO_4$ (431.2): C 72.40, H 7.01, N 3.25; Found: C 72.49, H 6.86, N 3.10.

2.6.2 3,6-Dimethoxy-9-(4-(4,4,5,5-tetramethyl-1,3,2-dioxaborolan-2-yl)phenyl)-9*H*-carbazole (5b)

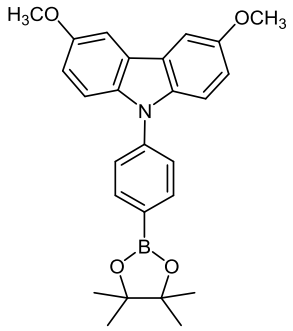

$C_{26}H_{28}BNO_4$ (429.32)

According to the GP 2 and after chromatography on silica gel (*n*-hexane/ethyl acetate 2:1) compound **5b** (0.52 g, 52%) was obtained as a colorless amorphous solid, Mp 108 °C, R_f (*n*-hexane/ethyl acetate 10:1): 0.25. ^{1}H NMR (300 MHz, $CDCl_3$): δ 1.39 (s, 12 H), 3.95 (s, 6 H), 7.03 (dd, *J* = 8.9, 2.5 Hz, 2 H), 7.37 (d, *J* = 8.9 Hz, 2 H), 7.51-7.60 (m, 4 H), 8.02 (d, *J* = 8.3 Hz, 2 H). ^{13}C NMR (75 MHz, $CDCl_3$): δ 25.1 (CH_3), 56.3 (CH_3), 84.2 (C_{quat}), 103.1, 111.0, 115.3, 124.0 (C_{quat}), 125.7, 136.1 (C_{quat}), 136.5, 141.0 (C_{quat}), 154.3 (C_{quat}).[1] IR (ATR): $\tilde{\nu}$ 3038 (w), 2976 (w), 2934 (w), 2907 (w), 2830 (w), 1605 (m), 1582 (w), 1518 (w), 1489 (m), 1464 (s), 1433 (w), 1396 (m), 1356 (s), 1327 (m), 1283 (w), 1261 (w), 1204 (s), 1175 (m), 1142 (s), 1107 (m), 1088 (s), 1032 (m), 1018 (m), 962 (w), 947 (w), 914 (w), 897 (w), 858 (m), 831 (m), 802 (m), 789 (m), 741 (w), 692 (w), 664 (s), 652 (m), 604 (w). EI-MS (70 eV): *m/z* (%) 429 (M^+, 11), 414 (13), 396 (13), 363 (13), 337 (10), 271 (14), 253 (12), 251 (11), 213 (12), 211 (10), 119 (14), 109 (17), 107 (19), 105 (18), 97 (21), 95 (25), 93 (17), 91 (18), 85 (17), 84 (19), 83 (37), 81 (35), 80 (20), 71 (24), 70 (23), 69 (80), 67 (25), 59 (28), 57 (46), 56 (48), 55 (73), 43 (100), 42 (13), 41 (59). Anal. calcd. for $C_{26}H_{28}BNO_4$ (429.2): C 72.74, H 6.57, N 3.26; Found: C 72.62, H 6.65, N 3.04.

[1] The quaternary carbon nucleus bound to the boron nucleus was not observed in the ^{13}C NMR spectrum.

2.6.3 9-(4-(4,4,5,5-Tetramethyl-1,3,2-dioxaborolan-2-yl)phenyl)-9*H*-carbazole (5c)

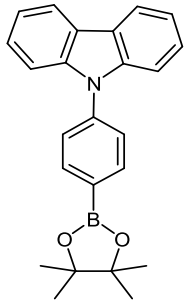

$C_{24}H_{24}BNO_2$ (369.27)

According to the GP 2 and after chromatography on silica gel (*n*-hexane/ethyl acetate 4:1) compound **5c** (1.87 g, 67%) was obtained as a colorless amorphous solid, Mp 159 °C, R_f (*n*-hexane/ethyl acetate 2:1): 0.24. ^{1}H NMR (300 MHz, $CDCl_3$): δ 1.42 (s, 12 H), 7.30 (ddd, *J* = 8.1, 6.7, 1.5 Hz, 2 H), 7.42 (ddd, *J* = 8.2, 6.7, 1.5 Hz, 2 H), 7.45-7.49 (m, 2 H), 7.61 (d, *J* = 8.4 Hz, 2 H), 8.07 (d, *J* = 8.4 Hz, 2 H), 8.15 (d, *J* = 8.0 Hz, 2 H). ^{13}C NMR (75 MHz, $CDCl_3$): δ 25.1 (CH_3), 84.2 (C_{quat}), 110.0, 120.2, 120.4, 123.6 (C_{quat}), 126.1, 126.2, 136.5, 140.5 (C_{quat}), 140.7 (C_{quat}).[1] IR (ATR): $\tilde{\nu}$ 3120 (w), 2974 (w), 2840 (w), 1605 (s), 1595 (m), 1516 (w), 1479 (m), 1452 (s), 1400 (s), 1360 (s), 1357 (s), 1333 (s), 1317 (s), 1298 (m), 1267 (m), 1233 (s), 1211 (w), 1184 (m), 1167 (m), 1142 (s), 1103 (m), 1088 (s), 1020 (s), 962 (m), 858 (m), 829 (m), 750 (s), 727 (s), 671 (m), 654 (s), 640 (m). EI-MS (70 eV): *m/z* (%) 370 (25), 369 (M^+, 100), 368 (24), 311 ($C_{20}H_{14}BNO_2^+$, 14), 270 (20), 269 (37), 268 (14), 243 (22), 242 ($C_{18}H_{12}N^+$, 10), 241 (13), 194 (13), 193 (88), 192 (28), 166 ($C_{12}H_8N^+$, 17), 165 (47), 116 ($C_6H_{12}O_2^+$, 18), 90 (16), 89 (18), 77 ($C_6H_5^+$, 20), 51 (13). Anal. calcd. for $C_{24}H_{24}BNO_2$ (369.2): C 78.06, H 6.55, N 3.79; Found: C 78.29, H 6.51, N 3.74.

2.6.4 9-(4-(4,4,5,5-Tetramethyl-1,3,2-dioxaborolan-2-yl)phenyl)-9*H*-carbazole (5d)

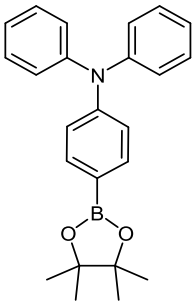

$C_{24}H_{26}BNO_2$ (371.29)

According to the GP 2 and after chromatography on silica gel (*n*-hexane/acetone 60:1) compound **5d** (1.00 g, 54%) was obtained as a colorless amorphous solid, Mp 91-92 °C. R_f (*n*-hexane/ethyl acetate 20:1) = 0.31. ^{1}H NMR (300 MHz, acetone-d^6): δ 1.32 (s, 12 H), 6.97 (dt, ^3J = 8.6 Hz, ^4J = 2.0 Hz, 2 H), 7.05 – 7.13 (m, 6 H), 7.27 – 7.36 (m, 4 H), 7.63 (dt, 3*J* = 8.6 Hz,

4*J* = 2.0 Hz, 2 H). ^{13}C NMR (75 MHz, acetone-d^6): δ 25.2 (CH3), 84.2 (C_{quat}), 122.1 (CH), 124.5 (CH), 125.9 (CH), 130.3 (CH), 136.7 (CH), 148.2 (C_{quat}), 151.5 (C_{quat}). MS (GC-MS) *m/z* (%): 371 ($[M]^+$,100), 271 ($[C_{18}H_{14}BNO]^+$, 31), 244 ($[C_{18}H_{14}N]^+$, 11), 168 ($[C_{12}H_{10}N]^+$, 13), 85 ($[C_6H_{13}]^+$, 50), 77 ($[C_6H_5]^+$, 42), 58 ($[C_3H_6O]^+$, 27). IR: $\tilde{\nu}$ [cm^{-1}] = 3038 (w), 2976 (w), 2928 (w), 2870 (w), 1586 (m), 1487 (m), 1456 (w), 1398 (m), 1358 (s), 1317 (s), 1287 (s), 1269 (s), 1213 (w), 1144 (s), 1028 (w), 1016 (m), 999 (w), 961 (m), 924 (w), 887 (w), 858 (m), 839 (w), 754 (s), 744 (m), 697 (m), 692 (s), 675 (m), 658 (s), 637 (m), 613 (w). Anal. calcd. for $C_{24}H_{26}BNO_2$ [371.3]: C 77.64, H 7.06, N 3.77; Found: C 77.36, H 7.01, N 3.60.

3 General Procedure (GP 3) for the Consecutive Three-component Synthesis of 3-Piperazinyl Prop-2-enylidene Indolone Bichromophores 4a-d

In a dry screw-cap Schlenk tube with a magnetic stir bar $PdCl_2(PPh_3)_2$ (14.2 mg, 0.02 mmol) and CuI (7.63 mg, 0.04 mmol) were dissolved in dry dichloromethane (5 mL) or dry acetonitrile (4 mL) under nitrogen. Then, the corresponding *ortho*-bromo anilides **1** (1.00 mmol) and the phenyl acetylene **2** (1.00 mmol) were successively added (for experimental details, see Table SI-3) and stirred for 10 min at room temp or at 50 °C. After addition of the terminal alkyne triethylamine (106 mg, 1.05 mmol) was added to the reaction mixture. The mixture turned brown and was then stirred at the temperatures T_1 and times t_1 indicated. Then, piperazine **3** (2.00 mmol) was added under nitrogen and the reaction mixture was stirred at the temperatures T_2 and times t_2 indicated. After cooling to room temp saturated aqueous ammonium chloride solution (10 mL) and dichloromethane (10 mL) was added to the red solution. The organic layer was separated and the aqueous phase was extracted with dichloromethane (3 x 30 mL). The combined organic layers were extracted with brine (15 mL) and dried (anhydrous magnesium sulfate). After filtration the filtrate was absorbed on celite® and purified by flash chromatography on silica gel to give the analytically pure merocyanines **4a-d** as red solids. Deviating workup procedures are given in the details to the analytics of the compounds **4a-d**.

Table SI-3. Experimental details of the consecutive three-component synthesis of 3-piperazinyl prop-2-enylidene indolones **4a-d**.

Entry	*ortho*-bromo anilide **1** [mg] (mmol)	phenylacetylene (**2**) [mg] (mmol)	T_1, t_1	piperazine **3** [mg] (mmol)	T_2, t_2	bichromophore **4** [mg] (%)
1[a]	317 (1.01) of **1a** (R^1 = Me, R^2 = H)	114 (1.12)	RT, 16 h	272 (1.08) of **3a** (R^4 = CH_2(*p*-biphenyl)	50 °C, 48 h	376 (64) of **4a**
2[a]	315 (1.00) of **1a**	114 (1.12)	RT, 16 h	321 (1.16) of **3b** (R^4 = CH_2(9-anthryl))	50 °C, 48 h	422 (69) of **4b**
3[b]	221 (0.49) of **1b**	57.3 (0.56)	RT, 20 h	276 (0.84) of **3b**	80 °C, 4 h	49.6 (14) of **4c**
4[c]	426 (0.94) of **1b**	119 (1.16)	50 °C, 15 h	537 (1.64) of **3c** (R^4 = *p*-C_6H_4(9-carbazolyl))	80 °C, 4 h	300 (40) of **4d**

[a]In dichloromethane as a solvent and induction period of 10 min at RT prior to starting the insertion-coupling step by addition of NEt_3. [b]In acetonitrile as a solvent and induction period of 10 min at RT prior to starting the insertion-coupling step by addition of NEt_3. [c]In acetonitrile as a solvent and induction period of 10 min at 50 °C prior to starting the insertion-coupling step by addition of NEt_3.

3.1 (*E*)-3-((*E*)-3-(4-([1,1'-Biphenyl]-4-ylmethyl)piperazin-1-yl)-1,3-diphenylallylidene)-1-methylindolin-2-one (4a)

According to the GP 3 and after chromatography on silica gel (*n*-hexane/ethyl acetate 5:1) compound **4a** (376 mg, 64 %) was obtained as a bright yellow-orange amorphous solid, Mp 198 °C, R_f (*n*-hexane/ethyl acetate 4:1): 0.18. ^{1}H NMR (600 MHz, $CDCl_3$): δ 2.53 (m, br, 4 H), 3.30 (m, br, 4 H), 3.34 (s, 3 H), 3.60 (s, 2 H), 5.46 (d, *J* = 7.8 Hz, 1 H), 6.44-6.47 (m, 1 H), 6.72 (d, *J* = 7.7 Hz, 1 H), 6.80-6.82 (m, 2 H), 6.85-6.89 (m, 2 H), 6.92 (d, *J* = 7.4 Hz, 2 H), 6.93-6.97 (m, 3 H), 6.98-7.02 (m, 2 H), 7.32-7.36 (m, 1 H), 7.39 (d, *J* = 7.8 Hz, 2 H), 7.42-7.45 (m, 2 H), 7.54 (d, *J* = 8.1 Hz, 2 H), 7.57-7.61 (m, 2 H), 7.80 (s, 1 H). ^{13}C NMR (151 MHz, $CDCl_3$): δ 25.8 (CH_3), 48.8 (CH_2), 52.9 (CH_2), 62.5 (CH_2), 105.9, 106.9, 114.8 (C_{quat}), 120.6, 121.4, 124.8 (C_{quat}), 125.1, 127.0, 127.16, 127.18, 127.3, 127.7, 127.87, 127.91, 128.2, 128.9, 129.4, 129.7, 130.4, 136.9 (C_{quat}), 140.2 (C_{quat}), 140.3 (C_{quat}), 140.5 (C_{quat}), 141.0 (C_{quat}), 156.3 (C_{quat}), 161.8 (C_{quat}), 167.1 (C_{quat}), 168.5 (C_{quat}). IR (ATR): $\tilde{\nu}$ 3071 (w), 2980 (m), 2972 (w), 2936 (w), 2882 (w), 2826 (w), 2797 (w), 1665 (s), 1607 (m), 1545 (s), 1535 (s), 1483 (m), 1470 (m), 1441 (m), 1398 (m), 1373 (m), 1348 (m), 1333 (s), 1304 (m), 1252 (s), 1225 (s), 1192 (m), 1153 (m), 1128 (w), 1084 (s), 1053 (m), 1009 (m), 999 (m), 968 (w), 922 (m), 874 (w), 837 (m), 808 (m), 772 (m), 758 (s), 746 (s), 729 (m), 714 (m), 696 (s), 650 (m), 611 (m). MALDI-TOF: *m/z* 588.2 ($M+H^+$). Anal. calcd. for $C_{41}H_{37}N_3O$ (587.8): C 83.78, H 6.35, N 7.15; Found: C 83.57, H 6.28, N 6.92.

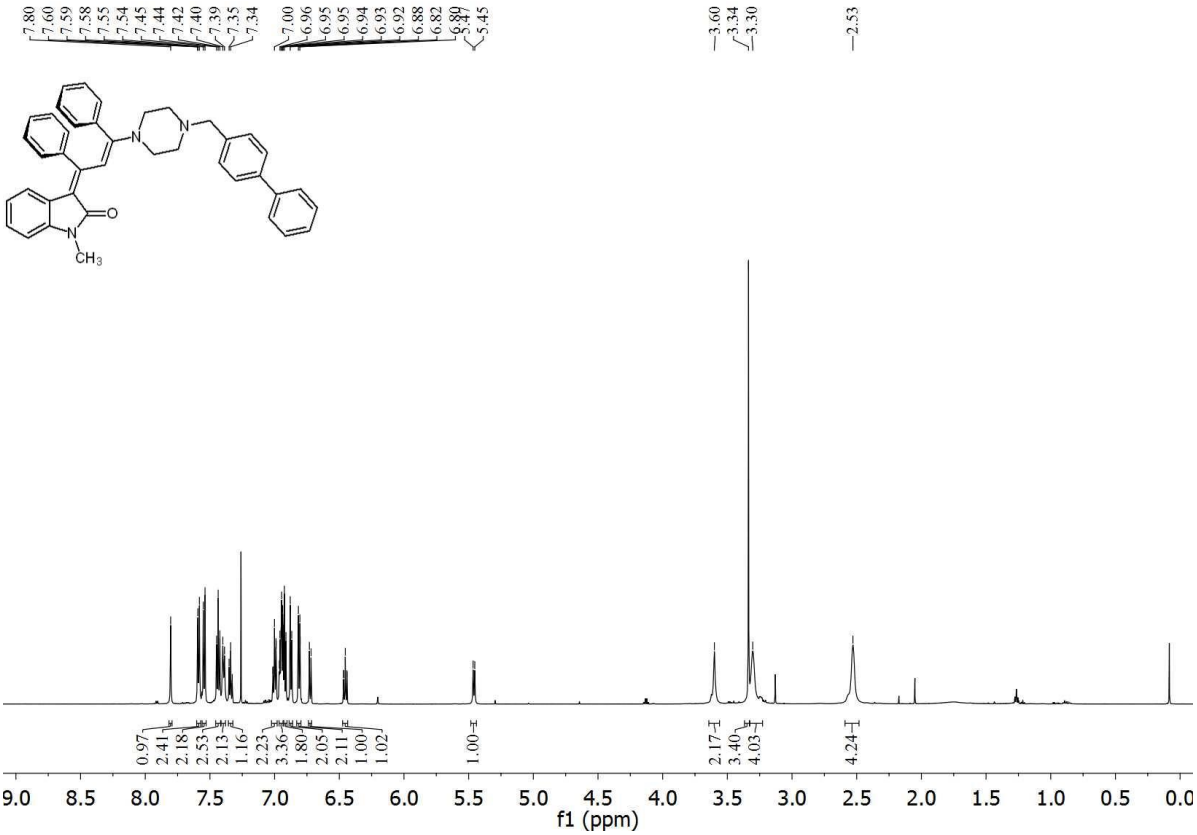

^{1}H NMR spectrum of **4a** ($CDCl_3$, 600 MHz, 293 K).

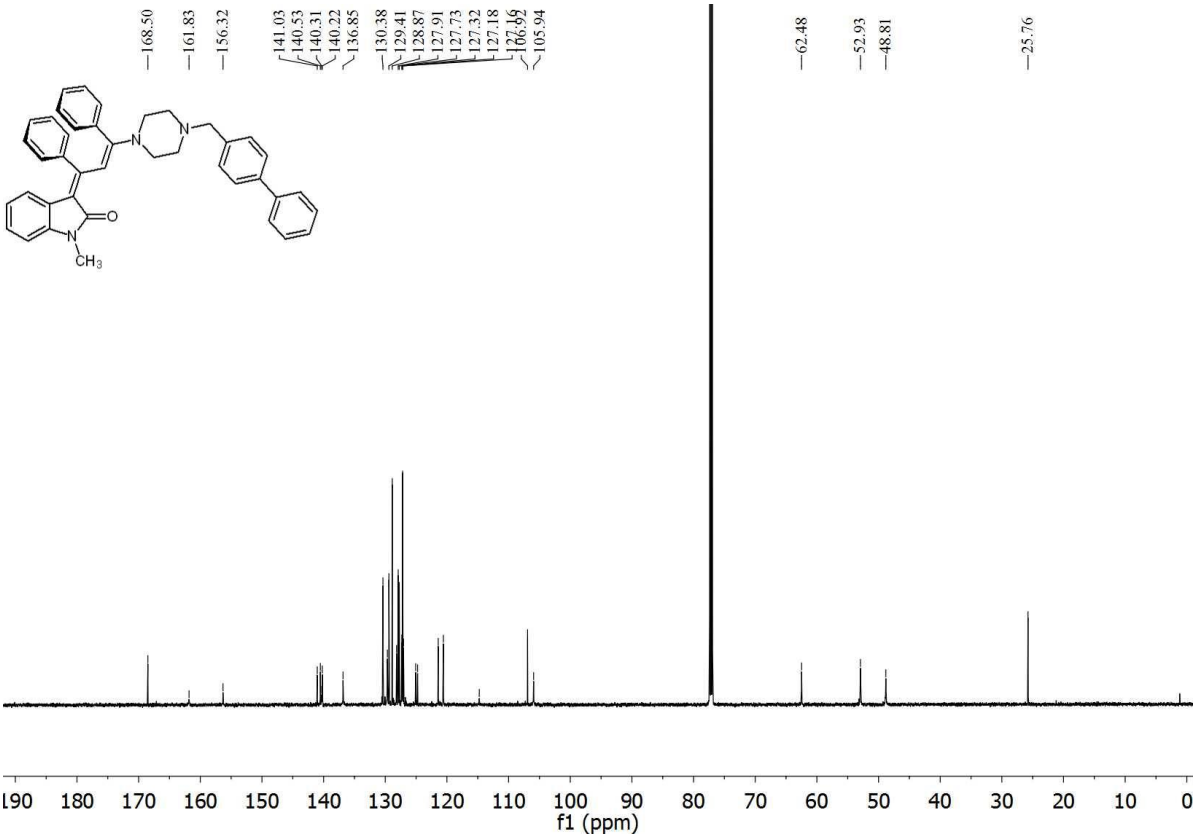

^{13}C NMR spectrum of **4a** ($CDCl_3$, 151 MHz, 293 K).

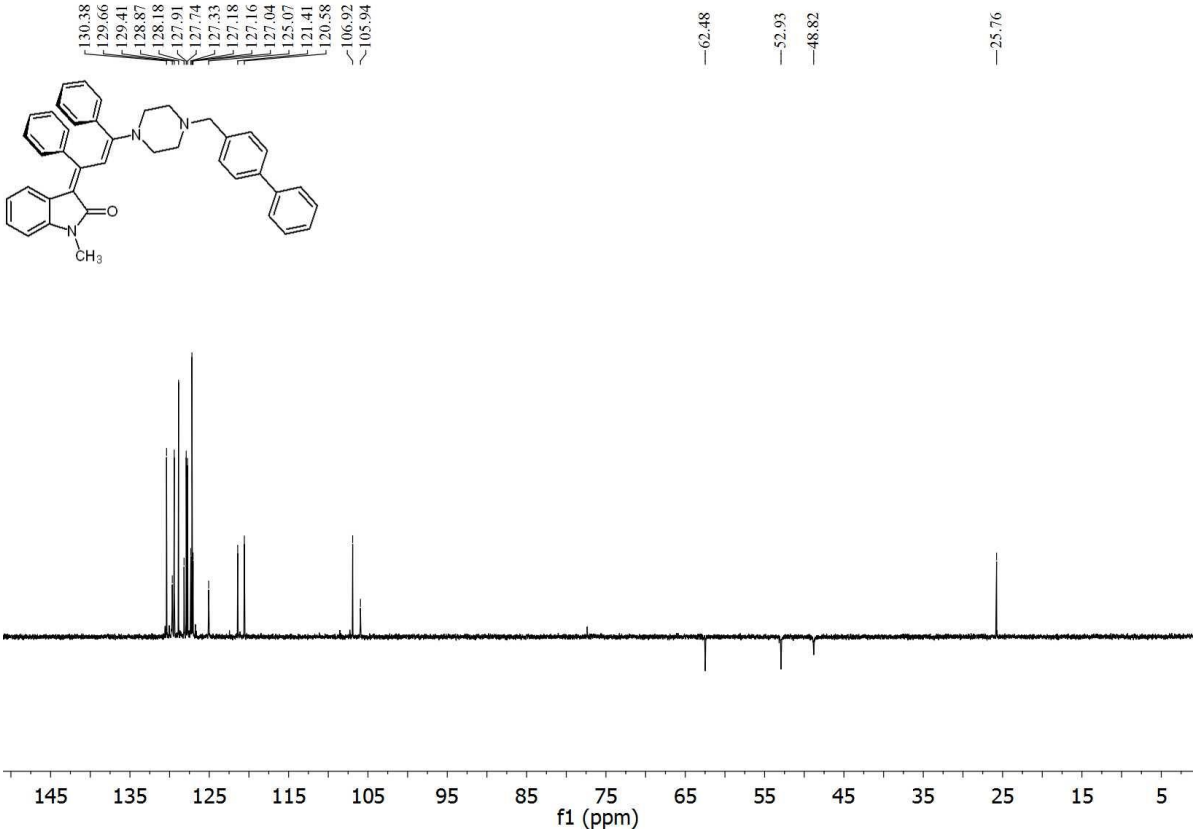

DEPT 135 ^{13}C NMR spectrum of **4a** ($CDCl_3$, 151 MHz, 293 K).

3.2 (*E*)-3-((*E*)-3-(4-(Anthracen-9-ylmethyl)piperazin-1-yl)-1,3-diphenylallylidene)-1-methylindolin-2-one (4b)

According to the GP 3 and after chromatography on silica gel (*n*-hexane/ethyl acetate 8:1) compound **4b** (422 mg, 69 %) was obtained as a dark orange amorphous solid, Mp 168 °C, R_f (*n*-hexane/ethyl acetate 5:1): 0.20. ^{1}H NMR (600 MHz, $CDCl_3$): δ 2.59-2.71 (m, 4 H), 3.15-3.25 (m, 4 H), 3.33 (s, 3 H), 4.48 (s, 2 H), 5.46 (d, *J* = 7.6 Hz, 1 H), 6.42-6.47 (m, 1 H), 6.72 (d, *J* = 7.5 Hz, 1 H), 6.76-7.03 (m, 11 H), 7.41-7.57 (m, 4 H), 7.78 (s, 1 H), 7.99 (dd, *J* = 8.2, 1.4 Hz, 2 H), 8.40 (s, 1 H), 8.47 (d, *J* = 8.8 Hz, 2 H). ^{13}C NMR (151 MHz, $CDCl_3$): δ 25.7 (CH_3), 49.1 (CH_2), 53.0 (CH_2), 54.1 (CH_2), 106.1, 106.9, 114.7 (C_{quat}), 120.5, 121.4, 124.8 (C_{quat}), 124.98, 125.02, 125.1, 125.8, 127.0, 127.68, 127.71, 127.9, 128.1, 129.1, 129.2 (C_{quat}), 129.4, 130.4, 131.45 (C_{quat}), 131.47 (C_{quat}), 136.9 (C_{quat}), 140.3 (C_{quat}), 140.5 (C_{quat}), 156.4 (C_{quat}), 162.0 (C_{quat}), 168.5 (C_{quat}). IR (ATR): $\tilde{\nu}$ 3100 (w), 2980 (w), 2949 (w), 2876 (w), 2832 (w), 2808 (w), 2770 (w), 1734 (w), 1670 (m), 1655 (m), 1603 (m), 1545 (s), 1537 (m), 1466 (m), 1443 (m), 1420 (w), 1395 (m), 1373 (m), 1331 (m), 1306 (m), 1240 (m), 1227 (s), 1198 (m), 1188 (m), 1153 (m), 1125 (m), 1082 (s), 1053 (m), 1040 (m), 1028 (m), 1003 (m), 993 (m), 922 (m), 880 (m), 835 (m), 808 (w), 790 (w), 770 (m), 748 (s), 727 (s), 712 (s), 693 (s), 689 (m), 669 (m), 648 (s). MALDI-TOF: *m/z* 612.3 ($M+H^+$). HRMS (ESI) calcd. for $C_{43}H_{37}N_3O+H^+$: 612.3009; Found: 612.3012.

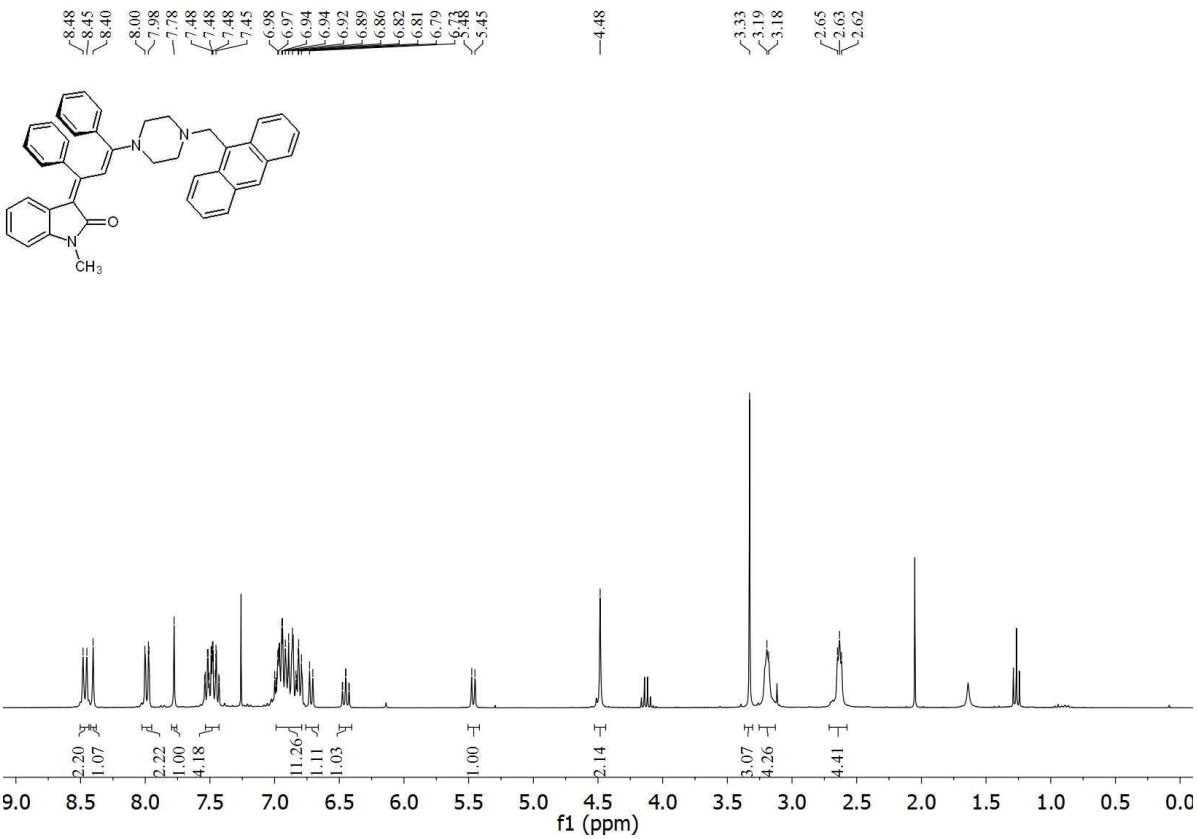

^{1}H NMR spectrum of **4b** ($CDCl_3$, 600 MHz, 293 K). *residual ethyl acetate

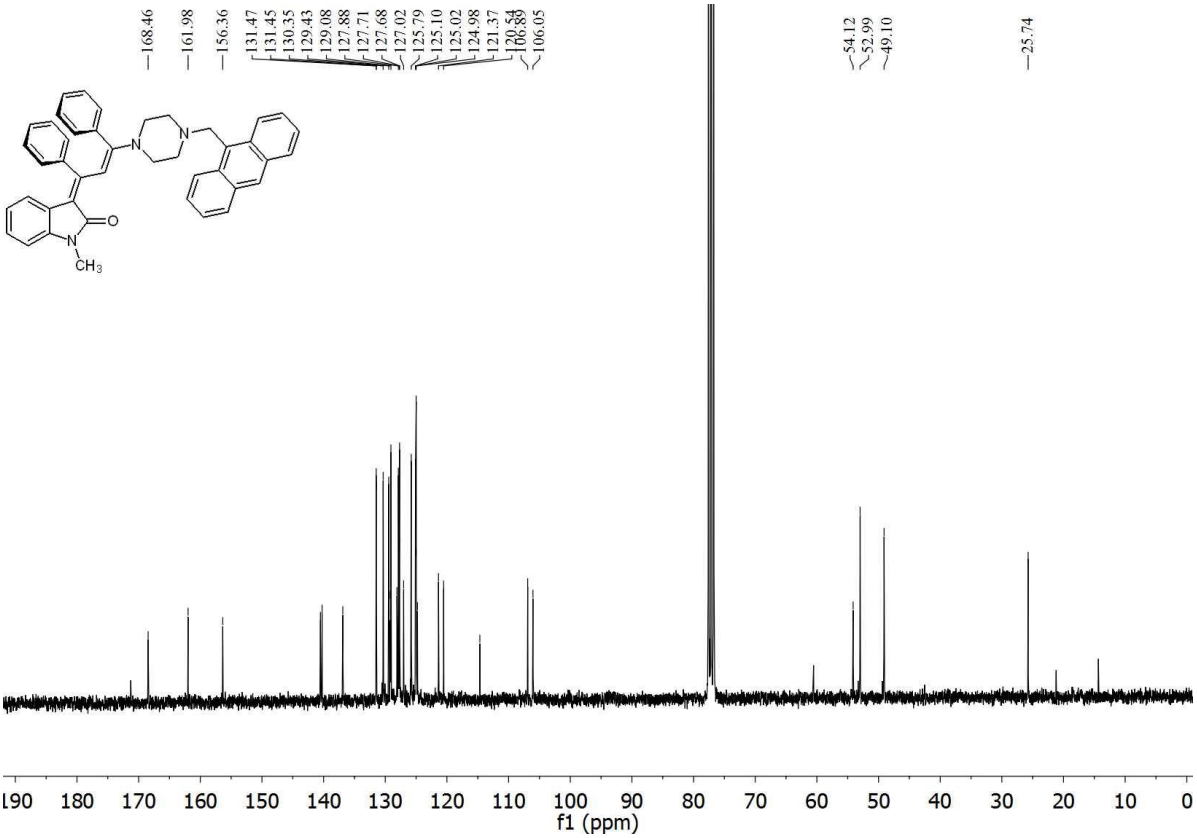

^{13}C NMR spectrum of **4b** ($CDCl_3$, 151 MHz, 293 K).

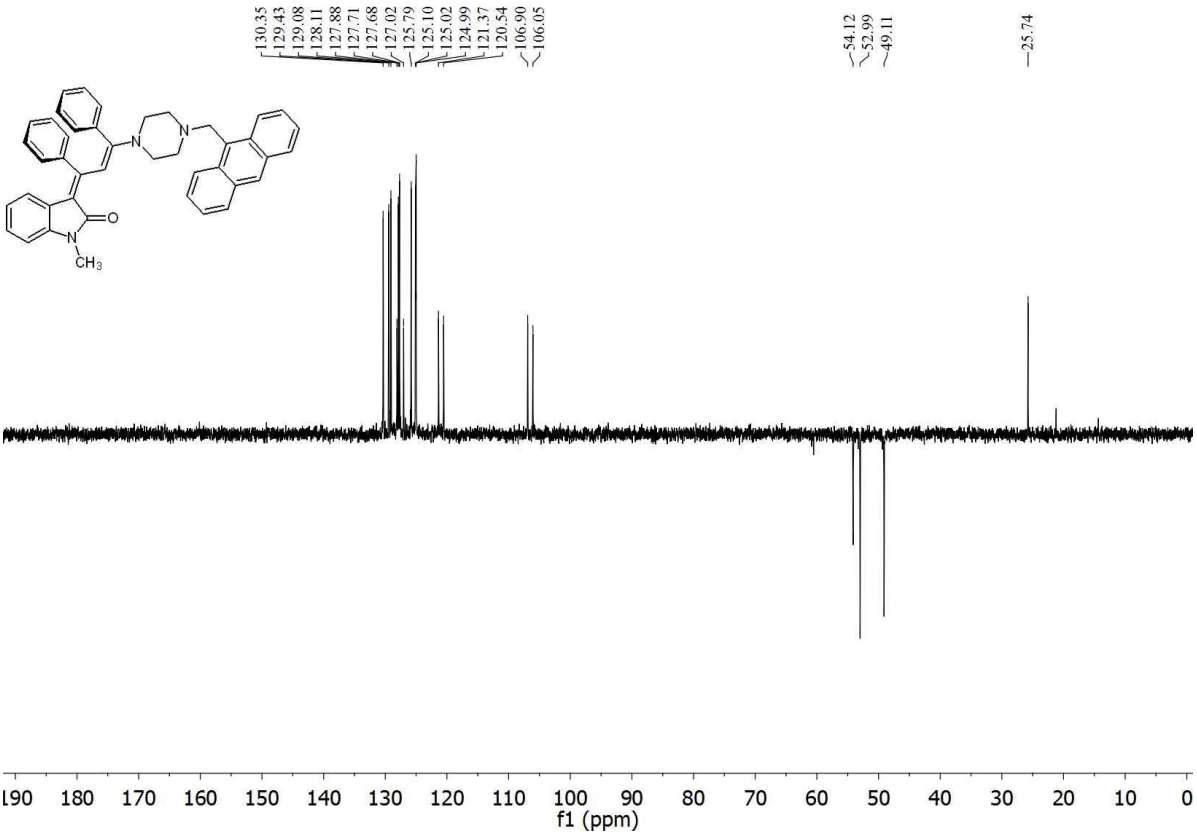

DEPT 135 ^{13}C NMR spectrum of **4b** ($CDCl_3$, 151 MHz, 293 K).

3.3 (*E*)-3-((*E*)-3-(4-(Anthracen-9-yl-methyl)piperazin-1-yl)-1,3-diphenylallylidene)-1-tosylindolin-2-one (4c)

According to the GP 3 and after chromatography on silica gel (*n*-hexane/ethyl acetate 10:1) compound **4c** (49.6 mg, 14 %) was obtained as an orange-red amorphous solid, Mp 223 °C, R_f (*n*-hexane/ethyl acetate 10:1): 0.03. ^{1}H NMR (300 MHz, $CDCl_3$): δ 2.40 (s, 3 H), 2.62 (m, br, 4 H), 3.21 (m, br, 4 H), 4.49 (s, 2 H), 5.36 (d, *J* = 7.8 Hz, 1 H), 6.49-6.53 (m, 1 H), 6.71 (d, *J* = 7.0 Hz, 2 H), 6.79 (d, *J* = 7.0 Hz, 2 H), 6.87-7.00 (m, 7 H), 7.29 (d, *J* = 8.3 Hz, 2 H), 7.45-7.54 (m, 4 H), 7.88 (d, *J* = 8.0 Hz, 1 H), 7.99-8.05 (m, 5 H), 8.43-8.47 (m, 3 H). ^{1}H NMR (600 MHz, CD_2Cl_2): δ 2.33 (s, 3 H), 2.56 (m, br, 4 H), 3.12-3.16 (m, 4 H), 4.42 (s, 2 H), 5.26 (br, 1 H), 6.39-6.42 (m, 1 H), 6.60-6.68 (m, 2 H), 6.69-6.81 (m, 2 H), 6.81-6.85 (m, 5 H), 6.91-6.93 (m, 2 H), 7.24 (d, *J* = 7.4 Hz, 2 H), 7.38-7.40 (m, 3 H), 7.45-7.47 (m, 2 H), 7.74 (d, *J* = 8.1 Hz, 1 H), 7.88 (d, *J* = 8.2 Hz, 2 H), 7.93 (d, *J* = 8.3 Hz, 2 H), 8.36 (s, 1 H), 8.39 (d, *J* = 8.9 Hz, 2 H). ^{13}C NMR (151 MHz, $CDCl_3$): δ 20.6 (CH_3), 48.5 (CH_2), 53.4 (CH_2), 54.2 (CH_2), 105.5 (C_{quat}), 108.8 (C_{quat}), 111.4 (CH), 120.0 (CH), 121.9 (CH), 123.7 124.0 (C_{quat}), (CH), 124.2 (CH),[2] 125.0 (CH), 125.0 (C_{quat}), 125.7 (C_{quat}), 126.8 (CH), 127.0 (CH), 126.9 (CH), 127.2 (CH), 128.2 (CH), 128.2 (C_{quat}), 128.3 (C_{quat}), 128.4 (C_{quat}), 128.6 (C_{quat}), 128.7 (CH), 129.3 (CH), 130.55 (CH), 130.6 (CH), 134.2 (C_{quat}), 135.9 (C_{quat}), 144.1 (C_{quat}), 164.2 (C_{quat}), 164.3 (C_{quat}), 164.5 (C_{quat}). IR (ATR): $\tilde{\nu}$ 3051 (w), 3026 (w), 2961 (w), 2928 (w), 2847 (w), 2806 (w), 2770 (w), 1667 (m), 1593 (m), 1526 (m), 1506 (s), 1485 (w), 1445 (m), 1435 (m), 1377 (m), 1366 (m), 1339 (s), 1325 (s), 1298 (m), 1248 (s), 1229 (s), 1167 (s), 1138 (m), 1119 (m), 1078 (s), 1038 (m), 1020 (w), 1001 (m), 988 (s), 961 (m), 924 (m), 903 (m), 885 (w), 870 (m), 847 (w), 814 (m), 802 (w), 770 (s), 731 (s), 700 (s), 681 (s), 656 (s). MALDI-TOF: *m/z* 752.2 ($M+H^+$), 597.2 (M^+-Tos), 561.2 ($C_{34}H_{31}N_3O_3S^+$). HRMS (ESI) calcd. for $C_{49}H_{41}N_3O_3S+H^+$: 752.2941; Found: 752.2941.

[2] Superposition of signals (broadening or overlap).

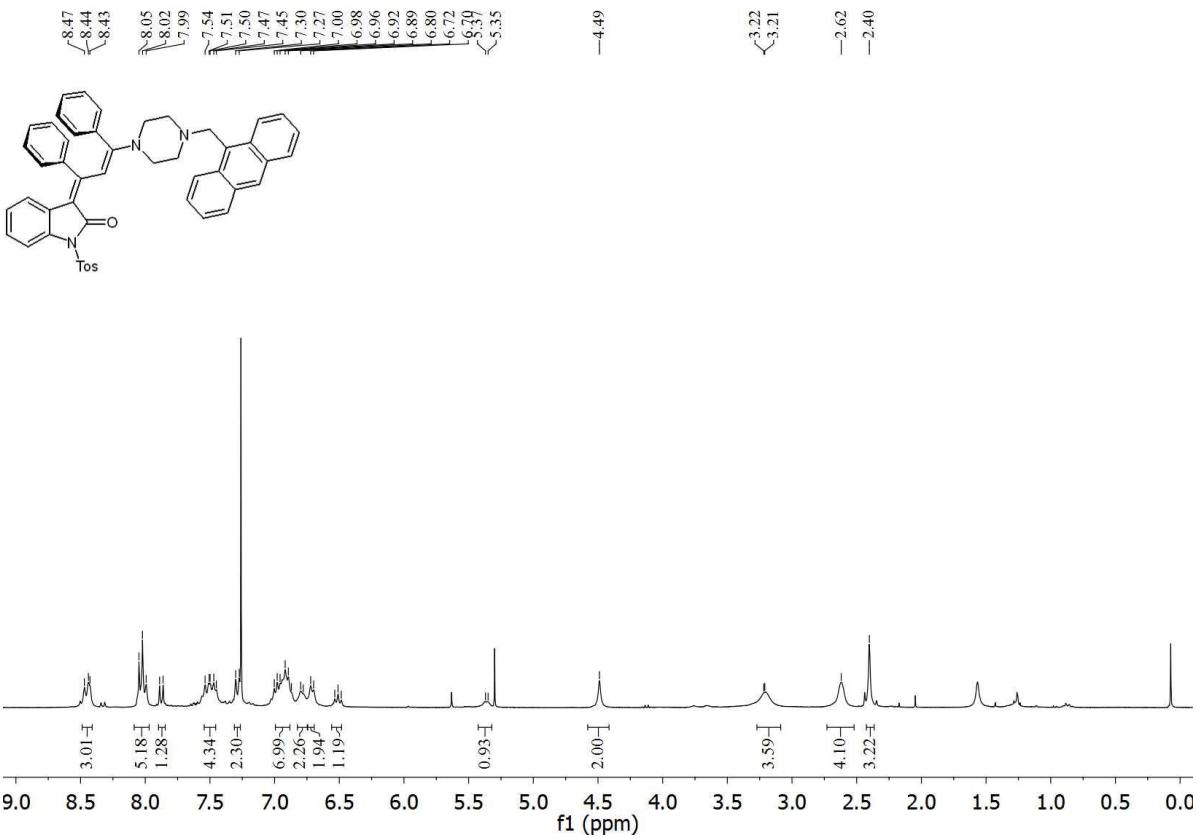

^{1}H NMR spectrum of **4c** ($CDCl_3$, 300 MHz, 293 K).

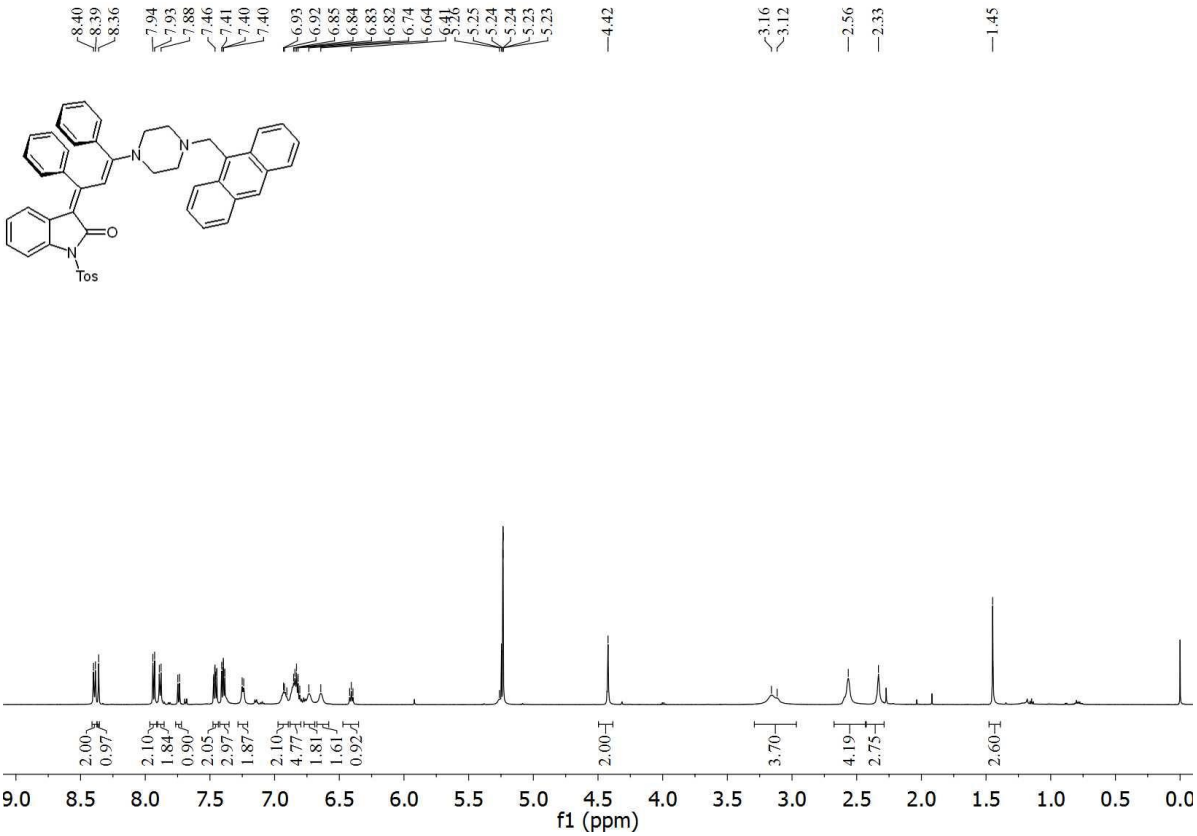

^{1}H NMR spectrum of **4c** (CD_2Cl_2, 600 MHz, 293 K).

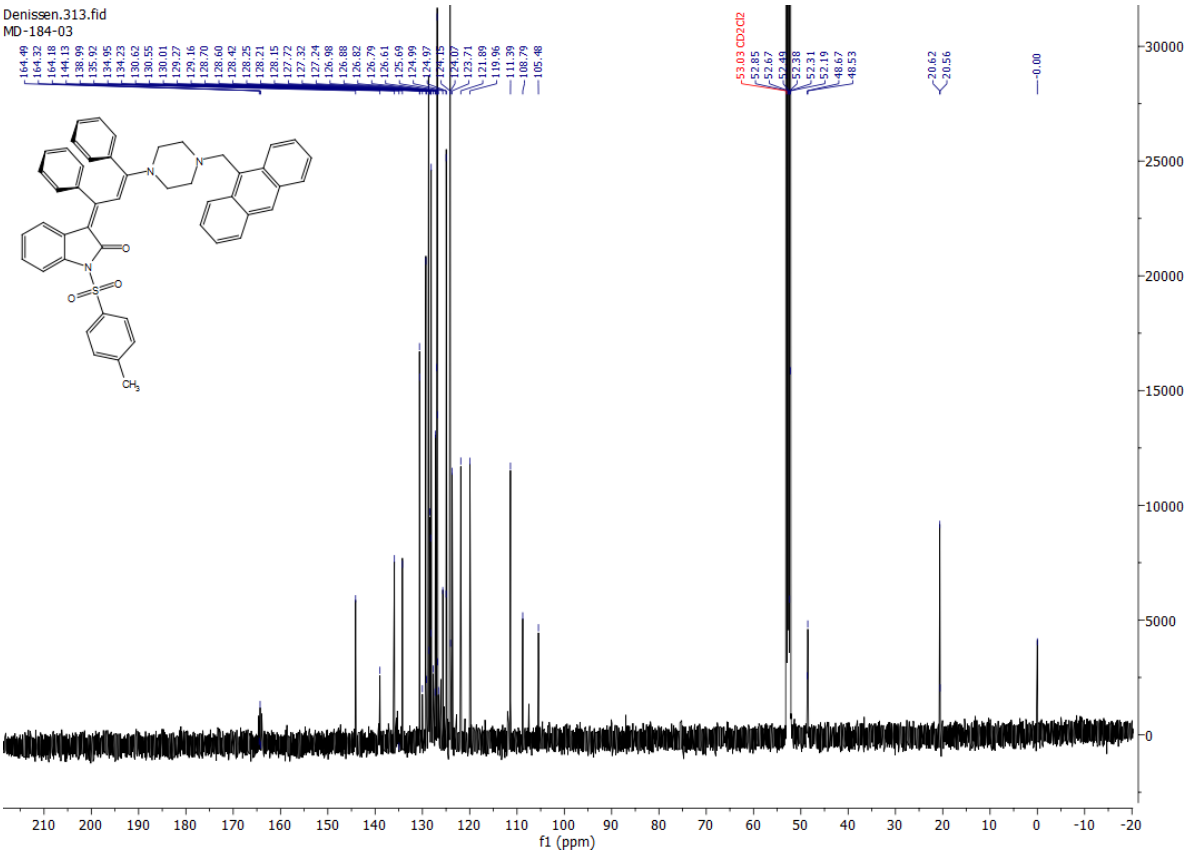

^{13}C NMR spectrum of **4c** ($CDCl_3$, 151 MHz, 293 K).

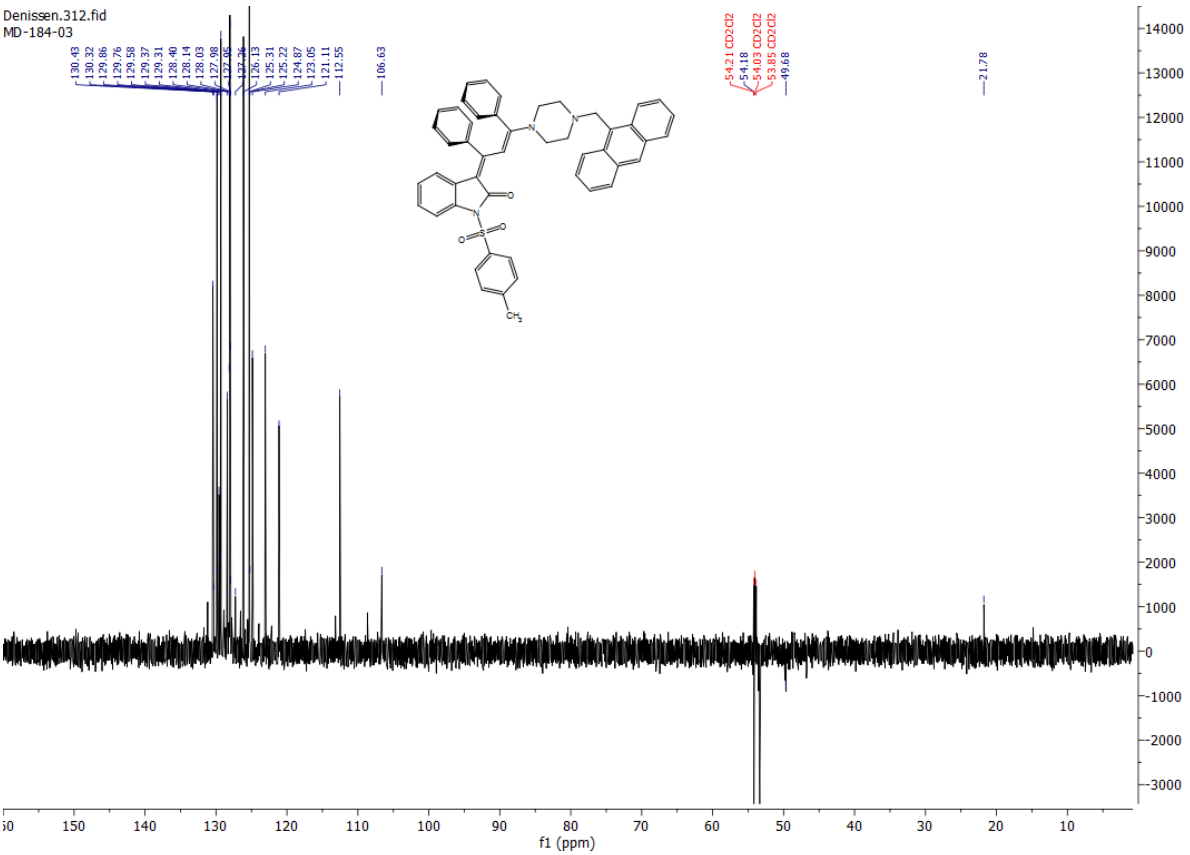

DEPT 135 ^{13}C NMR spectrum of **4c** ($CDCl_3$, 151 MHz, 293 K).

3.4 4-(4-(9*H*-Carbazol-9-yl)phenyl)-piperazin-1-yl)-1,3-diphenylallylidene)-1-tosylindolin-2-one (4d)

According to the GP 3, after chromatography on silica gel (*n*-hexane/ethyl acetate 30:1, *n*-hexane/ethyl acetate/dichloromethane 2:2:7), and after trituration with *n*-hexane or pentane compound **4d** (300 mg, 40 %) was obtained as an orange-red amorphous solid, Mp 233 °C, R_f (dichloromethane): 0.72. ^{1}H NMR (300 MHz, $CDCl_3$): δ 2.43 (s, 3 H), 3.33 (m, br, 4 H), 3.49 (m, br, 4 H), 5.42 (d, *J* = 7.2 Hz, 1 H), 6.53-6.56 (m, 1 H), 6.76 (d, *J* = 6.6 Hz, 2 H), 6.88 (d, *J* = 6.4 Hz, 2 H), 6.92-7.12 (m, 8 H), 7.27-7.48 (m, 11 H), 7.59 (s, 1 H), 7.91 (d, *J* = 8.1 Hz, 1 H), 8.07 (d, *J* = 7.9 Hz, 2 H), 8.15 (d, *J* = 7.3 Hz, 2 H). ^{13}C NMR (75 MHz, $CDCl_3$): δ 32.1 (CH_3), 48.8 (CH_2), 49.1 (CH_2), 107.0, 109.9, 111.6 (C_{quat}), 112.6, 117.1, 119.7, 120.4, 121.3, 123.1, 123.2 (C_{quat}), 123.9, 125.4, 125.9, 127.6, 127.9, 128.0, 128.2, 128.4, 128.7, 129.3, 129.7, 130.3, 135.6 (C_{quat}), 136.2 (C_{quat}), 136.8 (C_{quat}), 139.6 (C_{quat}), 139.7 (C_{quat}), 141.4 (C_{quat}), 141.7 (C_{quat}), 142.8 (C_{quat}), 144.7 (C_{quat}), 149.8 (C_{quat}), 149.9 (C_{quat}), 158.9 (C_{quat}), 164.1 (C_{quat}), 166.0 (C_{quat}). IR (ATR): $\tilde{\nu}$ 2988 (w), 2970 (w), 2901 (w), 1674 (w), 1595 (w), 1508 (s), 1501 (m), 1489 (m), 1452 (m), 1431 (w), 1375 (m), 1342 (m), 1321 (s), 1292 (w), 1227 (s), 1206 (w), 1165 (m), 1138 (w), 1113 (w), 1074 (s), 1013 (m), 961 (w), 932 (m), 905 (w), 858 (w), 812 (w), 772 (m), 748 (s), 725 (m), 689 (m), 660 (m). MALDI-TOF: *m/z* 803.3 ($M+H^+$), 649.3 (M^+-Tos). Anal. calcd. for $C_{52}H_{42}N_4O_3S$ (803.0): C 77.78, H 5.27, N 6.98, S 3.99; Found: C 77.49, H 5.53, N 6.68, S 3.75.

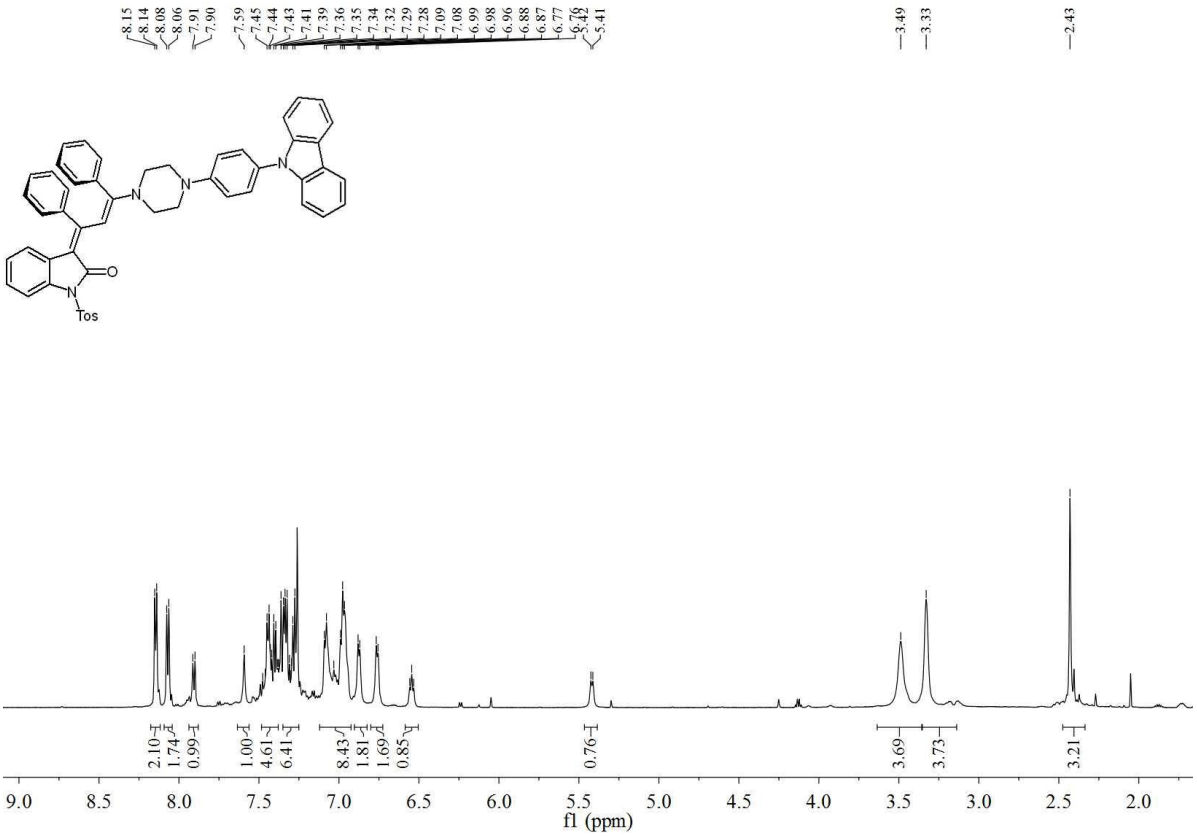

^{1}H NMR spectrum of **4d** ($CDCl_3$, 300 MHz, 293 K).

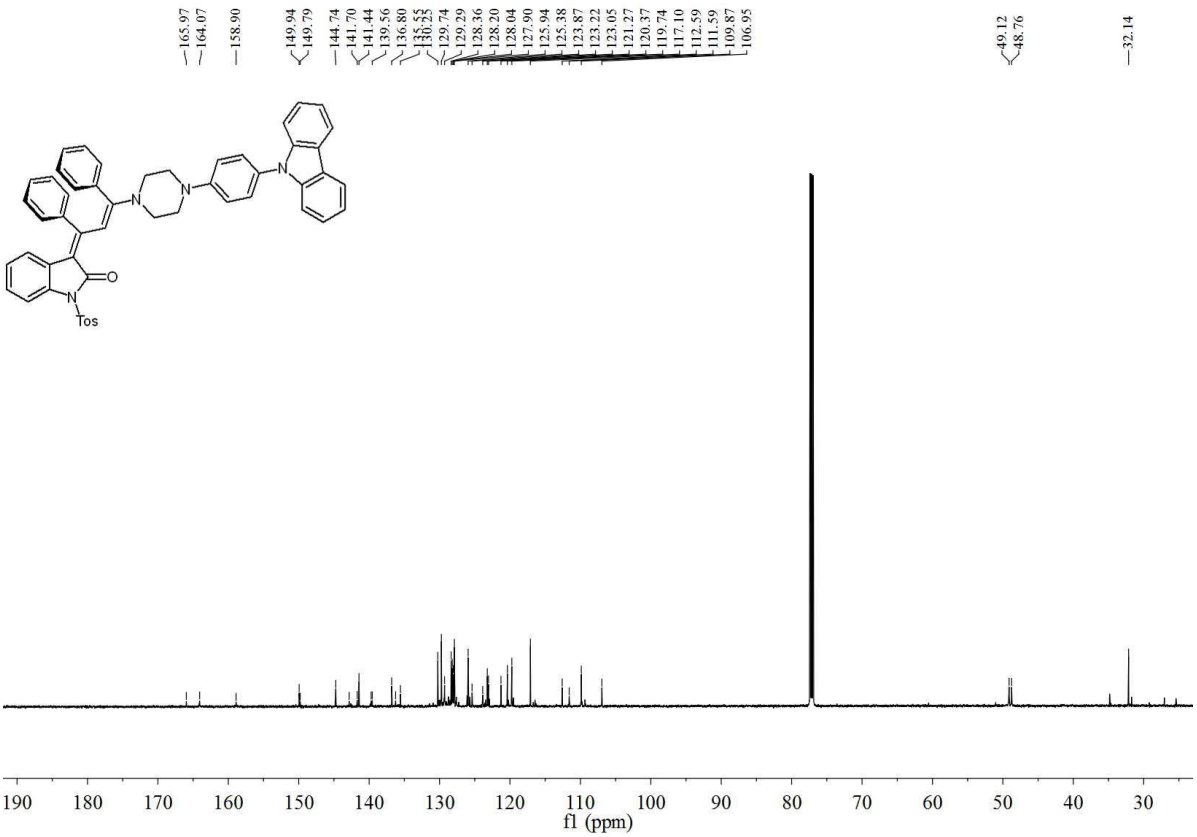

^{13}C NMR spectrum of **4d** ($CDCl_3$, 75 MHz, 293 K).

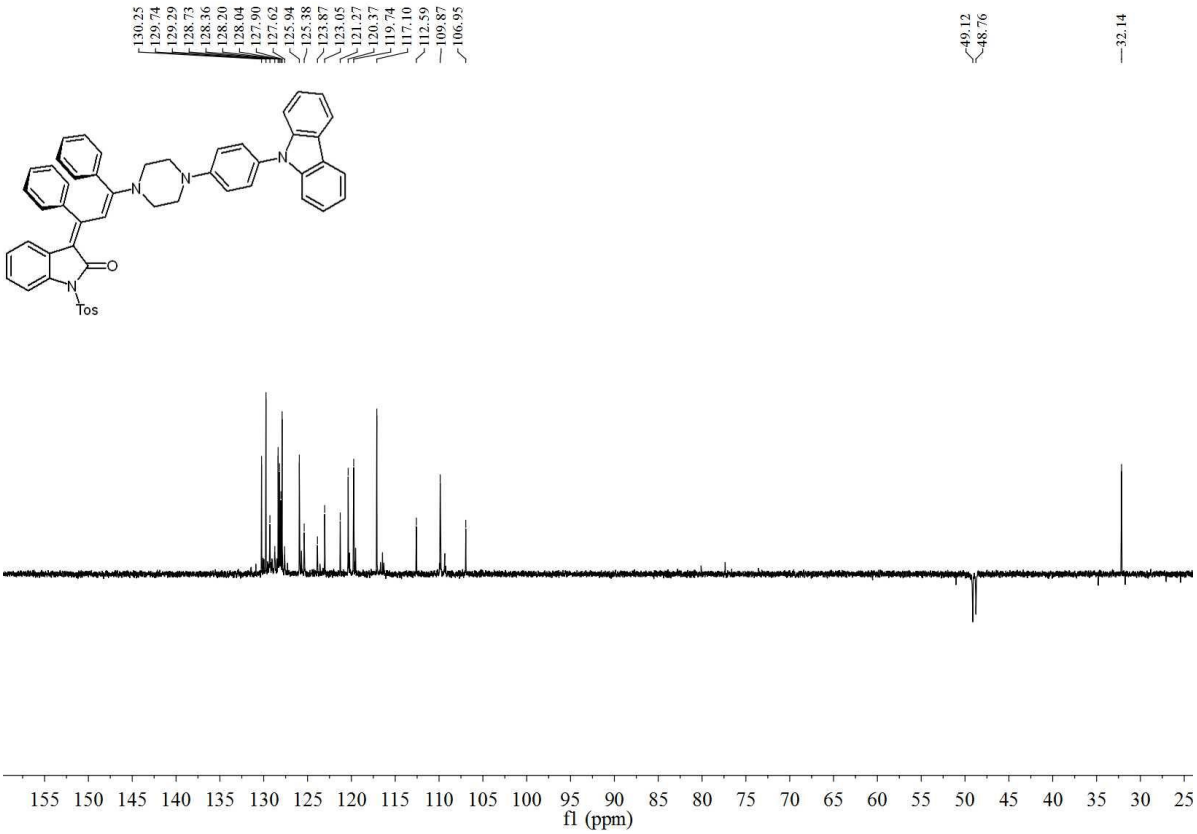

DEPT 135 ^{13}C NMR spectrum of **4d** ($CDCl_3$, 75 MHz, 293 K).

4 Optimization of the Suzuki Coupling

The extension of the three-component synthesis without adaption of the reaction conditions did not lead to the Suzuki coupling product **4e**. Unreacted brominated oxoindole-merocyanine **4i** could be isolated in 35% yield. Subsequently, the brominated oxoindole derivative **4i** was prepared as a key intermediate for the optimization of the Suzuki coupling (Scheme SI-1).

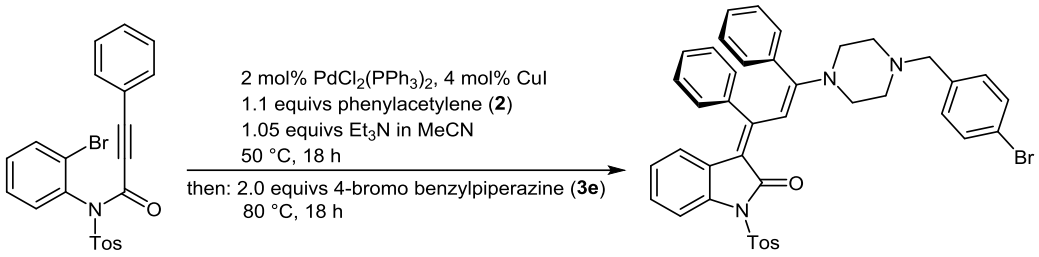

1b **4i** (32%)

Scheme SI-1. Three-component synthesis of the oxoindole-merocyanine **4i**.

(*E*)-3-((*E*)-3-(4-(4-Bromobenzyl)piperazin-1-yl)-1,3-diphenylallyliden)-1-tosylindolin-2-one (4i)

2 mol% (37.7 mg, 0.05 mmol) $PdCl_2(PPh_3)_2$ and 4 mol% (21.4 mg, 0.11 mmol) CuI, dry acetonitrile (9 mL) were placed under nitrogen in Schlenk tube with a magnetic stir bar. *ortho*-Bromo anilide **1b** (1.20 g, 2.64 mmol) were added to the reaction mixture, which was then heated under nitrogen to 50 °C (oil bath) for 10 min. To the warm solution phenylacetylene (**2**) (304 mg, 2.98 mmol) was added under nitrogen. Then, dry triethylamine (281 mg, 2.78 mmol) was added. The reaction mixture was then stirred at 50 °C for 18 h. After cooling to room temp 4-bromobenzylpiperazine (**3e**) (1.35 g, 5.29 mmol) was added under a stream of nitrogen. The mixture was heated to 80 °C (oil bath) for 18 h (the solution turned deep red). After cooling to room temp saturated aqueous ammonium chloride solution (30 mL) and dichloromethane (50 mL) were added. The aqueous layer was extracted with dichloromethane (3 x 25 mL) and the combined organic phases were washed with brine (30 mL) and dried (anhydrous magnesium sulfate). The solvents were removed in vacuo and the residue was absorbed on Celite®. After flash chromatography on silica gel (*n*-hexane/ethyl acetate 20:1, *n*-hexane/dichlormethane 5:1, *n*-hexane/acetone 4:1) the crude product was triturated with pentane and placed in the ultrasound bath. After decantation and drying of the solid compound 4i was (617 mg, 32%) was obtained as an amorphous orange powder, Mp 191 °C, R_f (*n*-hexane/ethyl acetate, 2:1): 0.18.

^{1}H NMR (600 MHz, $CDCl_3$): δ 2.42-2.46 (m, 7 H), 3.27 (br, 4 H), 3.48 (s, 2 H), 5.35 (d, *J* = 7.2 Hz, 1 H), 6.49-6.54 (m, 1 H), 6.71 (d, *J* = 6.6 Hz, 2 H), 6.79 (d, *J* = 6.8 Hz, 2 H), 6.89-7.01 (m, 7 H), 7.19 (d, *J* = 8.3 Hz, 2 H), 7.31 (d, *J* = 8.0 Hz, 2 H), 7.42-7.46 (m, 2 H), 7.48 (s, 1 H), 7.88 (d, *J* = 8.1 Hz, 1 H), 8.04 (d, *J* = 8.3 Hz, 2 H). ^{13}C NMR (75 MHz, $CDCl_3$): δ 21.8 (CH_3), 49.1

(CH_2), 53.0 (CH_2), 62.1 (CH_2), 106.8, 110.6 (C_{quat}), 112.5, 121.0, 121.2 (C_{quat}), 122.9, 125.0, 126.3 (C_{quat}), 127.5, 127.9, 128.1, 128.6, 129.3, 129.7, 130.2, 130.8, 131.6, 135.3 (C_{quat}), 136.3 (C_{quat}), 136.8 (C_{quat}), 136.9 (C_{quat}), 139.9 (C_{quat}), 144.6 (C_{quat}), 159.3 (C_{quat}), 164.7 (C_{quat}), 165.8 (C_{quat}). IR (ATR): $\tilde{\nu}$ 3057 (w), 3020 (w), 2823 (w), 2790 (w), 1672 (m), 1591 (w), 1526 (m), 1503 (s), 1485 (s), 1447 (m),1389 (m), 1368 (s), 1342 (s), 1319 (s), 1296 (m), 1285 (m), 1248 (s), 1236 (s), 1167 (s), 1150 (s), 1128 (s), 1092 (m), 1070 (s), 1043 (m), 995 (s), 959 (m), 941 (w), 924 (m), 905 (m), 866 (m), 849 (m), 833 (s), 814 (s), 795 (m), 770 (s), 739 (s), 727 (m), 702 (s), 689 (s), 658 (s), 646 (m). MALDI-TOF: *m/z* 731 (^{81}Br-M^+, 100), 729 (^{79}Br-M^+, 92), 652 ([M^+ - Br, 4), 576 (^{81}Br-M^+ - $TolSO_2$, 66), 574 (^{79}Br-M^+ - $TolSO_2$, 66). Anal. calcd. for $C_{41}H_{36}BrN_3O_3S$ (729.2): C 67.39, H 4.97, N 5.75, S 4.39; Found: C 67.12, H 5.19, N 5.45, S 4.09.

The optimization of the Suzuki step was performed in acetonitrile by using CsF as a base. Likewise, the effect of a co-solvent (1,4-dioxane) was tested and optimized (Scheme SI-2).

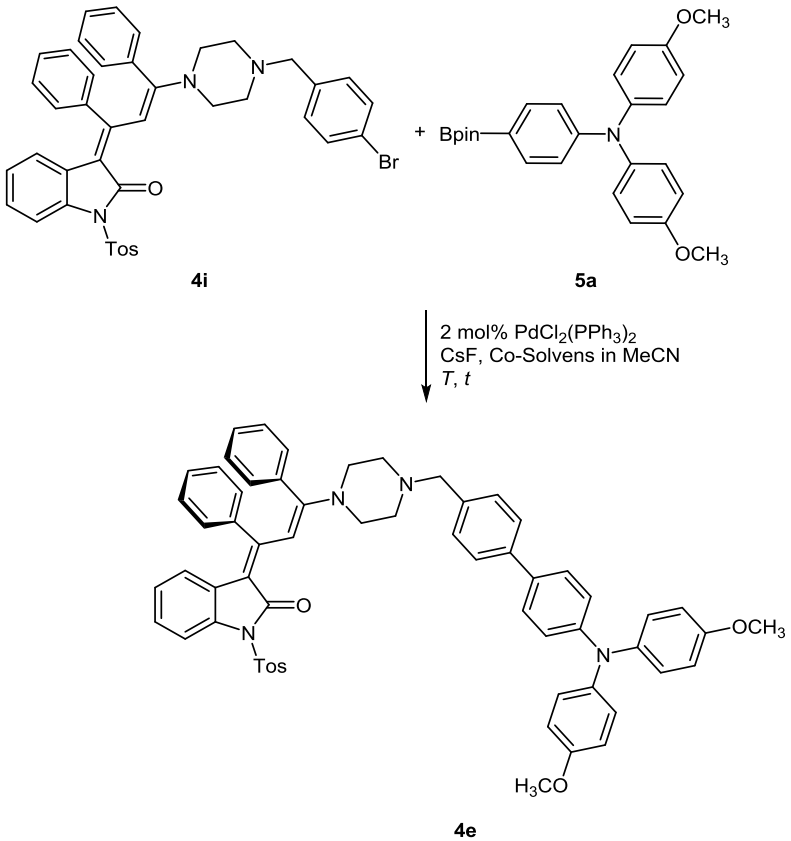

Schema SI-2. Optimization of Suzuki coupling using CsF as a base.

Due to low solubility the addition of 1,4-dioxane was necessary to increase the formation of product **4e** (Table SI-4, see entries 2-7).

Table SI-4. Experimental details of the optimization study using CsF as a base.

Entry	*T* [°C]	*t* [h]	Amount (CsF) [equivs]	*c* (1,4-dioxane) [M]	Yield (**4e**) [%]
1	80	18	3.0	-	42
2	80	18	3.0	0.12	72
3	80	18	8.8	0.12	37
4	120	18	3.0	0.12	59
5	80	48	3.0	0.12	77
6	80	18	3.0	0.06	85
7	80	18	3.0	0.04	56

These optimized reaction conditions of the Suzuki coupling (Table SI-3, entry 6) were implemented into the four-component reaction (Scheme SI-3).

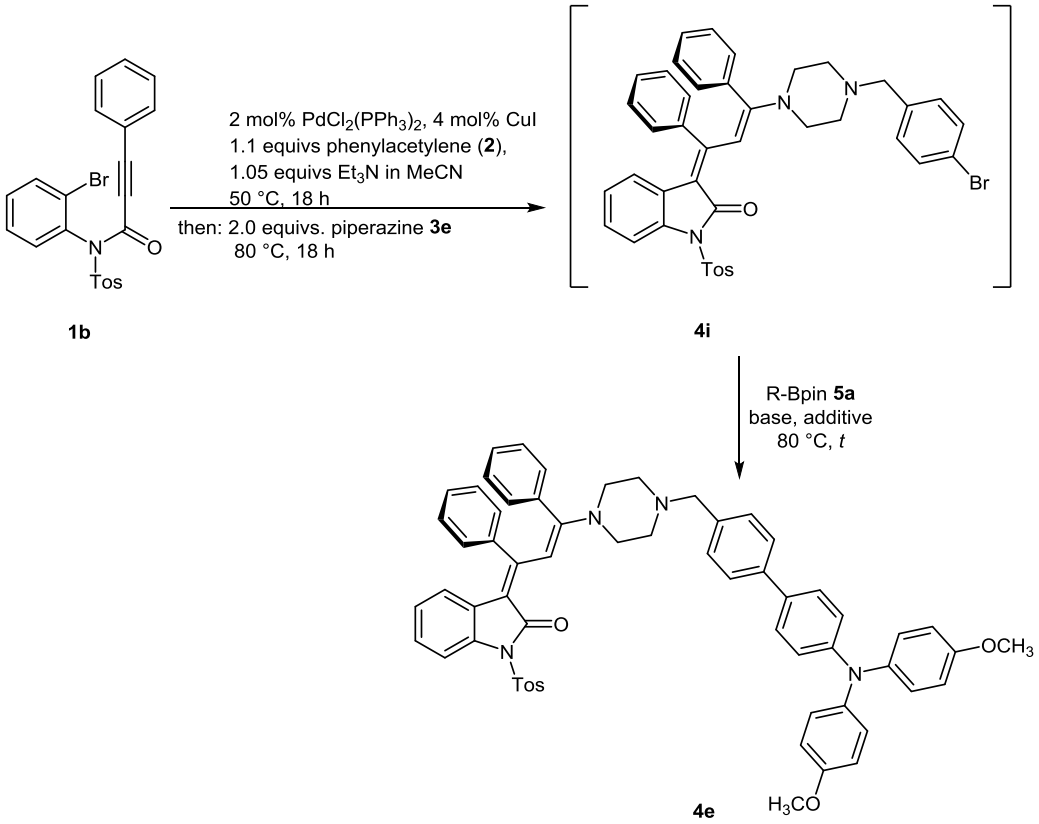

Scheme SI-3. Model reaction for the optimization of the four component synthesis.

The isolated yield of the brominated key intermediate **4i** and the product **4e** showed that the optimized conditions are not suitable in the reaction sequence (Table SI-3, entry 1). Therefore, the four-component synthesis had to be optimized, too. For the optimization the yield of the brominated oxoindole **11** as well as the yield of the product **4e** were monitored (Table SI-5).

Table SI-5. Experimental details of the reaction condition within the four component synthesis.

Entry	Base [equivs]	Additive	*t* [h]	Key intermediate **4i** [%]	Product **4e** [%]	Combined yield [%]
1	CsF (6.0)	-	18	36	11	47
2[a]	CsF (6.0)	-	18	11	4	15
3	CsF (6.0)	20 mol% PPh_3 H_2O	18	17	30	47
4	Cs_2CO_3 (6.0)	20 mol% PPh_3 H_2O	18	31	34	65
5	Cs_2CO_3 (6.0)	20 mol% PPh_3 H_2O	48	26	34	60
6	Cs_2CO_3 (6.0)	20 mol% PPh_3 H_2O TBAB	18	33	26	59
7	Cs_2CO_3 (8.0)	20 mol% PPh_3 H_2O	18	25	29	54

[a]The reaction was performed in a Schlenk flask.

None of the experiments of this optimization study showed a complete conversion of the key intermediate **4i**. The optimized reaction conditions (Table SI-4, entry 4) with respect to the catalytic system, the base, additives and reaction time were used for the optimization of the amount of boronate and base (Table SI-6).

Table SI-6. Additional optimazation of the four-component synthesis.

Entry	Cs_2CO_3 [equivs]	Boronate [equivs]	Key intermediate **4i** [%]	Product **4e** [%]	Combined yield [%]
1	6.0	2.4	31	34	65
2	6.0	6.0	-	50	50
3	12.0	6.0	28	18	46

Using 6.0 equivs of Cs_2CO_3 and boronate **5a** led to full conversion of the key intermediate **4i**. The product **4e** could be isolated in about 50% yield (Table SI-6, entry 2).

5 General Procedure (GP 4) for the Consecutive Four-component Synthesis of 3-Piperazinyl Prop-2-enylidene Indolone Bichromophores 4e-h

In a dry screw-cap Schlenk tube with a magnetic stir bar $PdCl_2(PPh_3)_2$ (3.51 mg, 5.00 μmol) and CuI (1.90 mg, 10.0 μmol) were dissolved in dry acetonitrile (1.75 mL) under nitrogen. Then, *ortho*-bromo anilide **1b** (113 mg, 0.25 mmol) were added and the reaction mixture was stirred at 50 °C (oil bath) for 10 min. Phenylacetylene (**2**) (28.6 mg, 0.28 mmol) and dry triethylamine (25.9 mg, 0.26 mmol) were successively added to the warm reaction mixture and the reaction mixture was stirred under nitrogen at 50 °C for 18 h. After cooling to room temp 4-bromo benzyl piperazine (**3e**) (128 mg, 0.50 mmol) was added under nitrogen and the reaction mixture was stirred under nitrogen at 50 °C for 18 h. After cooling to room temp 1,4-dioxane (1.75 mL), triphenylphosphane (13.1 mg, 50.0 μmol), and deionized water (0.25 mL) were successively added under nitrogen to the reaction mixture. Under vigorous stirring cesium carbonate (489 mg, 1.50 mmol), and after 5 min, pinacolyl boronate **5** (1.50 mmol) were added and the stoppered Schlenk tube was heated to 80 °C for 18 h (for experimental details, see Table SI-7). After cooling to room temp saturated aqueous ammonium chloride solution (10 mL) and dichloromethane (10 mL) was added to the red solution. The organic layer was separated and the aqueous phase was extracted with dichloromethane (3 x 30 mL). The combined organic layers were extracted with brine (15 mL) and dried (anhydrous magnesium sulfate). After filtration the filtrate was absorbed on celite® and purified by flash chromatography on silica gel (*n*-hexane, *n*-hexane/ethyl acetate 20:1, *n*-hexane/dichloromethane 5:1, *n*-hexane/acetone 4:1). The crude product was triturated with *n*-hexane and suspended under ultrasound to give after filtration and drying of insoluble product the analytically pure **4e-h** were obtained as amorphous red solids.

Table SI-7. Experimental details of the consecutive four-component synthesis of oxonol-merocyanine-based bichromophores **4e-h**.

Entry	*ortho*-bromo anilide **1b** [mg] (mmol)	phenylacetylene (**2**) [mg] (mmol)	pinacolyl boronate **5** [mg] (mmol)	bichromophore **4** [mg] (%)
1	113 (0.25)	31.8 (0.31)	646 (1.50) of **5a**	102 (50) of **4e**
2[a]	55 (0.12)	14.5 mg (0.14)	309 (0.72) of **5b**	34.7 (30) of **4f**
3	114 (0.25)	32.7 (0.32)	554 (1.50) of **5c**	104.7 (51) of **4g**
4	113 (0.25)	34.4 (0.33)	556 (1.50) of **5d**	143.8 (64) of **4h**

[a]The reaction was performed with $PdCl_2(PPh_3)_2$ (1.66 mg, 2.00 μmol), CuI (1.04 mg, 5.00 μmol), MeCN (0.85 mL), Et_3N (16.3 mg, 0.16 mmol), 4-$BrC_6H_4CH_2(CH_2CH_2)NH$ (**3e**) (61.2 mg, 0.24 mmol), 1,4-dioxane (0.85 mL), PPh_3 (6.7 mg, 26 μmol), deionized H_2O (0.12 mL), Cs_2CO_3 (235 mg, 0.72 mmol).

5.1 (*E*)-3-((*E*)-3-(4-((4'-(Bis(4-methoxyphenyl)amino)-[1,1'-biphenyl]-4-yl)methyl)piperazin-1-yl)-1,3-diphenylallylidene)-1-tosylindolin-2-one (4e)

According to GP 4 compound **4e** (102 mg, 50%) was obtained as an orange red amorphous solid, Mp 234 °C, R_f (*n*-hexane/acetone, 2:1): 0.30. ^{1}H NMR (600 MHz, $CDCl_3$, 298 K): δ 2.42 (s, 3 H), 2.48 (br, 4 H), 3.31 (br, 4 H), 3.56 (s, 2 H), 3.80 (s, 6 H), 5.34 (d, *J* = 6.9 Hz, 1 H), 6.49-6.51 (m, 1 H), 6.71 (d, *J* = 6.3 Hz, 2 H), 6.80 (d, *J* = 6.3 Hz, 2 H), 6.83-6.85 (m, 4 H), 6.88-6.95 (m, 5 H), 6.97-7.00 (m, 4 H), 7.07-7.10 (m, 4 H), 7.31 (d, *J* = 8.2 Hz, 2 H), 7.33 (d, *J* = 7.2 Hz, 2 H), 7.40 (d, *J* = 8.7 Hz, 2 H), 7.49-7.54 (m, 3 H), 7.88 (d, *J* = 8.2 Hz, 1 H), 8.04 (d, *J* = 8.3 Hz, 2 H). ^{1}H NMR (600 MHz, $CDCl_3$, 267 K):[3] δ 2.42 (s, 3 H), 3.57 (s, 2 H), 3.80 (s, 6 H), 5.27 (d, *J* = 7.5 Hz, 1 H), 6.50-6.53 (m, 1 H), 6.68 (d, *J* = 7.1 Hz, 2 H), 6.79 (d, *J* = 7.2 Hz, 2 H), 6.83-6.85 (m, 4 H), 6.90-6.94 (m, 5 H), 6.98-7.00 (m, 4 H), 7.08-7.11 (m, 4 H), 7.31-7.34 (m, 4 H), 7.39 (d, *J* = 8.7 Hz, 2 H), 7.47 (s, 1 H), 7.50 (d, *J* = 8.1 Hz, 2 H), 7.88 (d, *J* = 8.2 Hz, 1 H), 8.04 (d, *J* = 8.3 Hz, 2 H). ^{1}H NMR (600 MHz, CD_2Cl_2, 298 K): δ 2.43 (s, 3 H), 2.50 (br, 4 H), 3.32 (br, 4 H), 3.56 (s, 2 H), 3.79 (s, 6 H), , 6.48-6.51 (m, 1 H), 6.69-6.75 (m, 2 H), 6.79-6.83 (m, 2 H), 6.84-6.86 (m, 4 H), 6.90-6.95 (m, 7 H), 7.00-7.05 (m, 2 H), 7.06-7.08 (m, 4 H), 7.35 (d, *J* = 8.1 Hz, 4 H), 7.42 (d, *J* = 8.8 Hz, 2 H), 7.49 (s, 1 H), 7.51 (d, *J* = 8.2 Hz, 2 H), 7.83 (d, *J* = 8.1 Hz, 1 H), 7.98 (d, *J* = 8.3 Hz, 2 H).[4] ^{1}H NMR (600 MHz, CD_2Cl_2, 263 K):[5] δ 2.42 (s, 3 H), 3.54 (s, 2 H), 3.77 (s, 6 H), 5.25 (d, *J* = 8.0 Hz, 1 H), 6.46-6.49 (m, 1 H), 6.68 (d, *J* = 7.2 Hz, 2 H), 6.79 (d, *J* = 7.3 Hz, 2 H), 6.83 (d, *J* = 8.9 Hz, 4 H), 6.89-6.93 (m, 7 H), 6.98-7.02 (m, 2 H), 7.05 (d, *J* = 8.9 Hz, 4 H), 7.33-7.35 (m, 4 H), 7.40 (d, *J* = 8.6 Hz, 2 H), 7.46 (s, 1 H), 7.49 (d, *J* = 8.1 Hz, 2 H), 7.82 (d, *J* = 8.2 Hz, 1 H), 7.96 (d, *J* = 8.2 Hz, 2 H). ^{13}C NMR (151 MHz, $CDCl_3$): δ 20.7 (CH_3), 48.0 (CH_2), 51.9 (CH_2), 54.5 (CH_3), 61.3 (CH_2), 105.5 (CH), 111.3 (CH), 113.7 (CH), 119.7 (CH), 119.8 (CH), 121.7 (CH), 123.7 (C_{quat}), 125.2 (C_{quat}), 125.3 (C_{quat}), 125.6 (CH),[2] 126.4 (CH), 126.7 (CH), 126.7 (CH), 127.0 (C_{quat}), 127.4 (C_{quat}), 128.2 (C_{quat}), 128.5 (CH), 128.5 (CH), 129.0 (CH), 131.6 (C_{quat}), 134.1 (C_{quat}), 135.7 (C_{quat}), 138.8 (C_{quat}), 139.9 (C_{quat}), 143.4 (C_{quat}), 147.1 (C_{quat}), 154.9 (C_{quat}), 158.2 (C_{quat}), 164.7 (C_{quat}). IR (ATR): $\tilde{\nu}$ 2985 (w), 2970 (w), 2901 (w), 1674 (w), 1640 (w), 1595 (w), 1570 (m), 1563 (m), 1506 (s), 1489 (m), 1452 (m), 1380 (m), 1348 (m), 1321 (w), 1296 (w), 1287 (w), 1244 (s), 1233 (m), 1157 (m), 1153 (w), 1138 (w), 1078 (s), 1028 (m), 989 (w), 902 (w), 829 (w), 816 (m), 797 (w), 772 (m), 745 (w), 698 (w), 689 (m), 660 (m). MALDI-TOF: *m/z* 954.4 (M^+), 801.4 (M^+-Tos). Anal. calcd. for $C_{61}H_{54}N_4O_5S$ (954.4): C 76.70, H 5.70, N 5.87, S 3.36; Found: C 76.40, H 5.90, N 5.65, S 3.65.

[3] Piperazine protons cannot be resolved.
[4] One proton is superimposed by the signal of the deuterated solvent (CD_2Cl_2).
[5] Piperazine protons cannot be resolved.

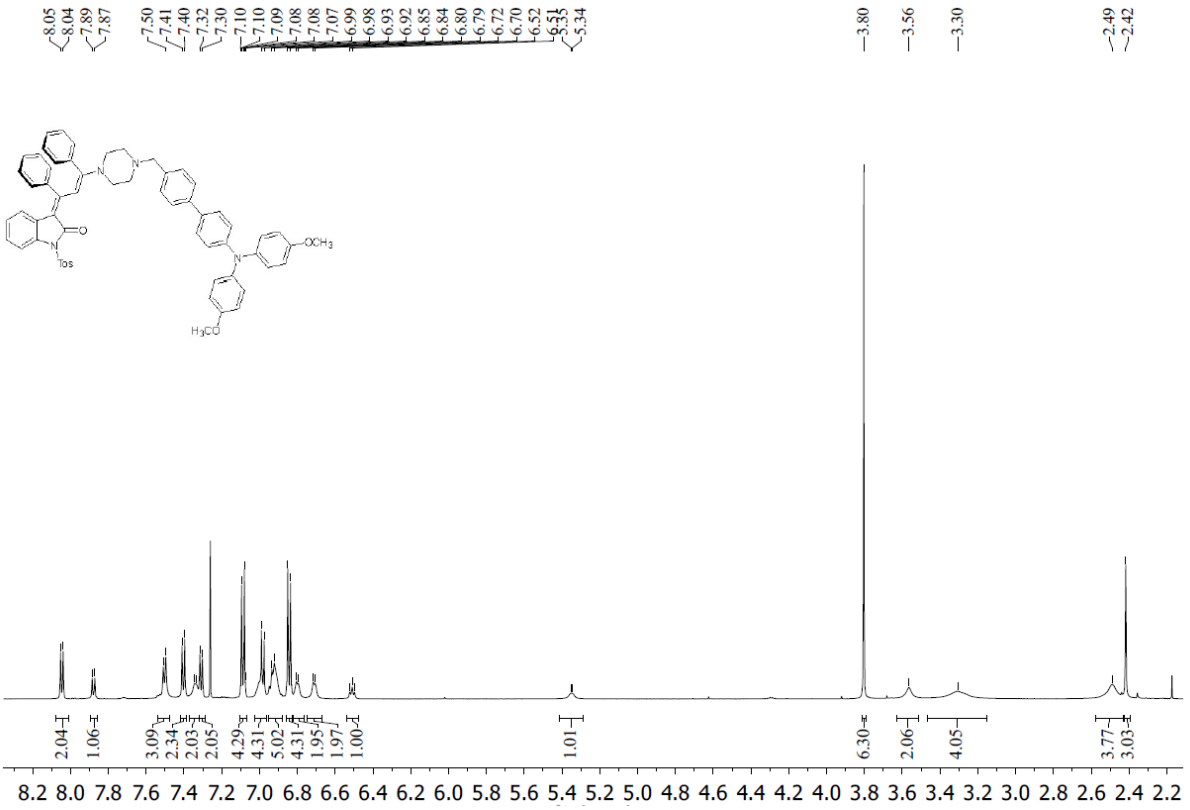

^{1}H NMR spectrum of **4e** ($CDCl_3$, 600 MHz, 298 K).

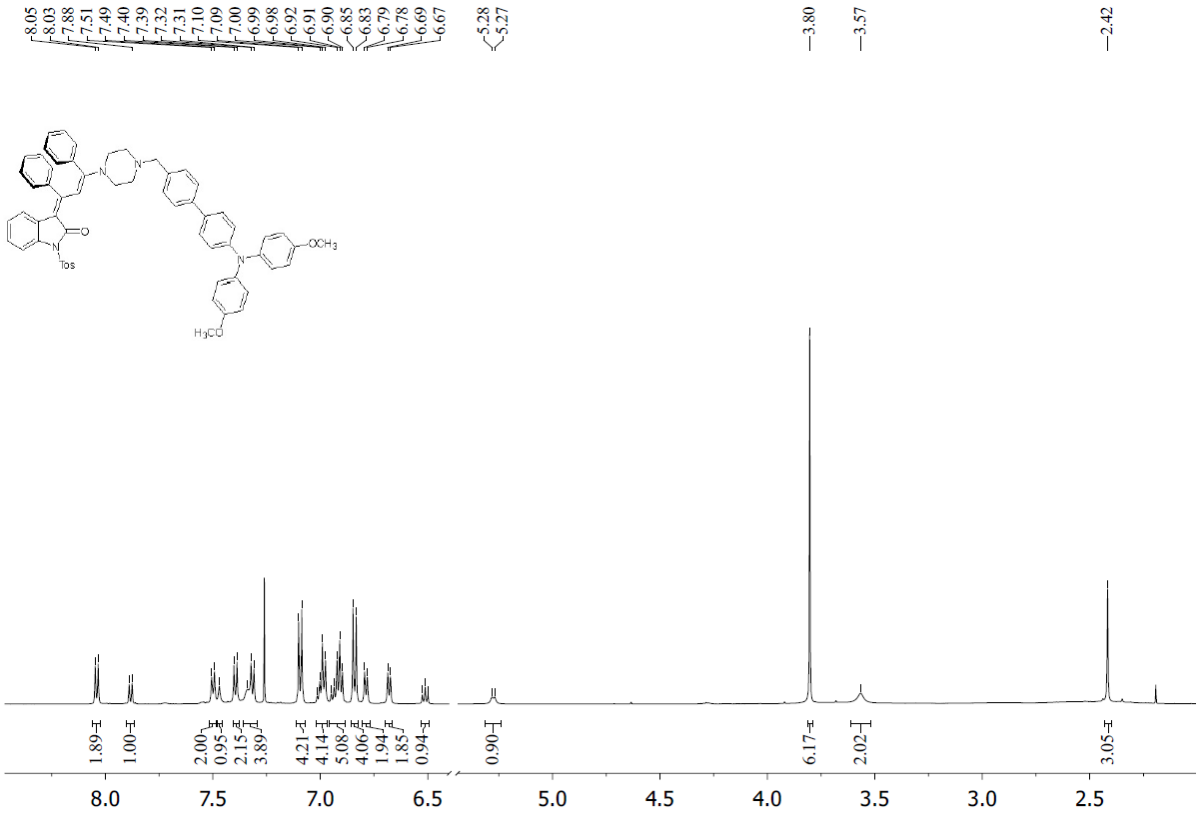

^{1}H NMR spectrum of **4e** ($CDCl_3$, 600 MHz, 263 K).

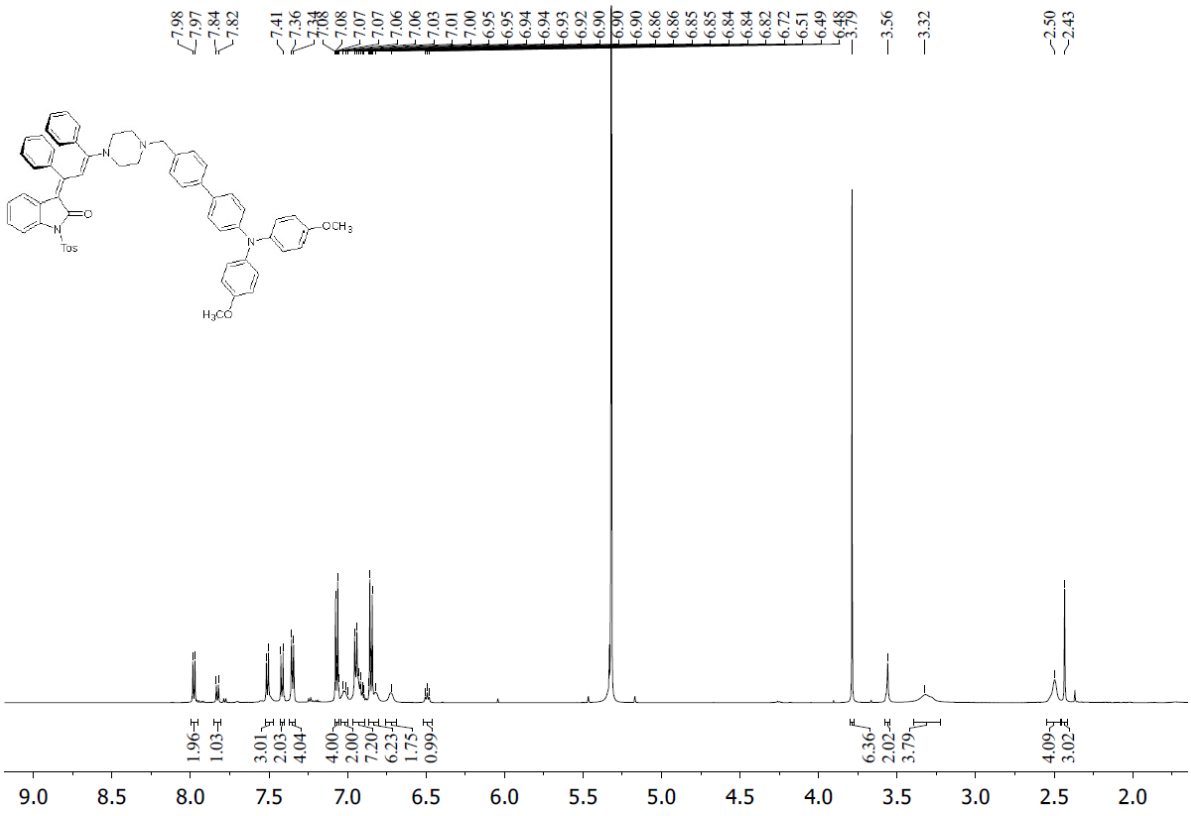

^{1}H NMR spectrum of **4e** (CD_2Cl_2, 600 MHz, 298 K).

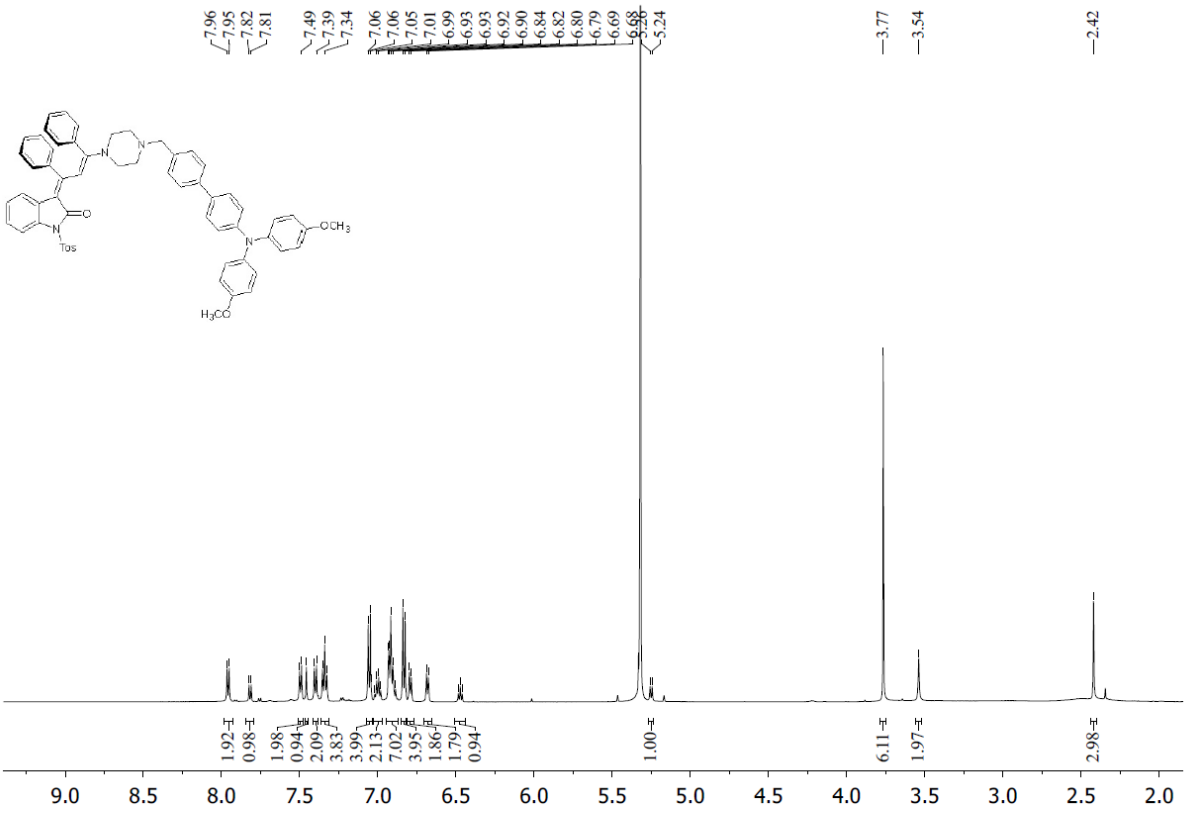

^{1}H NMR spectrum of **4e** (CD_2Cl_2, 600 MHz, 263 K).

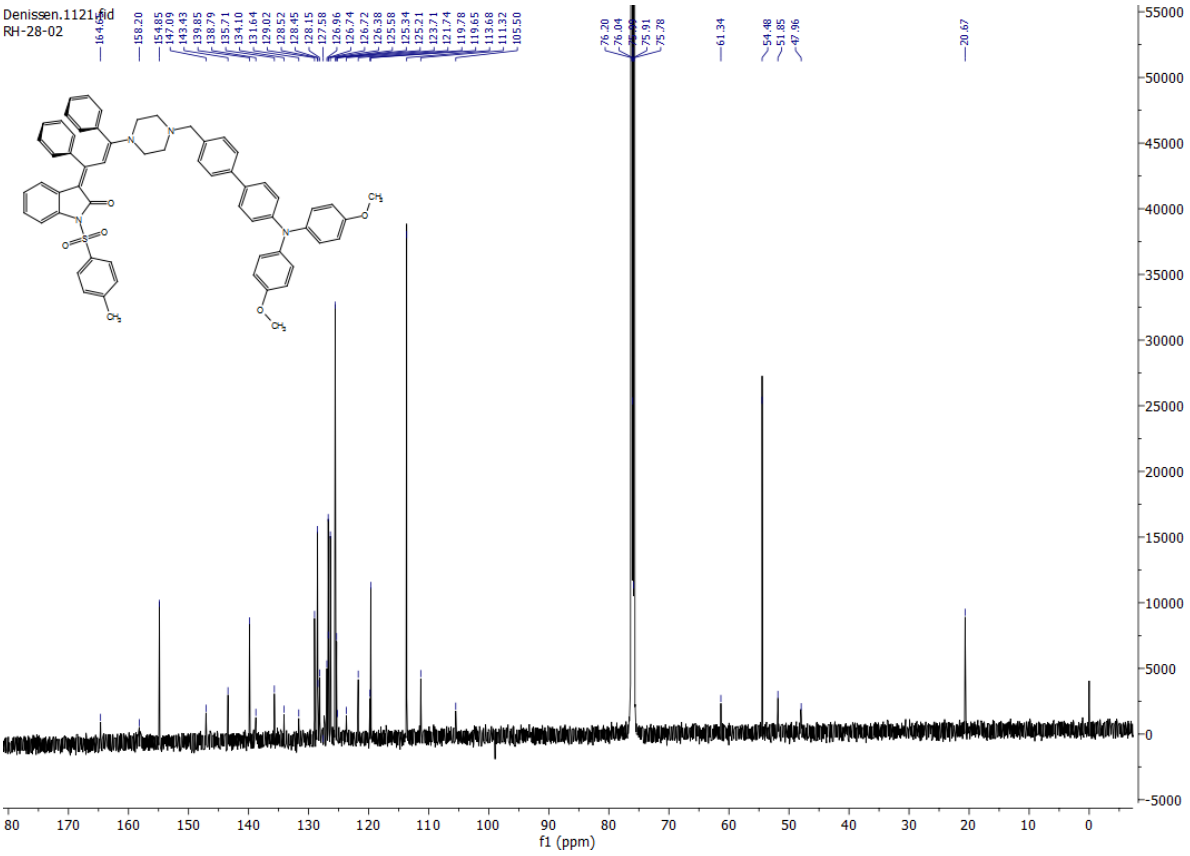

^{13}C NMR spectrum of **4e** ($CDCl_3$, 151 MHz, 293 K).

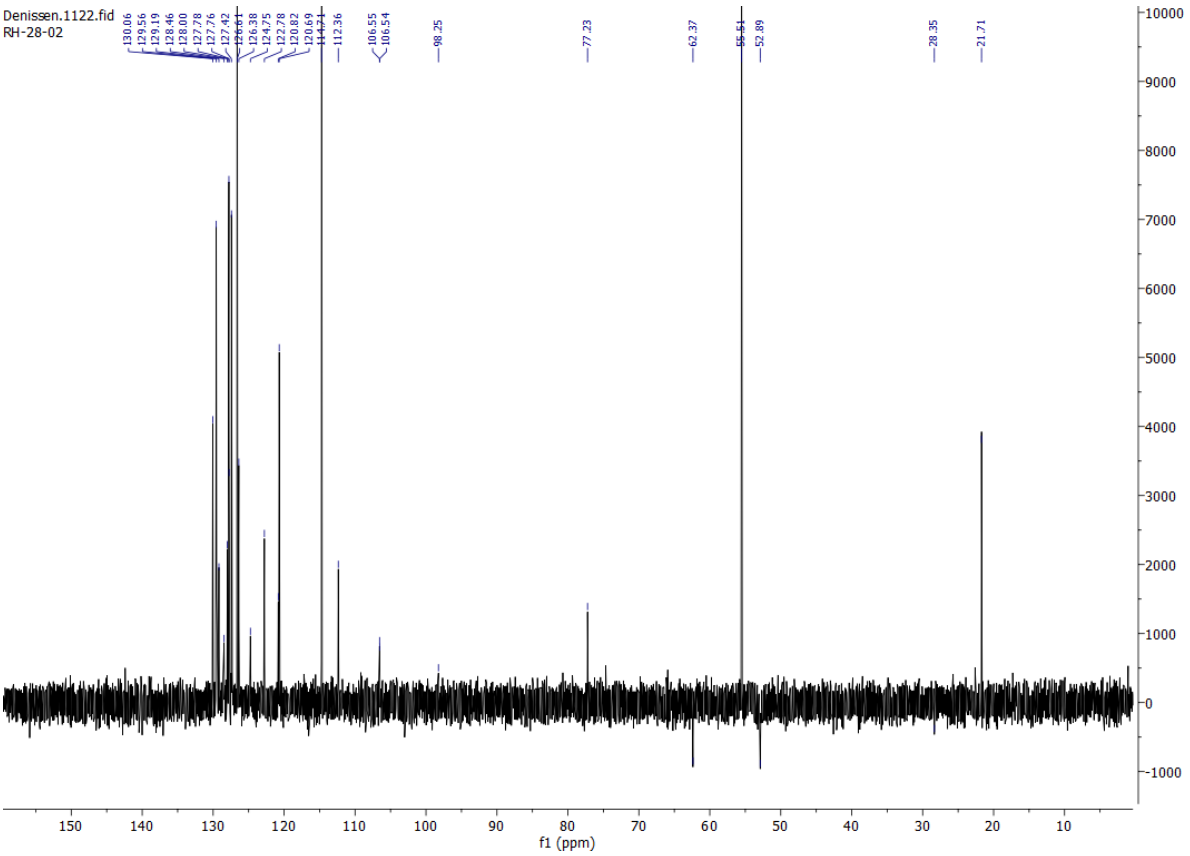

DEPT 135 ^{13}C NMR spectrum of **4e** ($CDCl_3$, 151 MHz, 293 K).

5.2 (*E*)-3-((*E*)-3-(4-((4'-(3,6-Dimethoxy-9H-carbazol-9-yl)-[1,1'-biphenyl]-4-yl)methyl)piperazin-1-yl)-1,3-diphenylallylidene)-1-tosylindolin-2-one (4f)

According to GP 4, after chromatography on silica gel (*n*-hexane/ethyl acetate 20:1, *n*-hexane/ dichloromethane 5:1, *n*-hexane/ acetone 4:1) and trituration with *n*-hexane or pentane compound **4f** (34.7 mg, 30 %) was obtained as a red to black amorphous solid, Mp 235 °C. R_f (*n*-hexane:acetone, 2:1): 0.08. ^{1}H NMR (600 MHz, $CDCl_3$, 298 K): δ 2.42 (s, 3 H), 2.54 (m, br, 3 H), 3.35 (m, br, 3 H), 3.63 (m, br, 2 H), 3.94 (s, 2 H), 3.96 (s, 6 H), 5.39 (m, br, 1 H), 6.50-6.55 (m, 1 H), 6.73 (d, *J* = 7.0 Hz, 2 H), 6.81 (d, *J* = 7.0 Hz, 2 H), 6.91-7.02 (m, 6 H), 7.06 (dd, *J* = 8.9, 2.5 Hz, 2 H), 7.32 (d, *J* = 8.1 Hz, 2 H), 7.40 (d, *J* = 8.9 Hz, 4 H), 7.43-7.52 (m, 1 H), 7.57 (d, *J* = 2.4 Hz, 2 H), 7.60-7.67 (m, 5 H), 7.78 (d, *J* = 8.5 Hz, 2 H), 7.88 (d, *J* = 8.1 Hz, 1 H), 8.05 (d, *J* = 8.3 Hz, 2 H). ^{1}H NMR (600 MHz, $CDCl_3$, 263 K): δ aliphatic protons see ^{1}H NMR at 298 K, 5.46 (d, *J* = 8.1 Hz, 1 H), 6.47-6.61 (m, 1 H), 6.64-6.75 (m, 2 H), 6.80 (d, *J* = 6.3 Hz, 2 H), 6.93-7.02 (m, 6 H), 7.05 (dd, *J* = 8.9, 2.4 Hz, 2 H), 7.29-7.41 (m, 3 H), 7.43 (d, *J* = 8.8 Hz, 4 H), 7.53 (d, *J* = 8.1 Hz, 1 H), 7.56 (d, *J* = 2.3 Hz, 2 H), 7.63-7.68 (m, 4 H), 7.76-7.77 (m, 2 H), 7.89 (d, *J* = 8.1 Hz, 1 H), 8.05 (d, *J* = 8.2 Hz, 2 H). ^{13}C NMR (75 MHz, $CDCl_3$) δ 21.7 (CH_3), 41.3 (CH_2), 53.0 (CH_2),[2] 56.1 (CH_3), 102.9 (CH),[2] 105.7 (C_{quat}), 107.8 (C_{quat}), 110.8 (CH),[2] 112.4 (C_{quat}), 115.2 (CH),[2] 123.7 (CH), 126.9 (CH),[2] 127.8 (CH),[2] 128.0 (CH),[2] 128.3 (CH), 129.2 (C_{quat}), 129.6 (CH),[2] 130.0 (CH),[2] 133.1 (C_{quat}), 136.2 (CH),[2] 144.9 (C_{quat}), 152.5 (C_{quat}), 154.1 (C_{quat}), 177.1 (C_{quat}). IR (ATR): $\tilde{\nu}$ 3160 (w), 3075 (w), 2959 (w), 2922 (w), 1667 (m), 1593 (w), 1560 (m), 1510 (m), 1487 (s), 1467 (s), 1439 (m), 1391 (m), 1375 (m), 1350 (s), 1321 (m), 1296 (m), 1248 (s), 1236 (s), 1207 (s), 1180 (s), 1151 (s), 1132 (m), 1107 (s), 1078 (s), 1022 (m), 1001 (m), 962 (m), 924 (m), 903 (m), 868 (m), 858 (m), 835 (s), 802 (s), 790 (s), 770 (m), 748 (m), 689 (s), 660 (s), 646 (m). MALDI-TOF: *m/z* 953.4 ($M+H^+$), 799.3 (M^+-Tos). Anal. calcd. for $C_{61}H_{52}N_4O_5S$ (952.4): C 76.87, H 5.50, N 5.88, S 3.36; Found: C 77.05, H 5.75, N 5.96, S 3.38.

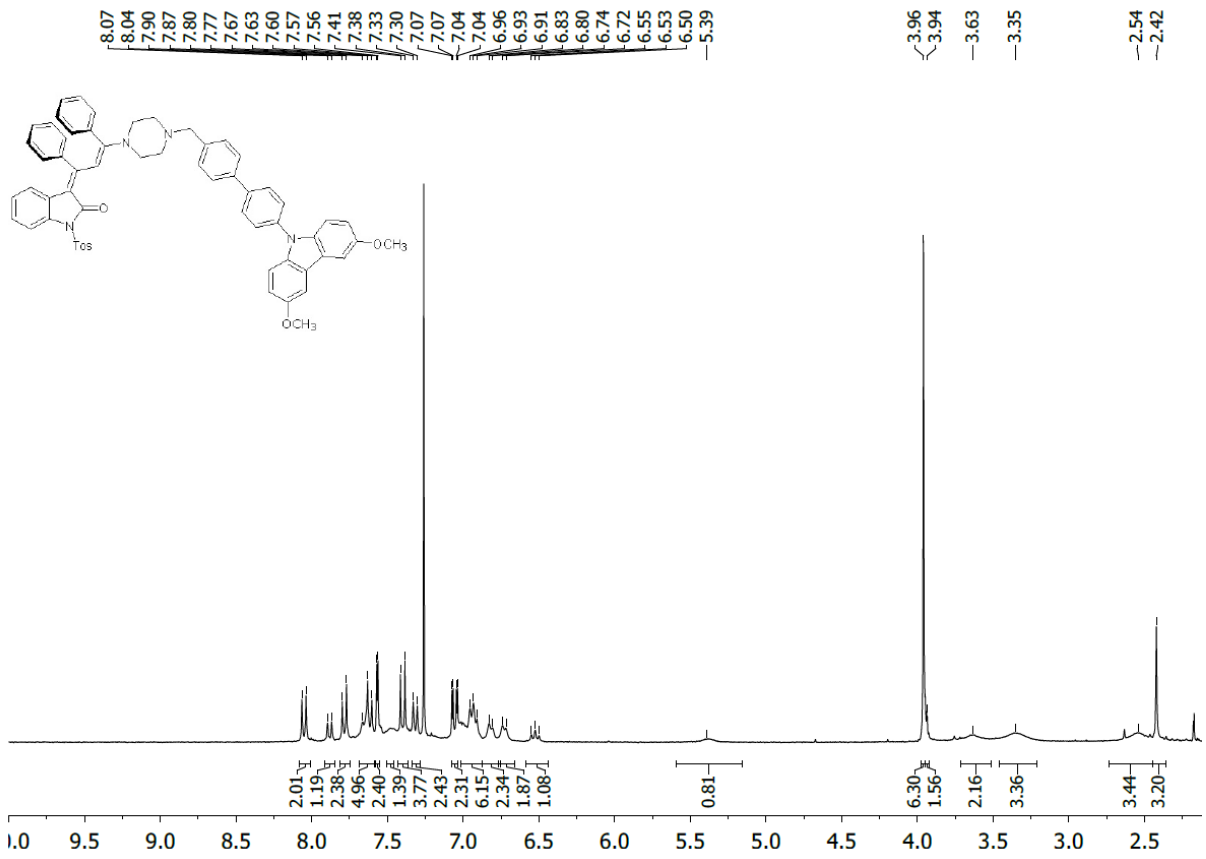

^{1}H NMR spectrum of **4f** ($CDCl_3$, 600 MHz, 298 K).

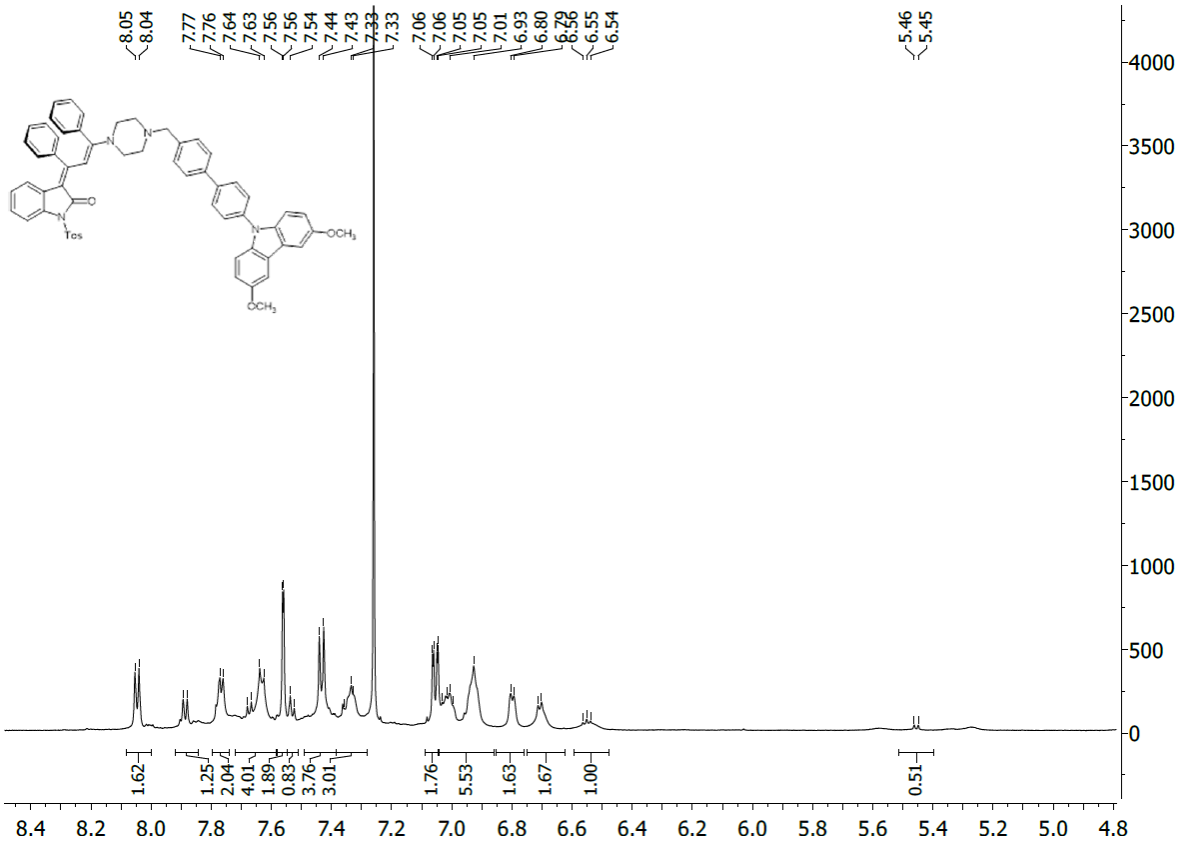

^{1}H NMR spectrum of **4f** ($CDCl_3$, 600 MHz, 263 K).

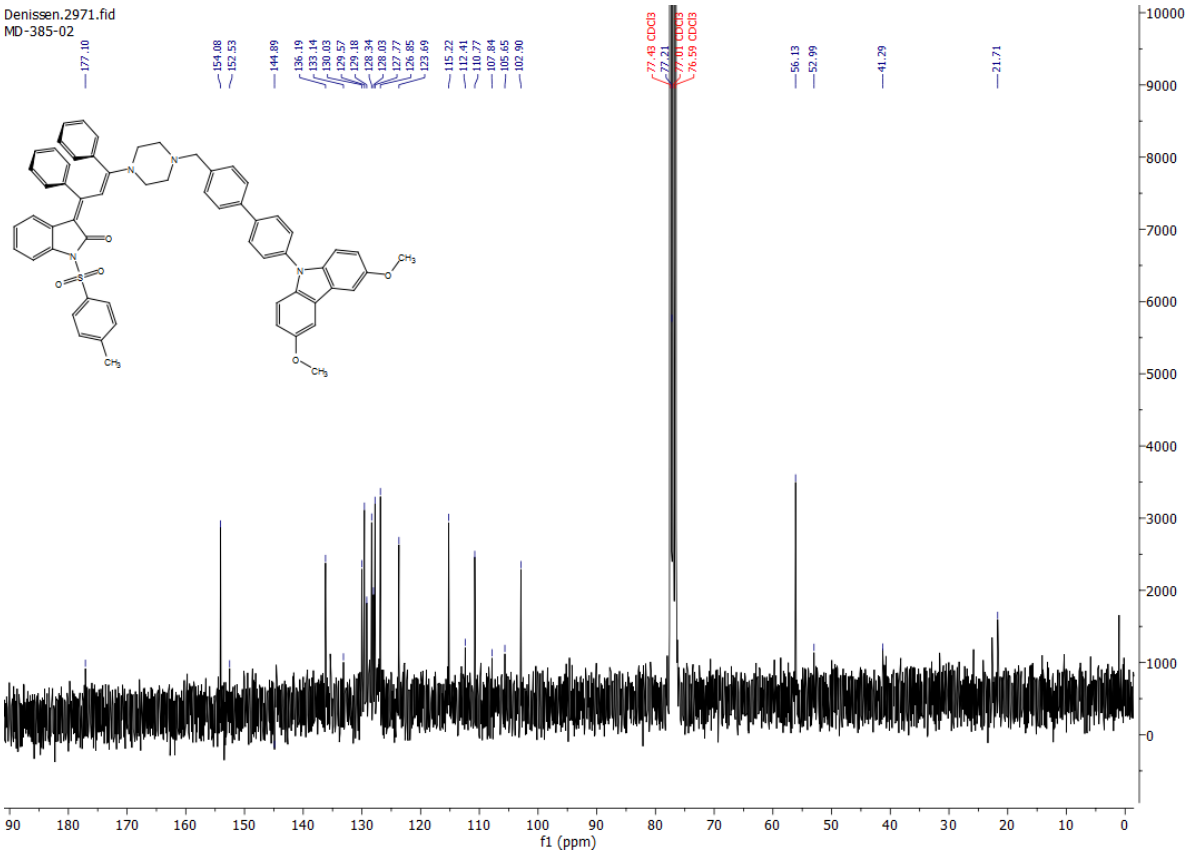

^{13}C NMR spectrum of **4f** ($CDCl_3$, 75 MHz, 293 K).

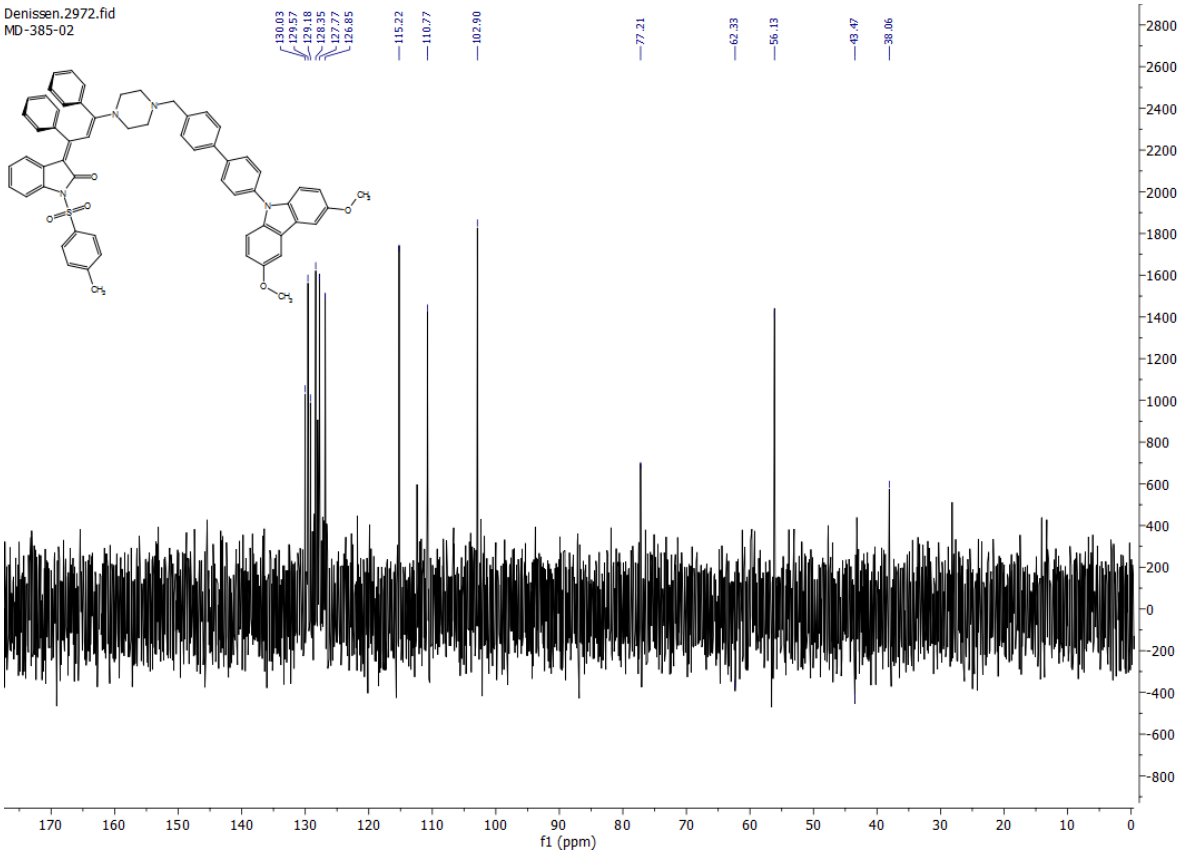

DEPT 135 ^{13}C NMR spectrum of **4f** ($CDCl_3$, 75 MHz, 293 K).

5.3 (*E*)-3-((*E*)-3-(4-((4'-(9*H*-Carbazol-9-yl)-[1,1'-biphenyl]-4-yl)methyl)piperazin-1-yl)-1,3-diphenylallylidene)-1-tosylindolin-2-one (4g)

According to the GP 4, after chromatography on silica gel (*n*-hexane/ethyl acetate 20:1, *n*-hexane/ dichloromethane 5:1, *n*-hexane/acetone 4:1) and trituration with *n*-hexane or pentane compound **4g** (105 mg, 51 %) was obtained as a red to black amorphous solid, Mp 153 °C. R_f (*n*-hexane/acetone, 2:1): 0.17. ^{1}H NMR (600 MHz, $CDCl_3$, 298 K): δ 2.42 (s, 3 H), 2.53 (m, br, 4 H), 3.33 (m, br, 3 H), 3.63 (s, 2 H), 3.76-3.89 (m, br, 1 H), 5.36 (s, 1 H), 6.51-6.53 (m, 1 H), 6.70 (d, *J* = 7.4 Hz, 2 H), 6.81 (d, *J* = 7.3 Hz, 2 H), 6.90-7.01 (m, 6 H), 7.29-7.32 (m, 4 H), 7.42-7.49 (m, 8 H), 7.64-7.67 (m, 4 H), 7.80-7.82 (m, 2 H), 7.89 (d, *J* = 8.2 Hz, 1 H), 8.06 (d, *J* = 8.2 Hz, 1 H), 8.16 (d, *J* = 7.7 Hz, 1 H). ^{1}H NMR (600 MHz, $CDCl_3$, 263 K): δ aliphatic protons see ^{1}H NMR at 298 K, 5.29 (s, 1 H), 6.52-6.54 (m, 1 H), 6.70 (d, *J* = 7.4 Hz, 2 H), 6.81 (d, *J* = 7.3 Hz, 2 H), 6.91-6.94 (m, 3 H), 6.95 (dd, *J* = 8.3, 7.7 Hz, 1 H), 7.00 (d, *J* = 7.6 Hz, 1 H), 7.02 (d, *J* = 7.6 Hz, 1 H), 7.31 (d, *J* = 7.5 Hz, 2 H), 7.32 (d, *J* = 7.6 Hz, 2 H), 7.43-7.46 (m, 4 H), 7.49-7.52 (m, 4 H), 7.65-7.66 (m, 4 H), 7.80-7.82 (m, 2 H), 7.89 (d, *J* = 8.2 Hz, 1 H), 8.05 (d, *J* = 8.2 Hz, 2 H), 8.18 (d, *J* = 7.7 Hz, 2 H). ^{13}C NMR (151 MHz, $CDCl_3$) δ 21.7 (CH_3), 49.1 (CH_2),[6] 52.9 (CH_2),6 109.8 (CH),[2] 112.4 (C_{quat}), 117.1 (C_{quat}), 120.0 (CH),[2] 120.3 (CH),[2] 120.4 (C_{quat}), 122.8 (C_{quat}), 123.4 (CH), 124.8 (C_{quat}), 126.0 (CH),[2] 127.1 (C_{quat}), 127.4 (CH),[2] 127.4 (C_{quat}), 127.8 (CH),[2] 128.0 (C_{quat}), 128.4 (CH),[2] 128.5 (C_{quat}), 129.2 (C_{quat}), 129.6 (CH),[2] 130.1 (CH),[2] 132.4 (C_{quat}), 133.6 (C_{quat}), 136.8 (C_{quat}), 140.9 (CH),[2] 144.5 (C_{quat}), 149.5 (C_{quat}), 165.8 (C_{quat}). MALDI-TOF: *m/z* 892.3 (M^+), 739.3 (M^+-Tos). HRMS (ESI) Anal. calcd. for $[C_{59}H_{48}N_4O_3S+H]^+$: 893.3520; Found: 893.3520.

[6] Not resolved due to line broadening

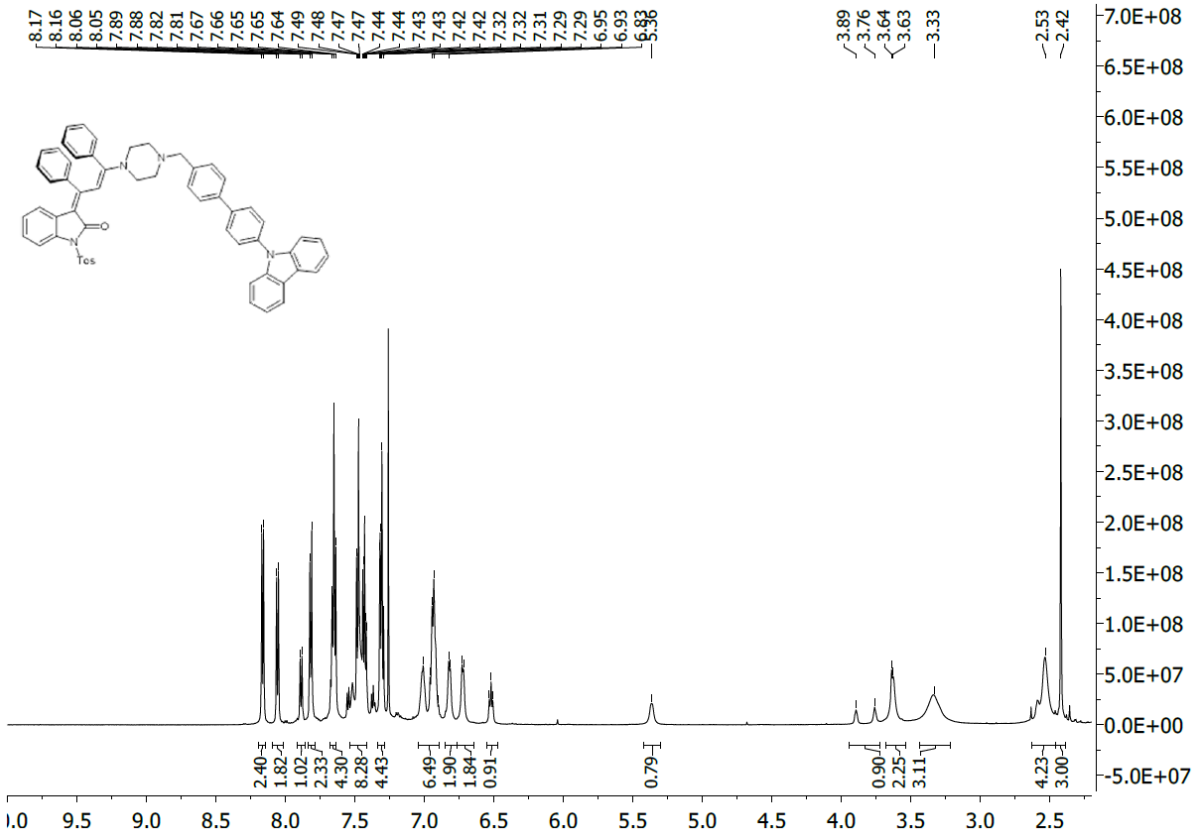

^{1}H NMR spectrum of **4g** ($CDCl_3$, 600 MHz, 298 K).

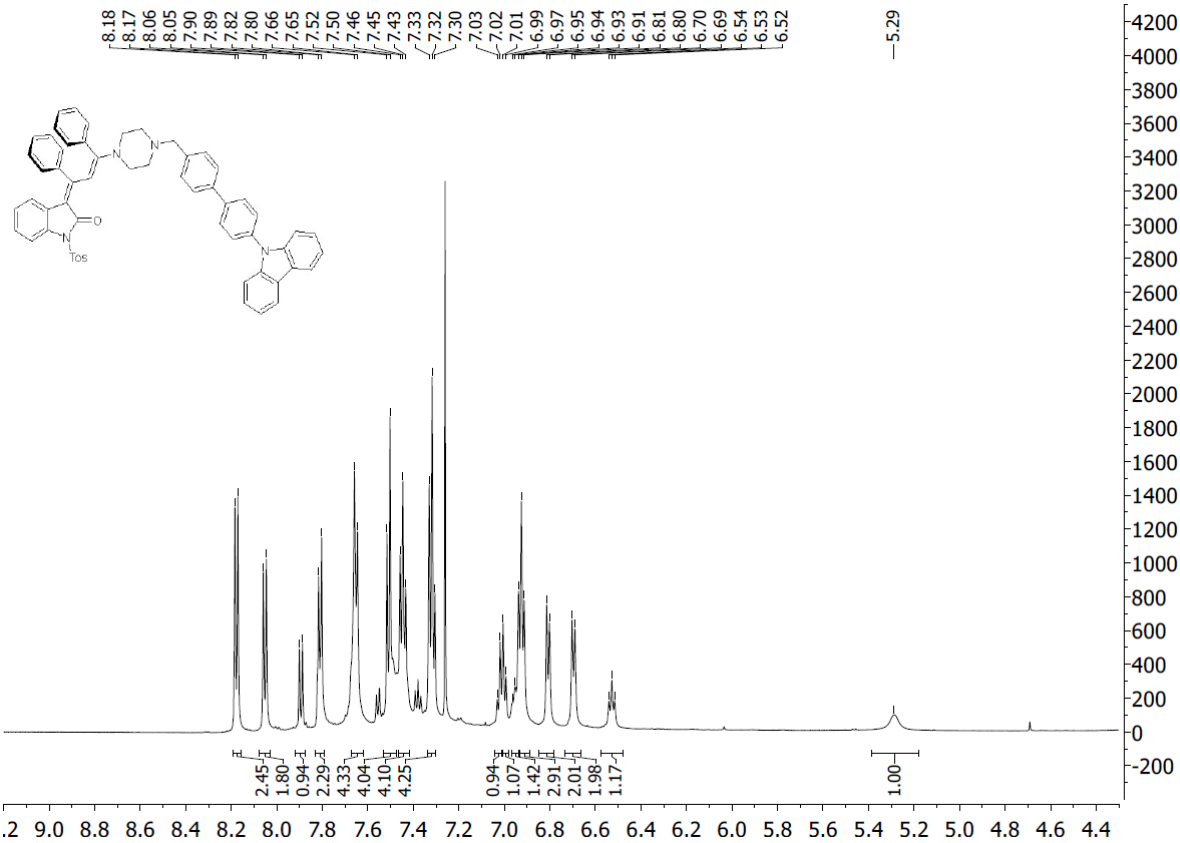

^{1}H NMR spectrum of **4g** ($CDCl_3$, 600 MHz, 263 K).

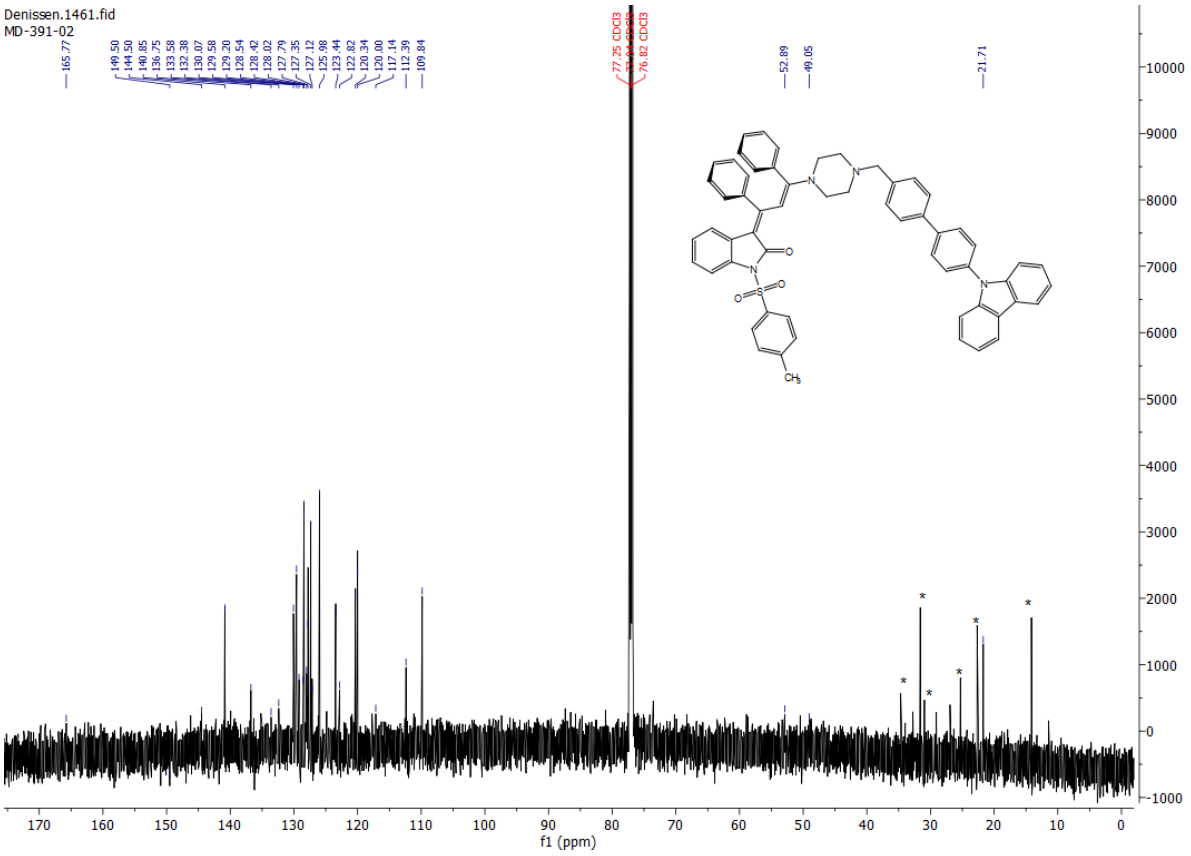

^{13}C NMR spectrum of **4g** ($CDCl_3$, 151 MHz, 293 K, *solvent impurities).

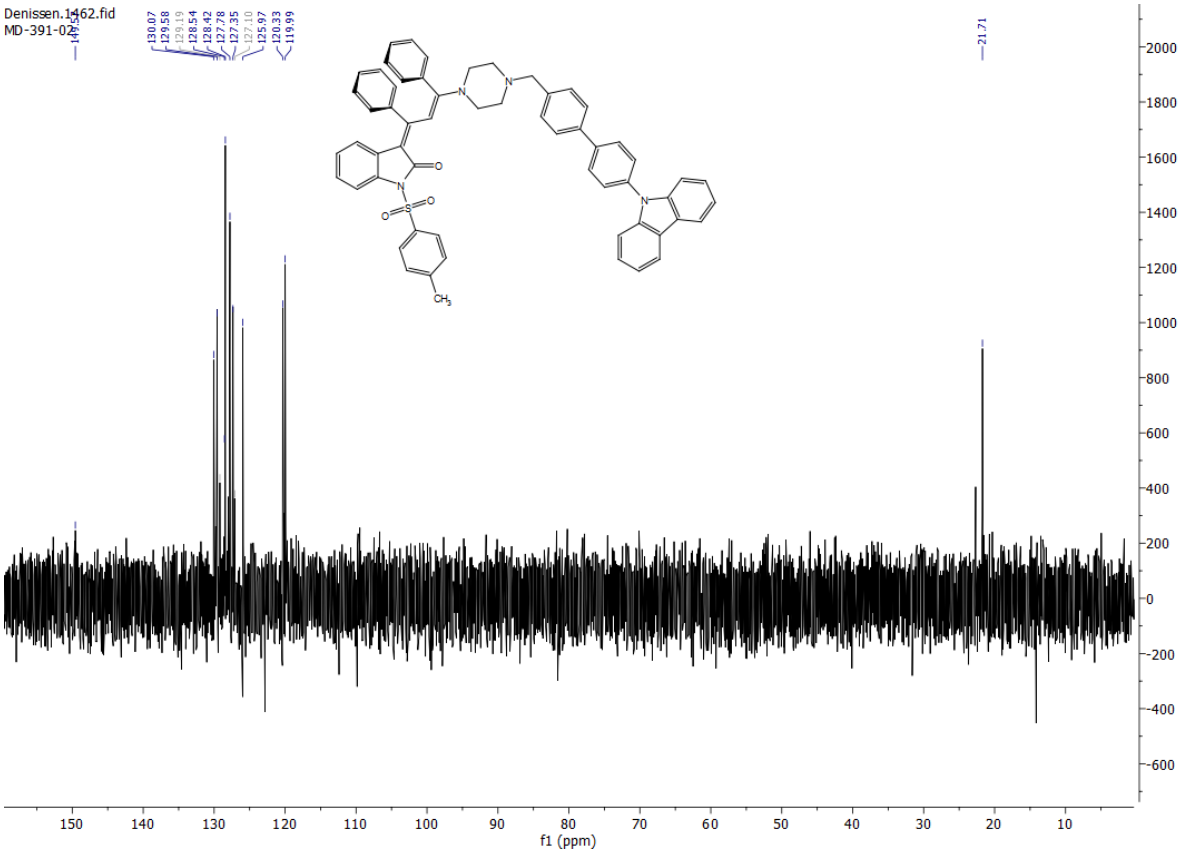

DEPT 135 ^{13}C NMR spectrum of **4g** ($CDCl_3$, 151 MHz, 293 K).

5.4 (*E*)-3-((*E*)-3-(4-((4'-(Diphenylamino)-[1,1'-biphenyl]-4-yl)methyl)piperazin-1-yl)-1,3-diphenylallylidene)-1-tosylindolin-2-one (4h)

According to the GP 4 compound **4h** (144 mg, 64%) was obtained as a dark red amorphous solid, Mp 140 °C, R_f (*n*-hexane/acetone, 2:1): 0.24, R_f (CH_2Cl_2/MeOH, 60:1): 0.26. ^{1}H NMR (600 MHz, $CDCl_3$, 298 K): δ 2.42 (s, 3 H), 2.48 (br, 4 H), 3.30 (br, 4 H), 3.57 (s, 2 H), 5.35 (br, 1 H), 6.48-6.52 (m, 1 H), 6.71 (d, *J* = 6.2 Hz, 2 H), 6.80 (d, *J* = 6.1 Hz, 2 H), 6.87-6.97 (m, 4 H), 7.00-7.05 (m, 5 H), 7.13 (d, *J* = 8.3 Hz, 8 H), 7.25-7.30 (m, 4 H), 7.31 (d, *J* = 8.1 Hz, 2 H), 7.34-7.38 (m, 3 H), 7.47 (d, *J* = 8.6 Hz, 2 H), 7.52-7.54 (m, 1 H), 7.88 (d, *J* = 8.2 Hz, 1 H), 8.05 (d, *J* = 8.3 Hz, 2 H). ^{1}H NMR (300 MHz, $CDCl_3$, 263 K): δ aliphatic protons see ^{1}H NMR at 298 K, 5.26 (d, *J* = 7.8 Hz, 1 H), 6.50-6.52 (m, 1 H), 6.68 (d, *J* = 7.2 Hz, 2 H), 6.79 (d, *J* = 7.2 Hz, 2 H), 6.90-6.95 (m, 4 H), 6.98-7.05 (m, 5 H), 7.14 (d, *J* = 8.2 Hz, 8 H), 7.26-7.29 (m, 4 H), 7.32 (d, *J* = 8.2 Hz, 2 H), 7.34-7.38 (m, 3 H), 7.45-7.47 (m, 2 H), 7.51-7.53 (m, 1 H), 7.88 (d, *J* = 8.3 Hz, 1 H), 8.04 (d, *J* = 8.3 Hz, 2 H). ^{13}C NMR (75 MHz, $CDCl_3$) δ 21.7 (CH_3), 49.0 (CH_2), 52.9 (CH_2),[6] 106.5 (CH), 110.2 (C_{quat}), 112.4 (CH), 120.8 (CH), 122.8 (CH), 122.9 (CH), 123.9 (CH), 124.4 (CH),[2] 124.8 (C_{quat}), 126.2 (C_{quat}), 126.6 (CH), 126.6 (C_{quat}), 127.7 (CH), 127.8 (CH),[2] 128.0 (C_{quat}), 128.5 (C_{quat}), 129.2 (CH), 129.3 (CH),[2] 129.5 (CH), 129.6 (CH), 130.1 (CH), 132.4 (C_{quat}), 134.8 (C_{quat}), 135.1 (C_{quat}), 136.1 (C_{quat}), 136.8 (C_{quat}), 139.7 (C_{quat}), 144.5 (C_{quat}), 147.2 (C_{quat}), 147.7 (CH),[2] 165.7 (C_{quat}). IR (ATR): $\tilde{\nu}$ 3059 (w), 3028 (w), 2960 (w), 2910 (w), 2812 (w), 1676 (m), 1632 (w), 1593 (m), 1526 (s), 1510 (s), 1489 (s), 1456 (m), 1445 (m), 1375 (s), 1354 (s), 1323 (s), 1283 (s), 1248 (s), 1188 (m), 1165 (s), 1153 (m), 1130 (m), 1072 (s), 1047 (w), 1028 (w), 995 (s), 959 (m), 926 (m), 905 (m), 868 (m), 835 (m), 800 (m), 750 (s), 745 (s), 735 (w), 694 (s), 689 (s), 660 (s), 623 (m). MALDI-TOF: *m/z* 894.4 (M^+), 741.4 (M^+-Tos). Anal. calcd. for $C_{59}H_{50}N_4O_3S$ (894.4): C 79.17, H 5.63, N 6.26; Found: C 79.20, H 5.87, N 6.06.

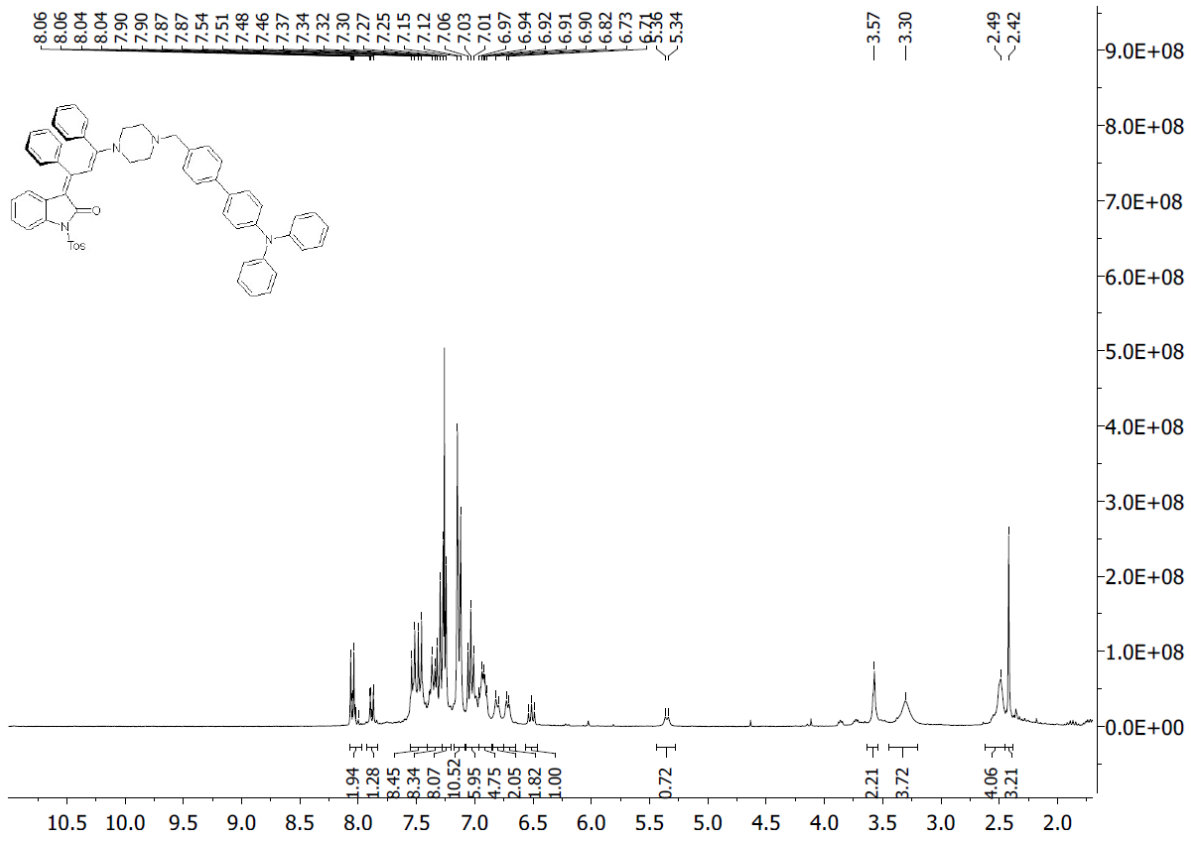

^{1}H NMR spectrum of **4h** ($CDCl_3$, 600 MHz, 298 K).

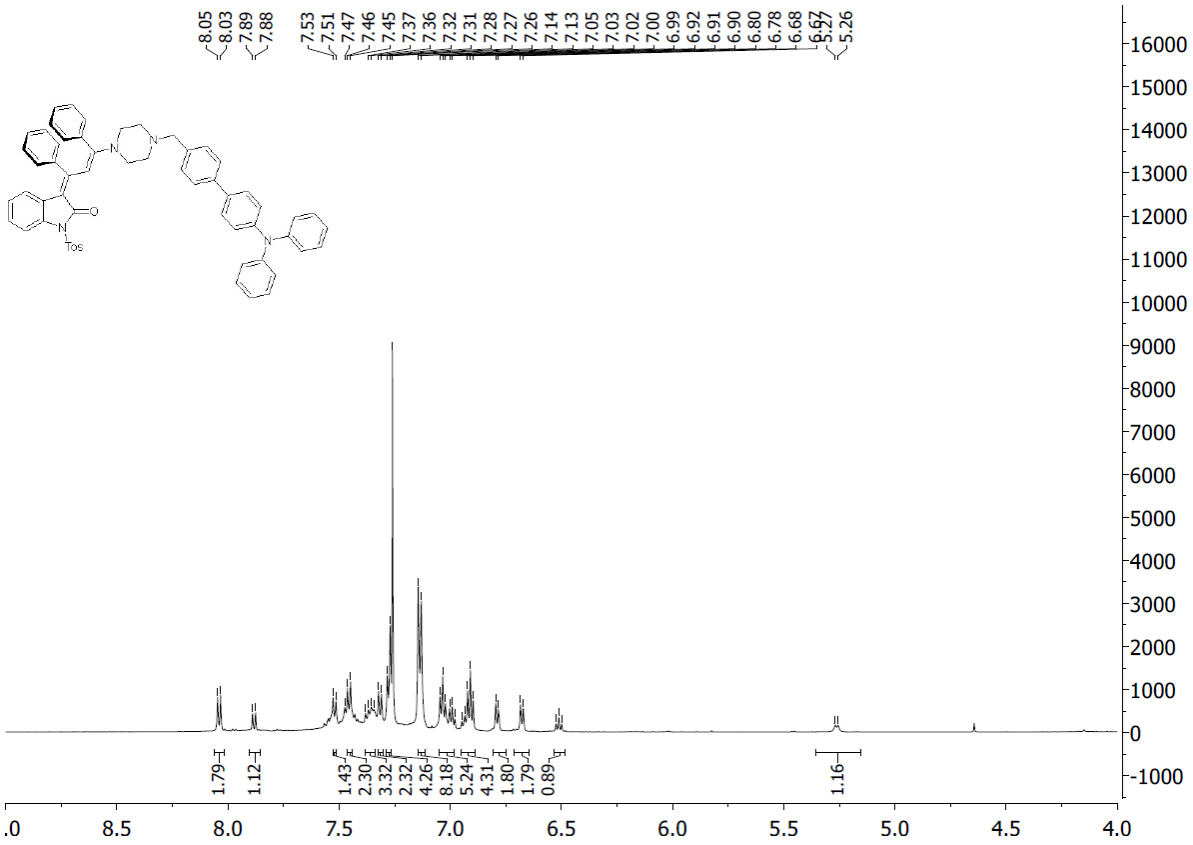

^{1}H NMR spectrum of **4h** ($CDCl_3$, 300 MHz, 263 K).

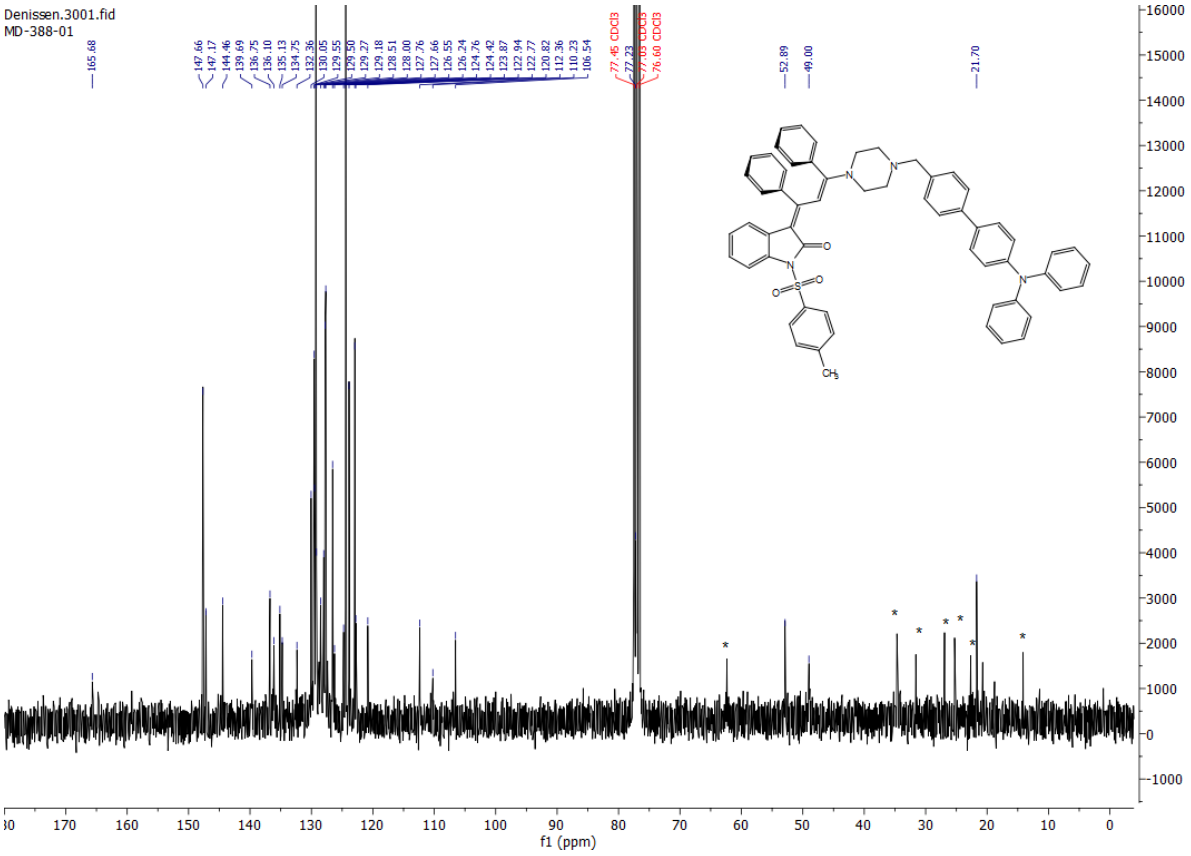

^{13}C NMR spectrum of **4h** ($CDCl_3$, 75 MHz, 293 K, *solvent impurities).

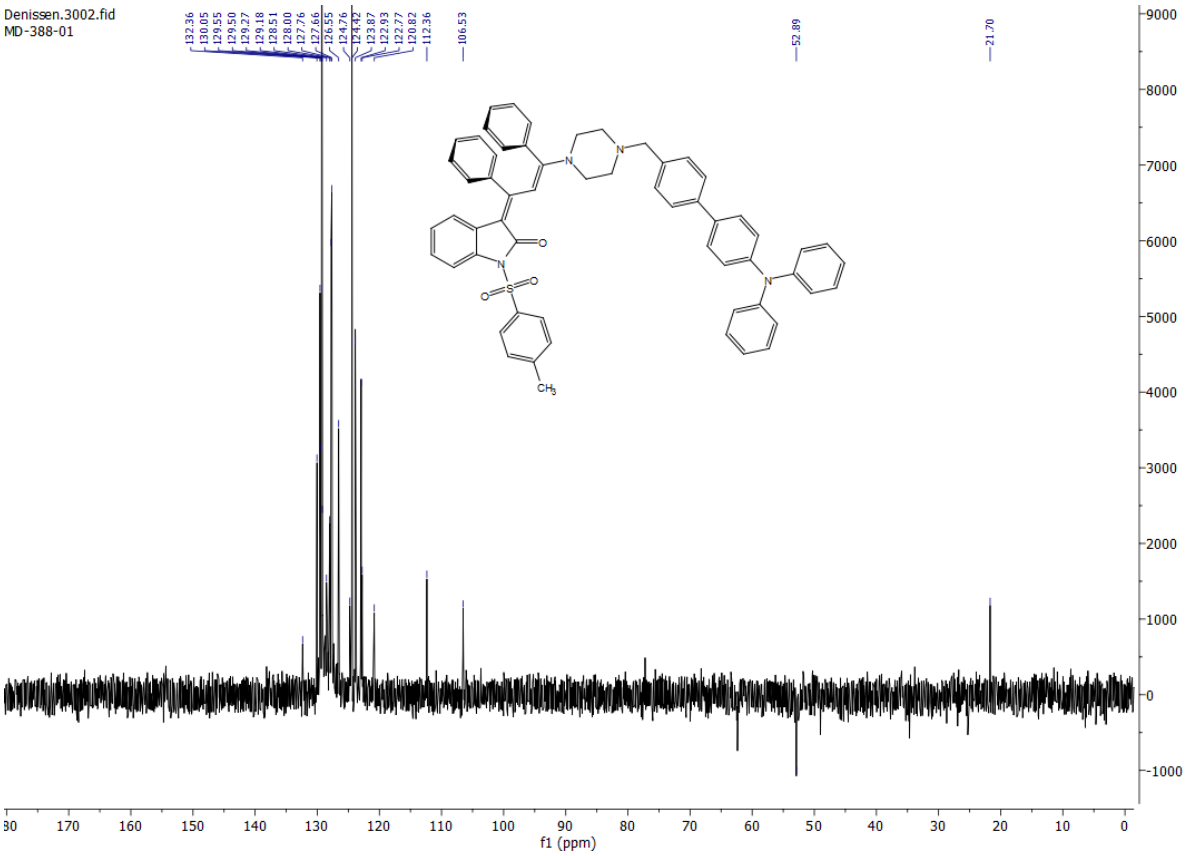

DEPT 135 ^{13}C NMR spectrum of **4h** ($CDCl_3$, 75 MHz, 293 K).

6 VT NMR-spectra of Compound 4e

As a consequence of the piperazinyl-*N*-benzyl substitution the room temperature ^{1}H NMR spectra indicate a dynamic behavior due to considerable line broadening around the coalescence temperatures. Furthermore, at room temperature all phenyl protons of the substituents at the merocyanine part are also broadened. Indeed, the unsymmetrical substitution pattern of the bridging piperazine leads to several coalescences between -5 and 25 °C as shown by VT-^{1}H NMR experiments with bichromophore **4e** (Figure SI-2). Upon cooling the line width of all signals on the 3-piperazinyl propenylidene indolone chromophore expectedly become sharper and the indicative methine resonance in β-position to the piperazinyl nitrogen atom gradually shifts to higher field. This finding can be interpreted as an increasing rigidification and reduced wagging of the phenyl rings at lower temperatures, and eventually upon crystallization (see the crystal structure).

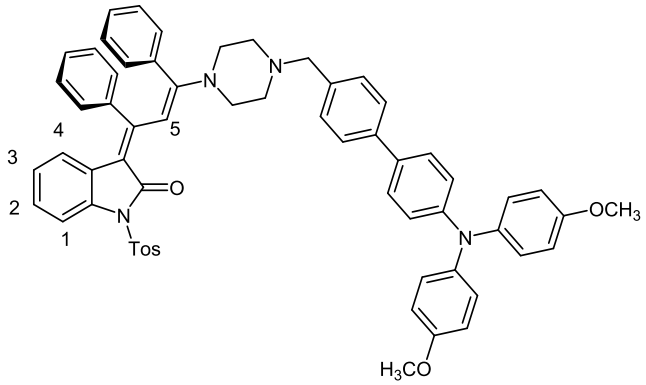

Figure SI-2. Structure of compound **4e**.

For the evaluation of the NMR spectra of compound **4e** optimization of the measuring temperature was mandatory. The aliphatic signals (piperazine core) as well as the aromatic signals (oxindole-merocyanine motif) show coalescence in different temperature ranges (Figure SI-3)

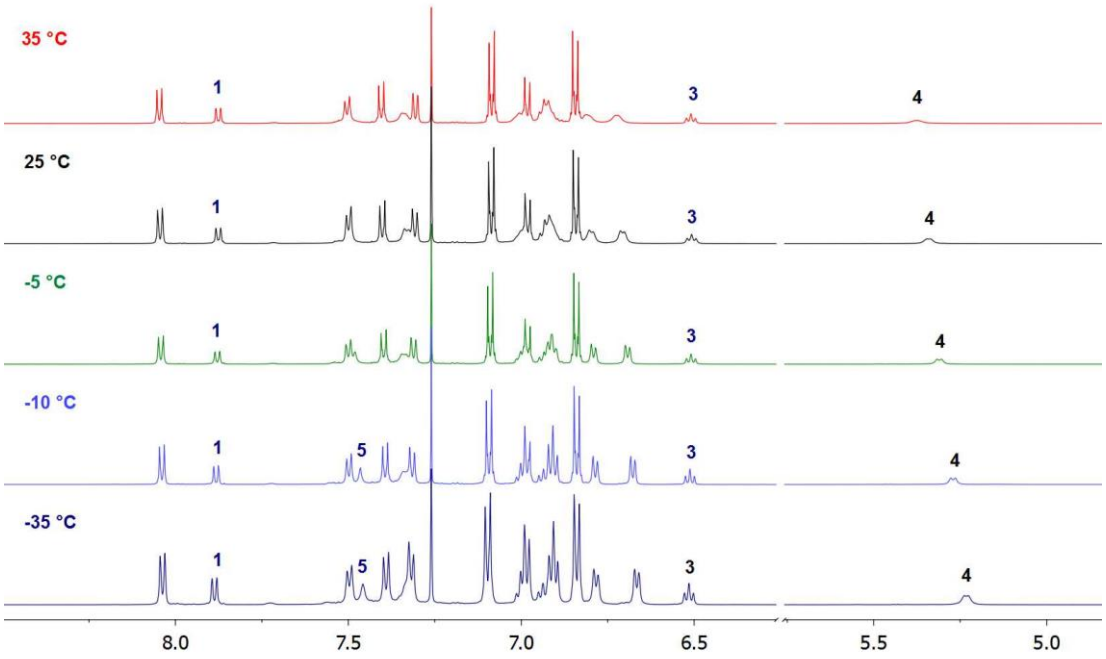

Figure SI-3. Sections of VT-^{1}H NMR spectra of compound **4e** in the aromatic and olefinic region (recorded at 600 MHz in $CDCl_3$ at 308, 298, 268, 263, and 238 K).

The measurements at room temperature show an inadequate resolution of the aromatic protons. Especially, the signals of protons of the oxoindole merocyanine core are broadened (Figure SI-3). This observation could be traced back to conformational changes of the vicinal phenyl substituents. At 25 and 35 °C the signal of the methine proton is superimposed by other aromatic and olefinic signals. Cooling down the solution the signal of the methine proton is shifted (H^5). The increased chromophore delocalization possibly leads to the observed high field shift (Figure SI-3).

The investigation of the molecular structure via VT-NMR gives insights into the motion of the phenyl substituents. The motion of the phenyl substituents implies the geometry of the oxo-indole motif and the delocalization as well. A torsion of the π-system leads to a hampered delocalization, which can be observed by a downfield shift of the signal H^5. No full rotation of the phenyl substituents is possible due to steric hindrance. Only „wobbling and swaying“ of the phenyl substituents is observed (Figure SI-4)

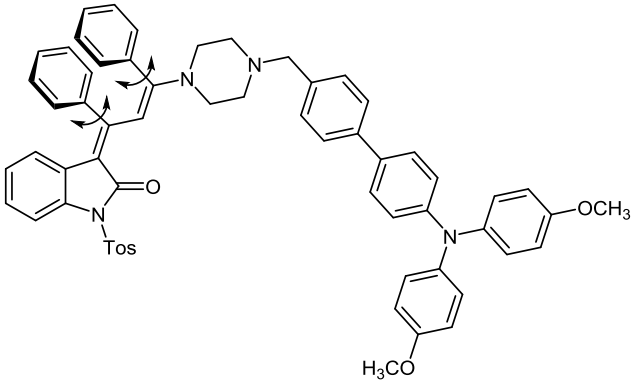

Figure SI-4. Frustated rotation of the vicinal phenyl substituents of compound **4e**.

The broadened signals at 35 °C shows the „wobbling“ of the phenyl substituents. Cooling leads to freezing of the thermodynamically favored conformation with sharp signals. Additionally, the thermodynamically favored conformation is stabilized by π-π-interactions of the phenyl substituents. At -35 °C the proton of the oxoindole core (H^4) is most high-field shifted, which is attributed to a perfect orthogonality of the phenyl substituent (anisotropy effect).

Besides, the torsion of the single bond of the merocyanine motif could also influence the electronic nature of the bichromophore system and the conformation of the phenyl substituents (Figure SI-5).

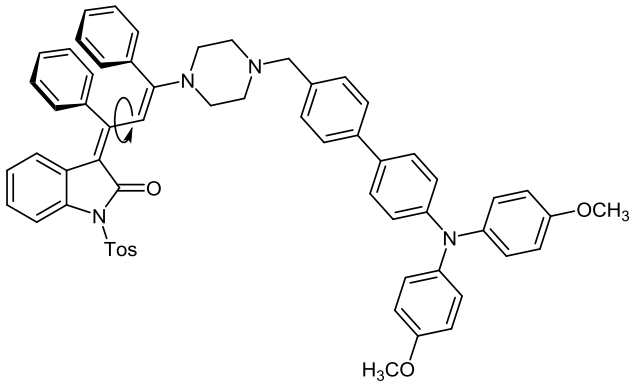

Figure SI-5. Torsion of the merocyanin motif.

In the aliphatic region of the NMR spectra a contrary coalesence behavior is observed. The optimized temperature of -10 °C is not suitable for the evaluation of the aliphatic signals. The signals of the eight piperazine protons split of into four broad signals, which are overlapped by the signals of the other aliphatic and benzylic protons (Figure SI-6). An optimization of the measuring temperature is also necessary to get insights into the conformation of the piperazine moiety.

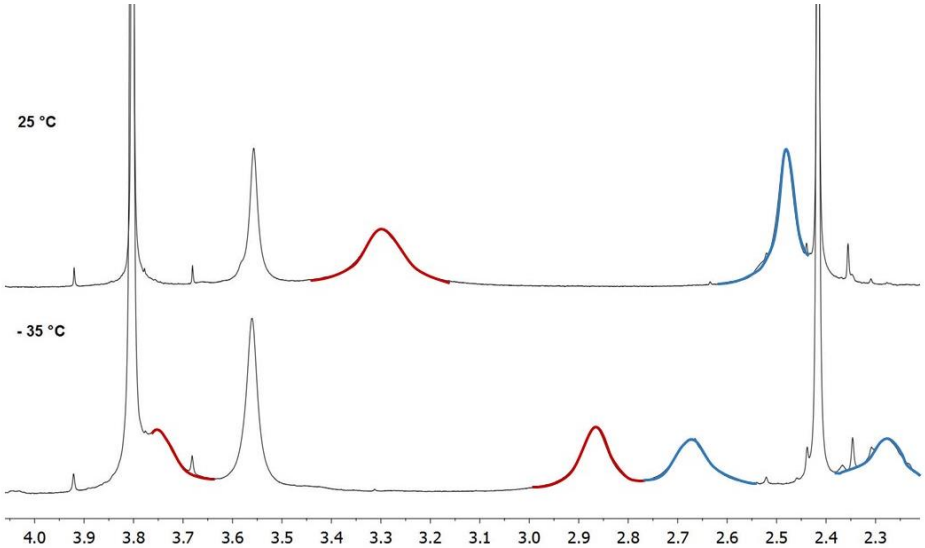

Figure SI-6. Sections of VT-^{1}H NMR spectra of compound **4e** in the piperazine region (recorded at 600 MHz in $CDCl_3$ at 298 and 238 K).

The signals of the aliphatic protons of the tosyl group (δ 2.42), of the methylene group (δ 3.56) and the methoxy substituents (δ 3.80) are not influenced within the optimization. At 25 and 35 °C, respectively, two broad multiplets (δ 3.30 and 2.48), which correspond to four protons for each signal are observed (Table SI-8). In this temperature the axial and equatorial protons are chemically equal (isochronous). The resulting spin system is characterized as an AA'BB' spin system.

Table SI-8. Chemical shifts δ of aliphatic protones (piperazine) measured in $CDCl_3$ depending on temperature.

Temperature	Piperazine (AA')	Piperazine (BB')
35 °C	3.30	2.49
25 °C	3.30	2.48
-5 °C	3.27/3.31	2.48
-10 °C	2.89/3.68	2.34/2.62
-35 °C	2.87/3.75	2.28/2.67

The measurements at low temperature confirm the ring inversion of the piperazine. Low temperature suppresses the exchange of axial and equatorial proton positions. The protons become chemically inequivalent and each signal splits of into two broad signals (Table SI-8). The observed spin system is characterized by an ABCD spin system. The point of coalescence lies in between -5 and 25 °C.

The signals of the four protons H^{7a} and H^{7b} (Figures SI-7 and SI-8) are not influenced by the conformational change of the vicinal phenyl substituents. The signals are assigned with a chemical shift of δ 6.84 (H^{7a}, J = 8.9 Hz, 4 H) und 7.08 (H^{7b}, J = 8.9 Hz, 4 H) at 267 K (Figure SI-8). The aromatic protons of the tosyl substituent are found as doublets at δ 7.31 (H^{1b}, J = 8.2 Hz, 2 H) and 8.04 (H^{1a}, J = 8.3 Hz, 2 H).

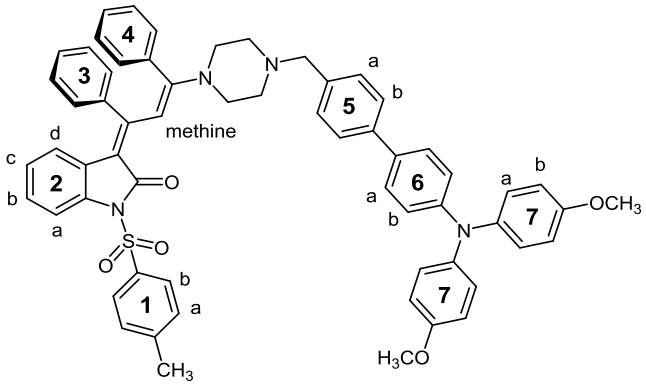

Figure SI-7. Structure **4e** for the assignment of chemical shifts and aromatic proton signals.

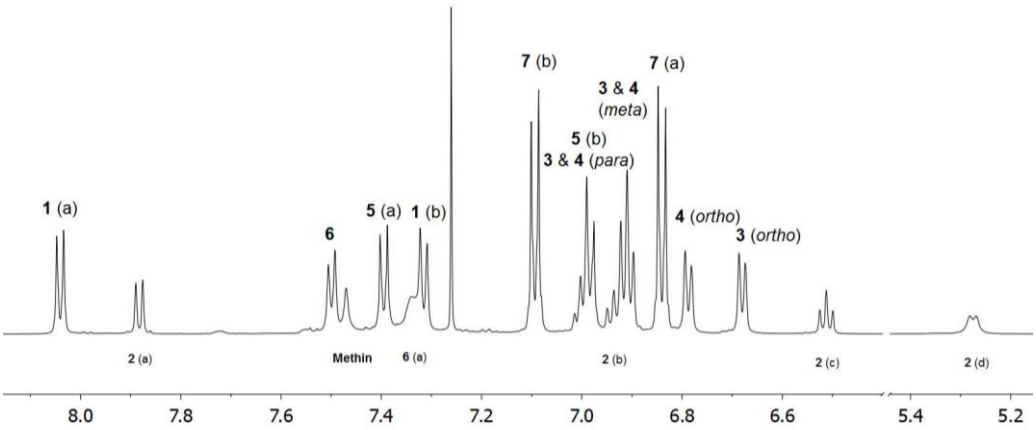

Figure SI-8. Section of ^{1}H spectrum of compound **4e** measured in CDCl3, 600 MHz, 267 K.

The assignment of the oxoindole and methine protons was done by additional TOCSY experiments (Figure SI-9).

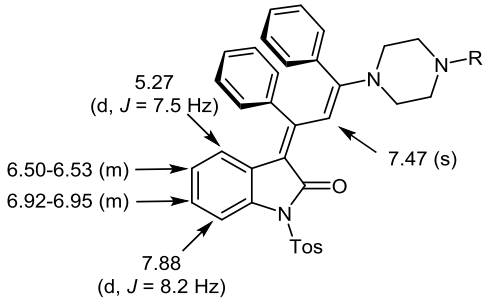

Figure SI-9. Assignment of chemical shifts and aromatic proton signals of the oxoindole-merocyanine (600 MHz, 267 K)

Further the assignment of the phenyl protons (H^3 and H^4) was possible (Figures SI-7 and SI-8). The bichromophore systems **4f-h** were investigated in the same way by VT-NMR spectroscopy and TOCSY experiments. In relation to the substituent different intra molecular mobility is observed.

7 Photophysical Data of Bichromophores 4

For comparison the constituting merocyanine chromophores *N*-Me-oxindole (**6**) and *N*-tosyl-oxindole (**7**) were chosen, whereas as UV absorbing subchromophore building block intermediates in the synthesis of piperazines **3** were selected, namely 4-(bromomethyl)-1,1'-biphenyl (**8**) for biphenyl, 9-(bromomethyl)anthracene (**9**) for anthracene, and *tert*-butyl 4-(4-(9*H*-carbazol-9-yl)phenyl)piperazine-1-carboxylate (**10**) for 9-phenyl carbazole (Figure SI-10, for detailed spectral data see also Supp Inf, Table SI-9). All absorption spectra are additive with respect to the constituting two chromophore units (Figure SI-11). In the absorption spectrum of anthryl-oxindole merocyanine bichromophore **4b** additionally the vibrational fine structure of the anthracene absorption band can be recognized (Figure SI-11b). A similar additive behavior of the constituting chromophores **6** and **8** is found in the absorption spectrum of bichromophore **4d** (Figure SI-12).

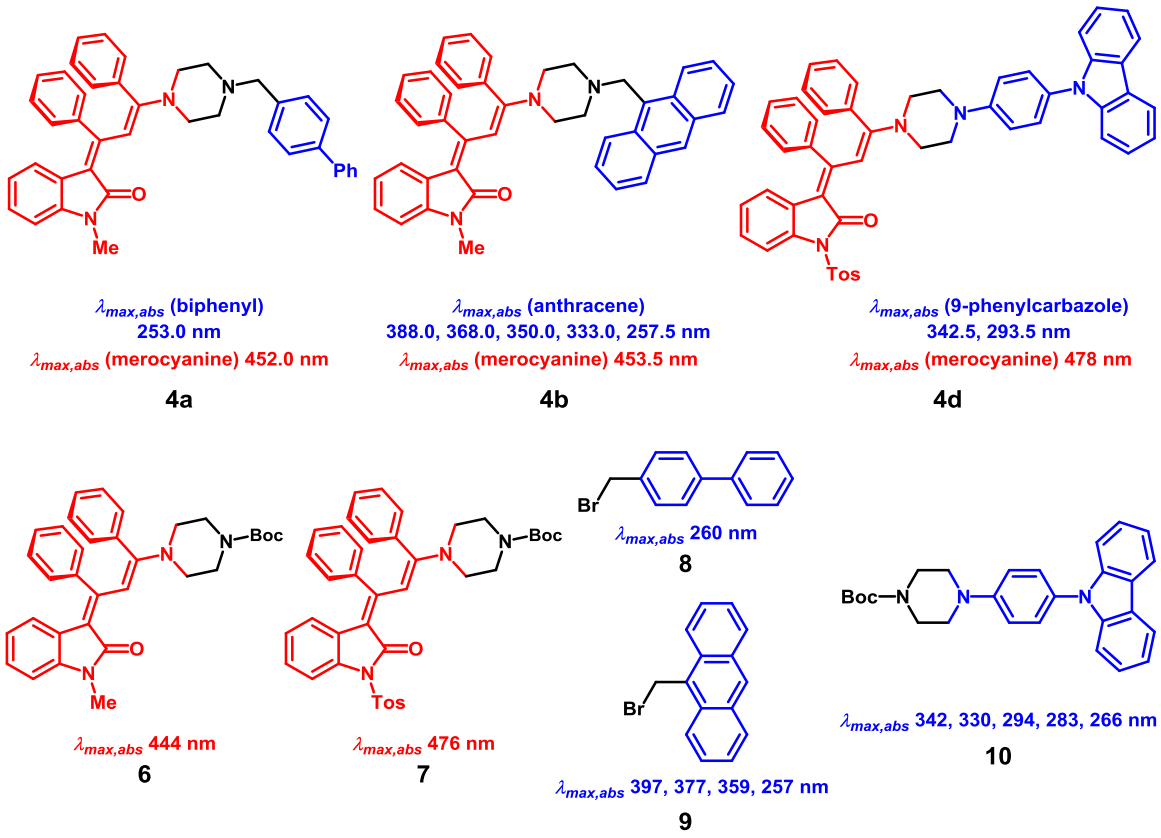

Figure SI-10. Assignment of the absorption bands in the bichromophores **4** by comparison with their constituting oxindole merocyanine (red, **6** and **7**) and UV-absorbing (blue, **8**, **9**, and **10**) subchromophores.

Table SI-9. Assignment of the chromophore units in the bichromophores **4a,b,d** by comparison with selected absorption bands $\lambda_{max,abs}$ (ε) [nm] of oxindole merocyanines **6** and **7**, biphenyl **8**, anthracene **9**, and 9-phenyl carbazole **10** derivatives (recorded in CH_2Cl_2 UVASOL® at T = 293 K, ([L·(mol·cm)$^{-1}$])).

subchromo-phore / bichromo-phore	*N*-Me-oxindole-merocyanine **6**[a]	*N*-Tos-oxindole-merocyanine **7**[a]	biphenyl **8**[b]	anthracene **9** [c]	9-phenyl carbazole **10**[d]
	444 (25700)	476 (20600)	260 (24800)	397 (8000) 377 (9000) 359 (6400) 257 (61300)	342 (3900) 330 (3900) 294 (24400) 283 (24000) 266 (25100)
4a	452 (25700)		253 (35300)		
4b	453.5 (21100)			388 (15800) 368 (11700) 350 (6900) 333 (4500) 258(128700)	
4d		478 (25400)			343 (8500) 294 (32300)

[d]Oxindole merocyanines **6** and **7** (ref. 9). [b]4-(Bromomethyl)-1,1'-biphenyl (**8**) (building block in the synthesis of piperazine **3a**). [c]9-(Bromomethyl)anthracene (**9**) (building block in the synthesis of piperazine **3b**). [d]*tert*-butyl 4-(4-(9*H*-carbazol-9-yl)phenyl)piperazine-1-carboxylate (**10**) (building block in the synthesis of piperazine **3c**).

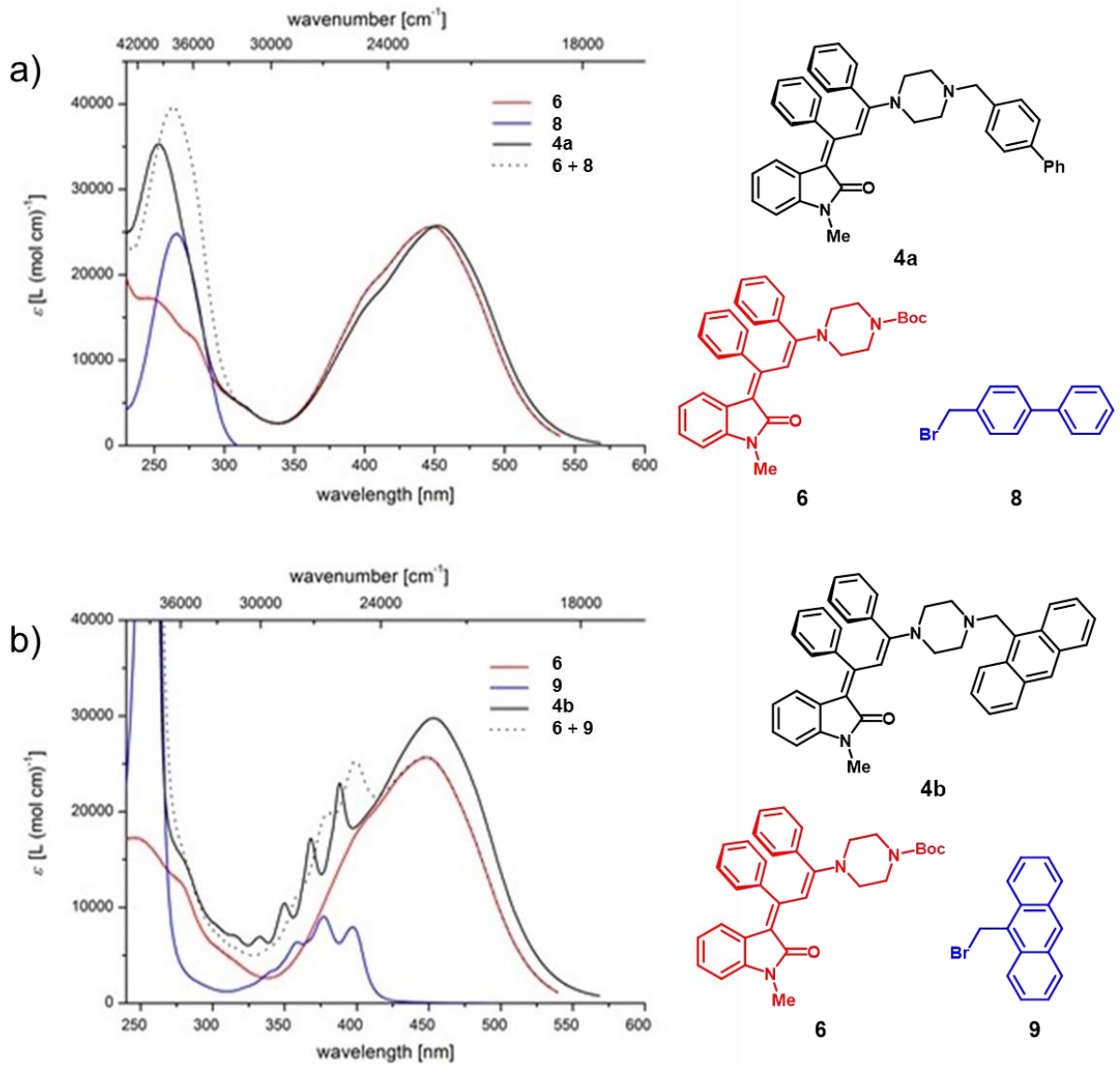

Figure SI-11. a) UV/VIS spectra of 3-piperazinyl propenylidene indolone merocyanine bichromophores **4a**, constituting of the merocyanine **6** and p-biphenylmethylbromide (**8**) and the corresponding sum spectrum of **6** and **8** (recorded in CH_2Cl_2 UVASOL® at *T* = 293 K). b) UV/VIS spectra of 3-piperazinyl propenylidene indolone merocyanine bichromophore **4b**, constituting merocyanine **6** and 9-anthrylmethylbromide (**9**) and the corresponding sum spectrum of **6** and **9** (recorded in CH_2Cl_2 UVASOL® at *T* = 293 K).

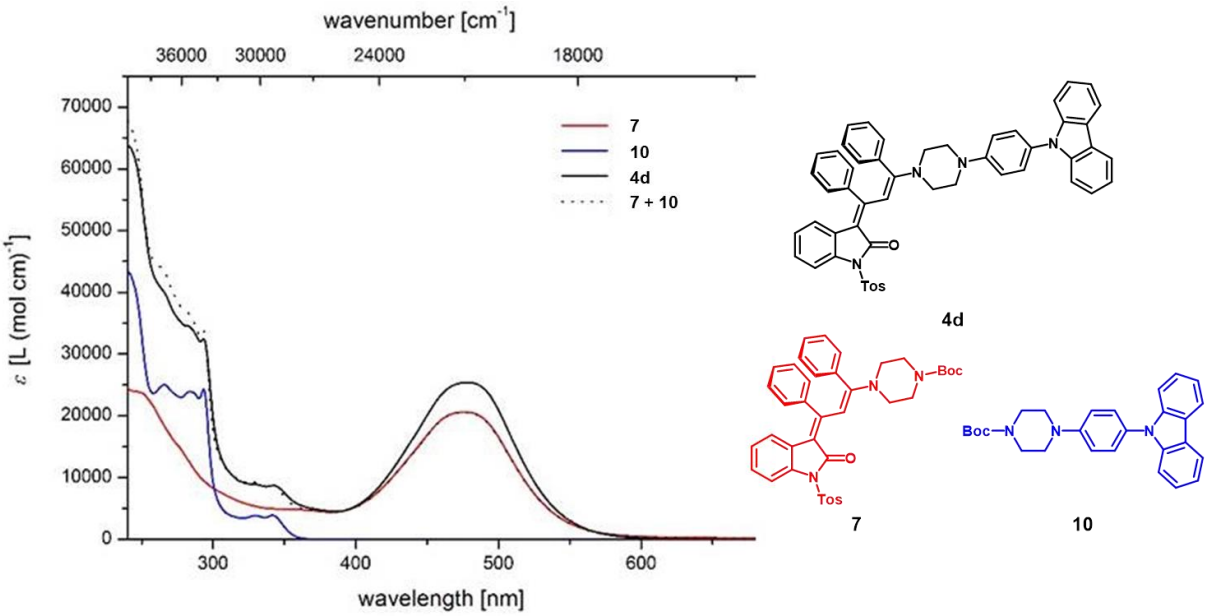

Figure SI-12. UV/VIS spectra of 3-piperazinyl propenylidene indolone merocyanine bichromophore **4d**, constituting merocyanine **7** and *tert*-butyl 4-(4-(9*H*-carbazol-9-yl)phenyl)piperazine-1-carboxylate (**10**) and the corresponding sum spectrum of **7** and **10** (recorded in CH_2Cl_2 UVASOL® at T = 293 K).

The emission spectrum of compound **4b** shows the anthracene emission signature in solution upon excitation at 350 nm, which however is absent in the drop-casted film (Figure SI-13a). Excitation of the drop-casted film at 454 nm exclusively shows the AIE typical merocyanine emission band around 600 nm (Figure SI-13b).

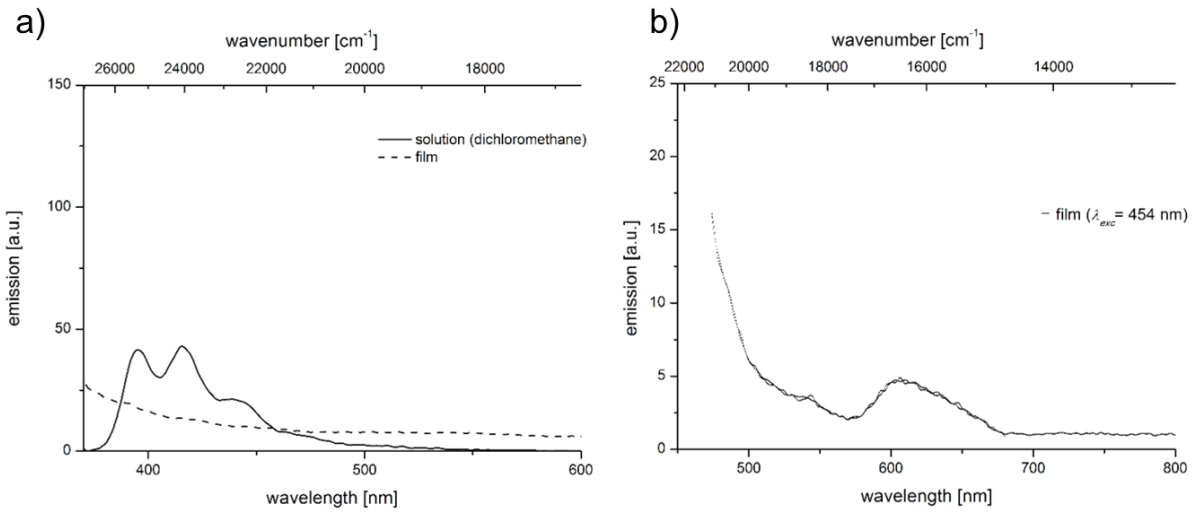

Figure SI-13. a) Emission spectra of bichromophore **4b** in CH_2Cl_2 UVASOL® (solid line) and in a drop-casted film (λ_{exc} = 350 nm; T = 293 K). b) Emission spectrum of the drop-casted film of bichromophore **4b** (λ_{exc} = 454 nm; T = 293 K).

The longest wavelength absorption band of bichromophore **4e** only shows a modest positive solvatochromicity (Figure SI-14, Table SI-10).

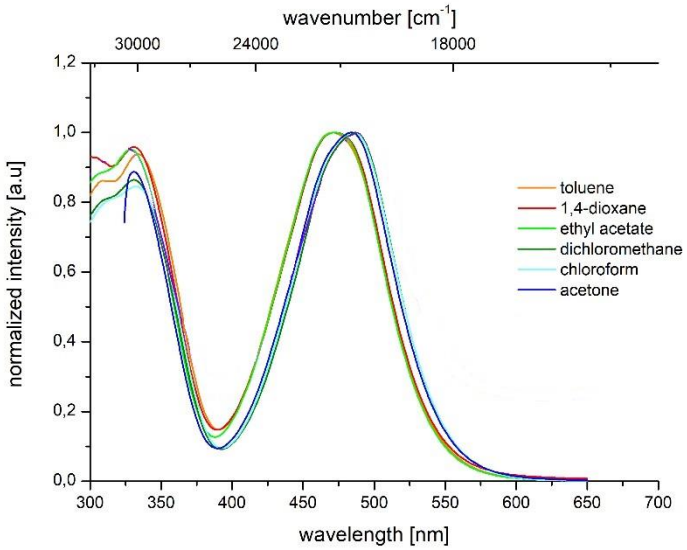

Figure SI-14. Normalized absorption spectra of compound **4e** in selected solvents with different polarity measured at 293 K.

Table SI-10. Selected absorption data of bichromophore **4e** in solvents of different polarity (recorded at T = 293 K).

solvent	$\lambda_{max,abs}$ (ε) [nm] ([L· (mol · cm)$^{-1}$])
toluene	333.5 (26600), 471.0 (28300)
1,4-dioxane	330.5 (30500), 472.0 (32100)
ethyl acetate	328.0 (24400), 473.0 (25600)
chloroform	333.0 (29900), 485.0 (35400)
dichlormethane	330.5 (30200), 486.5 (34700)
acetone	331.0 (27900), 484.0 (31700)

Upon excitation at λ_{exc} = 330 nm (triarylamine) in solvents of different polarity a positive solvatochromocity of the triarylamine chromophore becomes apparent (Figure SI-15a). However, upon excitation at λ_{exc} = 485 nm (merocyanine) in the same solvents, only in acetonitrile emission can be detected (Figure SI-15b). As the merocyanine only emits upon aggregation or in the solid state a partial aggregation of bichromophore **4e** in acetonitrile can be assumed in this concentration regime.

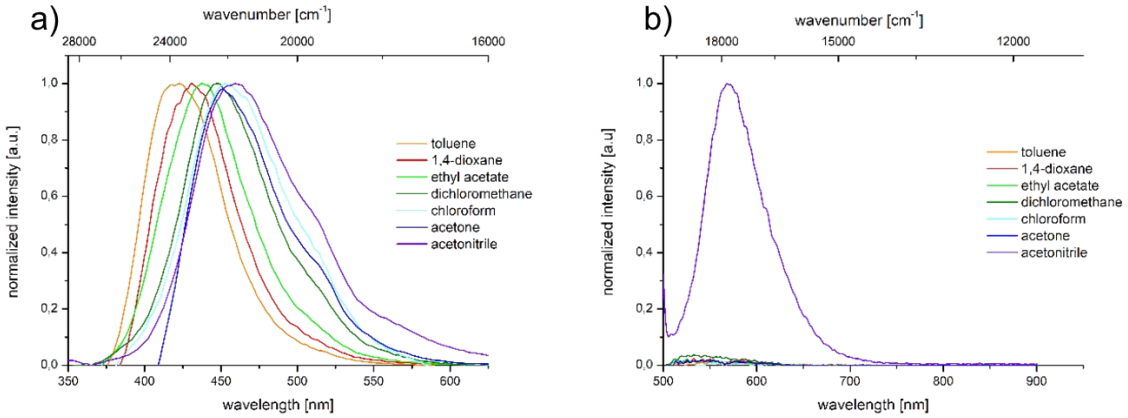

Figure SI-15. a) Normalized emission spectra of bichromophore **4e** (c(**4e**) ~ 1·10^{-4} M) in seven solvents of different polarity. Left: normalized emission bands, λ_{exc} = 330 nm at T = 293 K. b) Normalized emission spectra of bichromophore **4e** relative to the emission intensity in acetonitrile, λ_{exc} = 485 nm at T = 293 K.

Absorption spectra of acetonitrile-water mixtures of compound **4e** show that with increasing water content a small bathochromic shift of the longest wavelength absorption band with concomitant hypochromic decrease of the molar absorption coefficient (Figure SI-16) occur. Monitoring the change of the emission spectra of compound **4e** with increasing water content of the acetonitrile-water mixtures reveals that at a low water content only the emission signal of the triarylamine chromophore around 450 nm at λ_{exc} = 330 nm is detected, whereas the merocyanine emission around 550 nm is absent (Figure SI-17). At high water content the triarylamine emission is completely absent and only the emission of the merocyanine is detected at both excitation wavelengths.

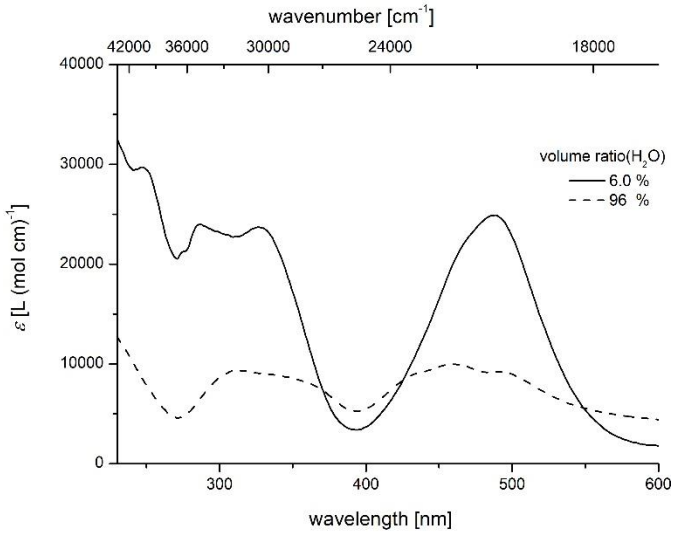

H_2O [vol%]	$\lambda_{max,abs}$ (ε) [nm] ([L·(mol·cm)$^{-1}$])
6.0	488.5 (24900) 326.5 (23700)
96	491.5 (9200) 459.5 (10000) 308.5 (9300)

Figure SI-16. Absorption spectra of bichromophore **4e** in acetonitrile-water mixtures (c(**4e**) = 1.1 · 10^{-5} M at 293 K).

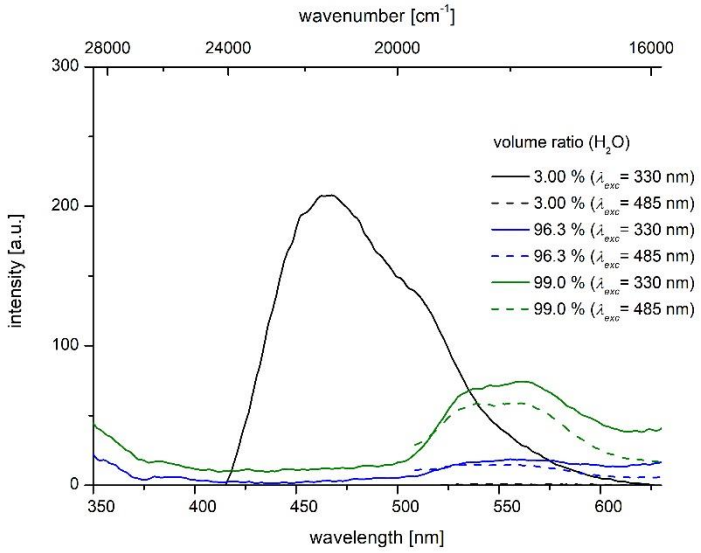

Figure SI-17. Emission spectra of bichromophore **4e** in 97:3 (black), 2.7:96.3 (blue) and 1:99 vol% (green) acetonitrile-water mixtures (c(**4e**) = 5.4 · 10^{-6} M at 293 K) (solid lines, λ_{exc} = 330 nm; dashed lines λ_{exc} = 485 nm).

The fluorescence quantum yields Φ_f of bichromophore **4e** in acetonitrile-water mixtures with increasing water content are quite low and essentially do not change at both excitation

wavelengths (Table SI-11). However, the excited state lifetimes τ of both chromophores change with increasing water content. While the lifetime of the triarylamine emission steadily decreases with increasing water content, the lifetime of the merocyanine emission increases considerably for a water content exceeding 95 vol%. In summary the appearance of the merocyanine emission at high water content occurring exclusively in the solid state or in aggregates indicates that in the acetonitrile-water system the merocyanine emission becomes dominant due to energy transfer from the triarylamine chromophore.

Table SI-11. Fluorescence quantum yields Φ_f and lifetimes τ of donor-acceptor-bichromophore **4e** in acetonitrile-water mixtures with increasing water content (λ_{exc} = 330 nm; λ_{exc} = 485 nm).

water content [vol%]	quantum yield Φ_f		lifetime τ [ns]	
	λ_{exc} = 330 nm	λ_{exc} = 485 nm	λ_{exc} = 330 nm	λ_{exc} = 485 nm
0	< 0.01	< 0.01	4.53	<0.2
50	< 0.01	< 0.01	5.09	<0.2
75	< 0.01	< 0.01	2.81	<0.2
85	< 0.01	< 0.01	<0.2	<0.2
95	< 0.01	< 0.01	<0.2	3.25

Solvent systems at the other polarity end are dichloromethane-cyclohexane mixtures. The absorption spectra of dichloromethane-cyclohexane mixtures with increasing dichloromethane content expectedly show the positive absorption solvatochromism of the merocyanine band whereas the absorption of the shorter wavelength absorbing triarylamine is only affected to a minor extent in the electronic ground state (Figure SI-18).

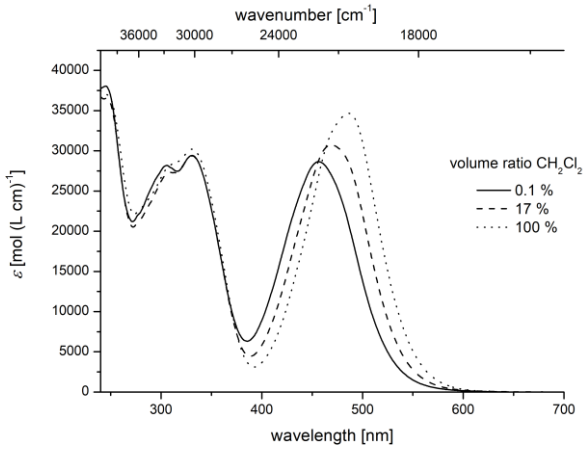

CH_2Cl_2 [vol%]	$\lambda_{max,abs}$ (ε) [nm] ([L·(mol·cm)$^{-1}$])
0.10	456.0 (28600) 331.0 (29400) 306 (28200)
17.0	469.0 (30700) 331.0 (29400) 309.5 (27300)[a]
100	486.5 (34700) 330.5 (30200) 309.5 (28200)[a]

[a] shoulder

Figure SI-18. Absorption spectra of bichromophore **4e** in 0.1:99.9 vol% (solid line), 17:83 vol%(dashed line) and 100:0 vol% (doted line) dichloromethane-cyclohexane mixtures (c(**4e**) = 1.7 · 10^{-5} M at 293 K), $\lambda_{max,abs}$ (ε).

At a very low content of dichloromethane (1 or 0.1 vol%) the dichloromethane-cyclohexane mixtures of bichromophore **4e** start to show dual emission with contributions from the constituting merocyanine (λ_{em} ~ 590 nm) and triarylamine subchromophores (λ_{em} ~ 590 nm) (see manuscript text). Evidence of this dual emission originating from partial intramolecular energy transfer is supported by the fluorescence excitation spectra recorded at the emission band λ_{em} = 590 nm of bichromophore **4e** for contents of 1.0 and 0.1 vol% of dichloromethane in cyclohexane (Figure SI-19). This confirms that both absorption bands at 330 and 500 nm contribute to the dual emission (Figure SI-19).

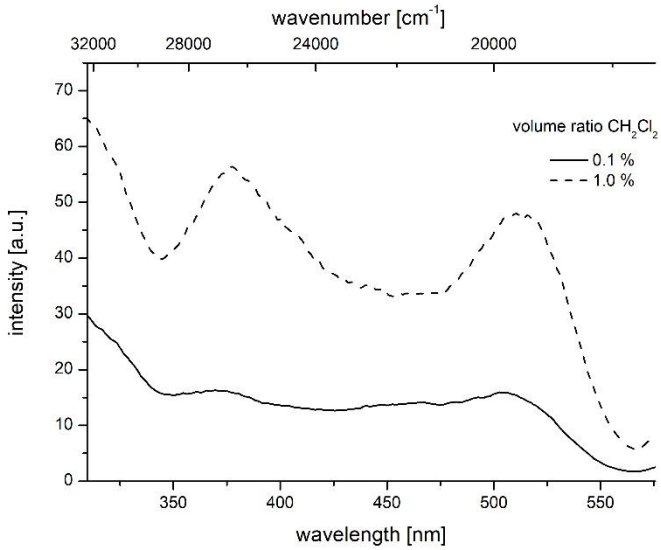

Figure SI-19. Excitation spectra of the emission band λ_{em} = 590 nm of bichromophore **4e** in 0.1:99.9 vol% (solid line), 1:99 vol% (dashed line) and 100:0 vol% (doted line) dichloromethane-cyclohexane mixtures (c(**4e**) = 2.1 · 10^{-5} M at 293 K).

The fluorescence quantum yields Φ_f of bichromophore **4e** in dichloromethane-cyclohexane mixtures with increasing cyclohexane content are quite low, however, upon excitation at λ_{exc} = 375 nm decreasing lifetimes τ of the triarylamine emission in the nanosecond range can be detected with increasing cyclohexane content (Table SI-12). Simultaneously the triarylamine emission maximum gradually shifts hypsochromically (with decreasing polarity of the solvent mixture), whereas the merocyanine band shifts bathochromically (Figure SI-20).

To confirm our hypothesis of white light emission resulting from a combination of the simultaneous blue and orange emission we included the absorption and emission spectra obtained for dye **4e** in dichloromethane-cyclohexane mixtures of increasing cyclohexane content shown below. The pink absorption line (or more correct the wavelength dependent optical density) clearly reveals scattering as to be expected from the photograph (see manuscript, Figure 4C). The corresponding emission spectra show the changes in the intensity ratios of the blue and orange emission induced by the increasing cyclohexane content of the

solvent mixture with this dual emission in combination with the proper intensity ratio of both emission bands eventually accounting for the observed white emission.

Table SI-12. Fluorescence quantum yields Φ_f and lifetimes τ of donor-acceptor-bichromophore **4e** in dichloromethane-cyclohexane mixtures with increasing cyclohexane content (λ_{exc} = 375 nm).

cyclohexane content [vol%]	quantum yield Φ_f λ_{exc} = 350 nm	lifetime τ [ns] λ_{exc} = 375 nm	lifetime τ [ns] λ_{exc} = 375 nm
0	< 0.01	3.48 (λ_{em} = 426 nm)	3.62 (λ_{em} = 543 nm)
50	< 0.01	2.39 (λ_{em} = 419 nm)	3.23 (λ_{em} = 543 nm)
99	< 0.01	1.09 (λ_{em} = 409 nm)	2.64 (λ_{em} = 560 nm)
99.9	0.01	1.11 (λ_{em} = 400 nm)	0.252 (λ_{em} = 570 nm)

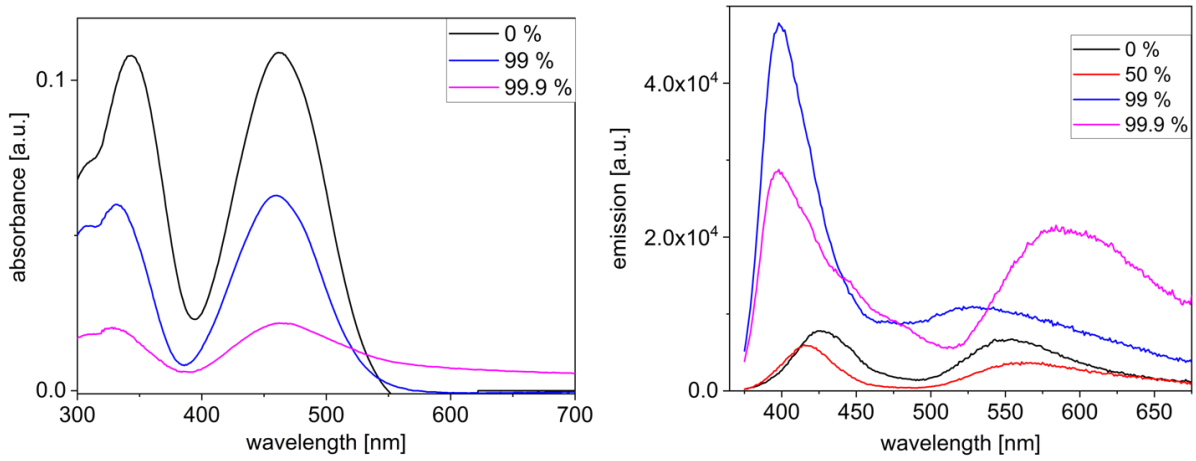

Figure SI-20. Absorption (left) and emission (right) spectra of bichromophore **4e** in 100:0 vol% (black lines), 50:50 vol% (red line, only emission), 1:99 vol% (blue lines), and 0.1:99.9 vol% (red lines) dichloromethane-cyclohexane mixtures (c(**4e**) = 2.1 · 10^{-5} M at 293 K).

By weighting of the energy distributions from the measured fluorescence spectra the tristimulus values X, Y and Z can be calculated. From these the chromaticity coordinates x and y are determined and visualized in the CIE 1931 color space chromaticity diagram. The chromaticity coordinates x and y describe the apparently perceived emission color in good agreement (Table-SI13). In addition the mixing color can be modulated by variation of the dichloromethane:cyclohexane ratio and by variation of the concentration of bichromophore **4e**.

Table SI-13. Chromaticity coordinates x and y of bichromophore **4e** in a CIE 1931 normal valence system determined 5 min after forming the dichloromethane-cyclohexane mixtures.

relative concentration of the saturated solution of bichromophore **4e**	vol% ratio (CH_2Cl_2/cyclohexane)	x	y
high (~ 10^{-5} M)	0.1:99.9	0.32	0.35
	1:99	0.28	0.33
low (~ 10^{-6} M)	0.1:99.9	0.31	0.34

After 12 h the emission behavior of the suspensions has changed as detected by fluorescence spectrocopy (Figure SI-21). For the 1:99 vol% dichloromethane-cyclohexane mixture an increase intensity of the blue band is found, however, the red emission band does not change its intensity (Figure SI-21a). In the 0.1:99.9 vol% dichloromethane-cyclohexane mixture a significant blue shift of the emission spectra can be detected after 12 h, accompanied by a loss of intensity of the red emission band (Figure SI-21b).

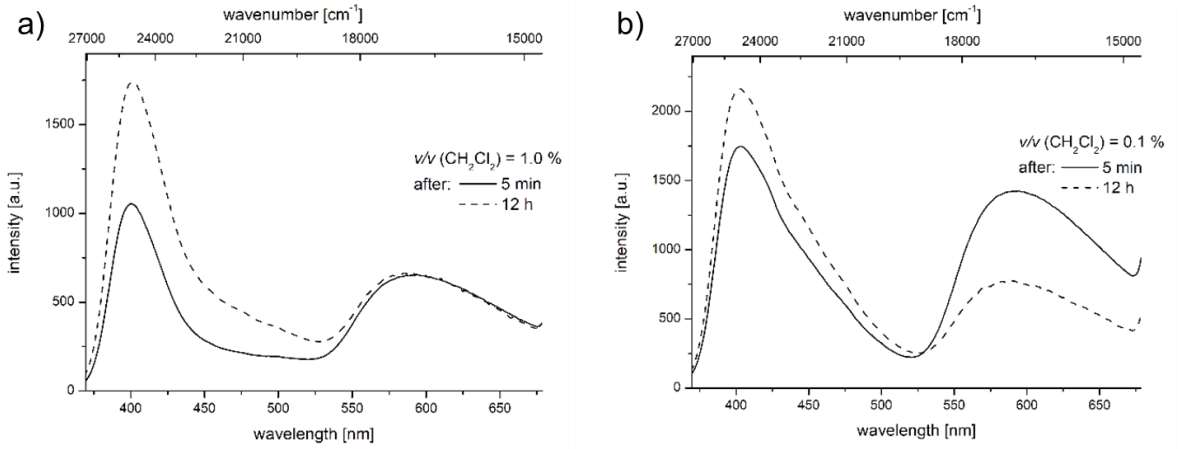

Figure SI-21. Emission spectra of bichromophore **4e** in dichloromethane-cyclohexane mixtures of 1:99 (left) and 0.1:99.9 (right) (c(**4e**) = ~ 10^{-5} M) after 5 min (solid lines) und nach 12 h (dashed lines).

Aging leads to the formation of particles of a critical size that finally preciptate as a consequence of gravitational forces.[10] Thereby, the emission contribution of bichromophore **4e** in solution resulting from the triarylamine fluorescence becomes increasingly important. The DVLO (Derjaguin, Landau, Verwey, and Overbeek) theory rationalizes the coagulation of particles by short and long distance interactions,[11] and describes the stability of colloids by attractive dispersion and repulsive electrostatic interactions.[12] Indeed, after 12 h the precipitation of the particles can be observed upon eyesight.

Furthermore, we encapsulated bichromophore **4e** in polystyrene particles (PSP) according to the depicted protocol (Figure SI-22).[13]

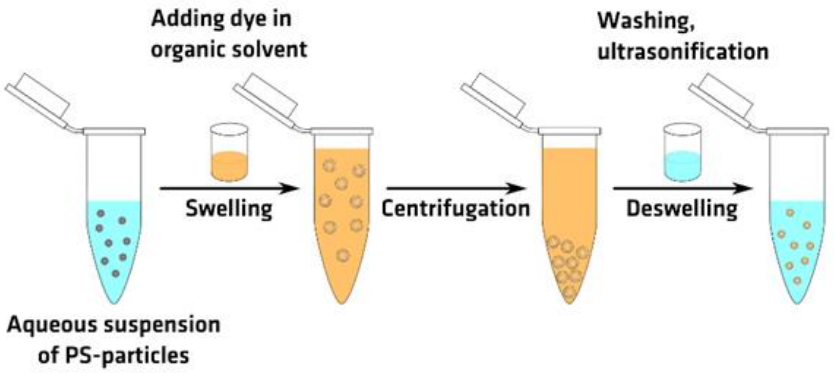

Figure SI-22. Encapsulation of bichromophore **4e** in a polymer particle.

Emission spectra excited at λ_{exc} = 330 nm and λ_{exc} = 485 nm and fluorescence excitation spectra show for bichromophore **4e** two emission scenarios (Figure SI-23). Excitation at 330 nm leads to a predominant emission of the triarylamine chromophore with a longer wavelength side band (Figure SI-23). In contrast, excitation at 485 nm exclusively leads to the merocyanine emission with a maximum over 600 nm (Figure SI-23). For both excitation wavelengths the fluorescence quantum yields Φ_f are low and the lifetimes lie in the margin of aggregated species (Table SI-14). However, from the absence of dual emission it can be concluded that the emission results mainly from a restricted motion of the chromophoric subunits in the PSP.

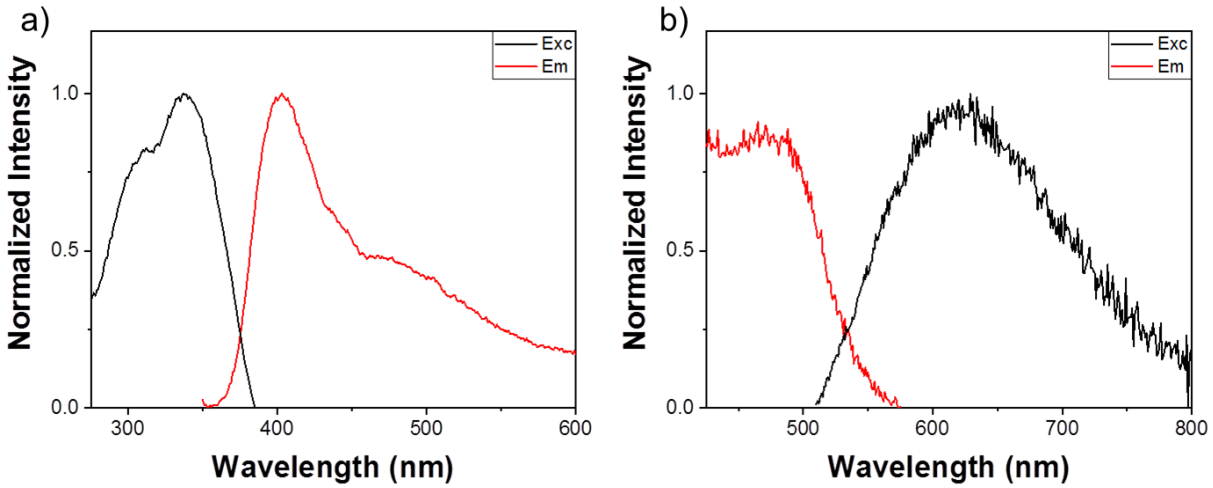

Figure SI-23. Excitation and emission spectra of donor-acceptor-bichromophore **4e** in 1 µm-sized PSP-COOH; a) λ_{exc} = 330 nm; b) λ_{exc} = 485 nm.

Table SI-14. Fluorescence quantum yields Φ_f and lifetimes τ of donor-acceptor-bichromophore **4e** in PSP (polystyrene particle) (λ_{exc} = 330 nm and λ_{exc} = 485 nm).

	fluorescence quantum yield Φ_f		lifetime τ [ns]	
	λ_{exc} = 330 nm	λ_{exc} = 485 nm	λ_{exc} = 330 nm	λ_{exc} = 485 nm
PSP	<1	<1	0.955	<0.2

The efficiency of the energy transfer can be modulated by varying the chromophore concentration (Figure SI-24) as shown by the weighted contribution of the integral emission intensities of both emission bands from 340-520 nm and 520-670 nm (Figure SI-24).

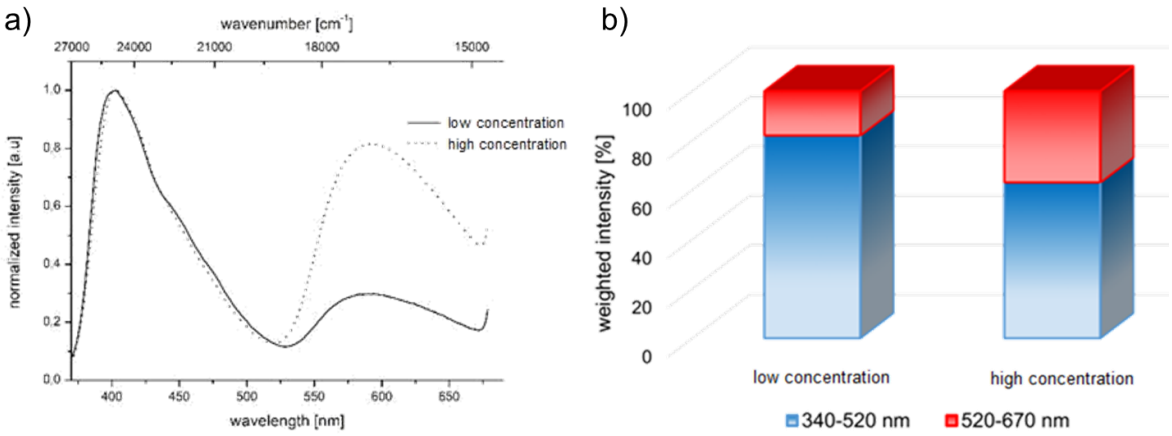

Figure SI-24. a) Emission spectra of bichromophore **4e** in a dichloromethane-cyclohexane mixture of 0.1:99.9 at high (dotted line) and low (solid line) concentration. b) Comparison of the weighted intensity of the emission maxima relative to the overall emission of the corresponding sample.

8 X-Ray Structure Analysis of Bichromophore 4e

Table SI-20. Details of refinement on structure **4e**.

Chemical formula	$C_{61}H_{54}N_4O_5S$	
Molecular weight	955.14	
Temperature	292 K	
Wavelength	1.54178 Å (Cu $K\alpha$)	
Crystal system	monoclinic	
Space group	*C2/c*	
Cell parameters	*a* = 41.915(3) Å	α = 90°
	b = 9.9907(9) Å	β = 116.974(5)°
	c = 26.883(2) Å	γ = 90°
Volume of cell	10032.8(15) Å^3	
Z	8	
Density (calculated)	1.265 g/cm^3	
Absorption coefficient μ	1.01 mm^{-1}	
F(000)	4032	
Crystal size	0.10 x 0.03 x 0.01 mm^3	
Measured Theta	3.4 – 59.8°.	
Indices	$-45 \le h \le 46$, $-11 \le k \le 11$, $-30 \le l \le 30$	
Data collection	Bruker APEX-II CCD diffractometer	
Measured reflections	51816	
Independent reflections	7447 [R(int) = 0.077]	
Refinement on F^2	Full-matrix least-squares on F^2	
Data/ Restrains/ Parameter	7447 / 0 / 643	
S	1.10	
Final R-values [$F^2>2\sigma(F^2)$]	*R1* = 0.049, w*R2* = 0.117	
Max/min electron density $\Delta\rho$	0.48 und -0.19 eÅ^{-3}	

A closer inspection of the bond length in bichromophore **4e** reveals bond length alternation in the electronic ground state (C1-C2 1.463(3) Å, C2-C9 1.390(3) Å, C9-C16 1.422(3) Å, C16-C17 1.379(3) Å) (Figure SI-25a). The C-N bond between butadiene and piperazine is found with 1.358(3) Å and accounts for a partial double bond character, i.e. a push-pull system. The π-π-interaction of the neighboring phenyl rings contributes to the planarization of the merocyanine chromophore in the solid state (Figure SI-25b). This is additionally supported by a minor deviation of the butadienyl moiety from coplanarity with a torsional angle β (C2-C9-C16-C17) of 11.3(4)°. The centroid distance *a* of the vicinal phenyl rings accounts to a = 3.597 Å with an opening angle α of 15.1(2)°.

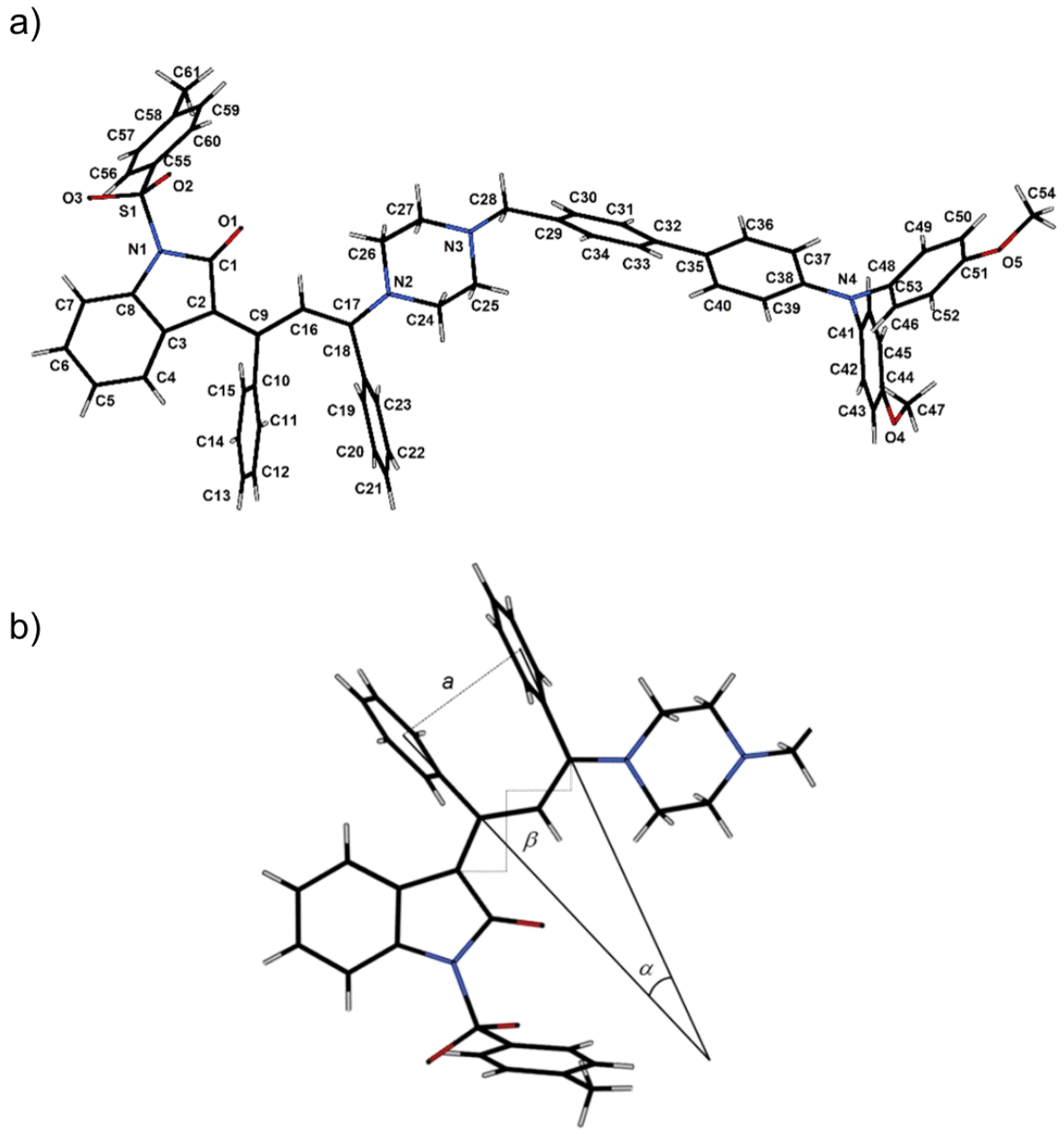

Figure SI-25. a) Wireframe plot of the crystal structure of bichromophore system **4e**. b) π-π-Interaction of the neighboring phenyl rings and coplanarity of the merocyanine chromophore in the truncated structure of bichromophore system **4e**.

The 3-piperazinyl propenylidene indolone units are separated by 9.99 Å, which corresponds to the cell's b-axis. The intermolecular distances of the triarylamine units are shorter (5.10 und 6.06 Å) (Figure SI-26, blue lines) and the intermolecular distances between indolone and triarylamine lie at 7.200 Å (Figure SI-27, violet lines). The arrangement of the molecules in the elementary cells is shown in the cut of the crystal packing (Figure SI-28)

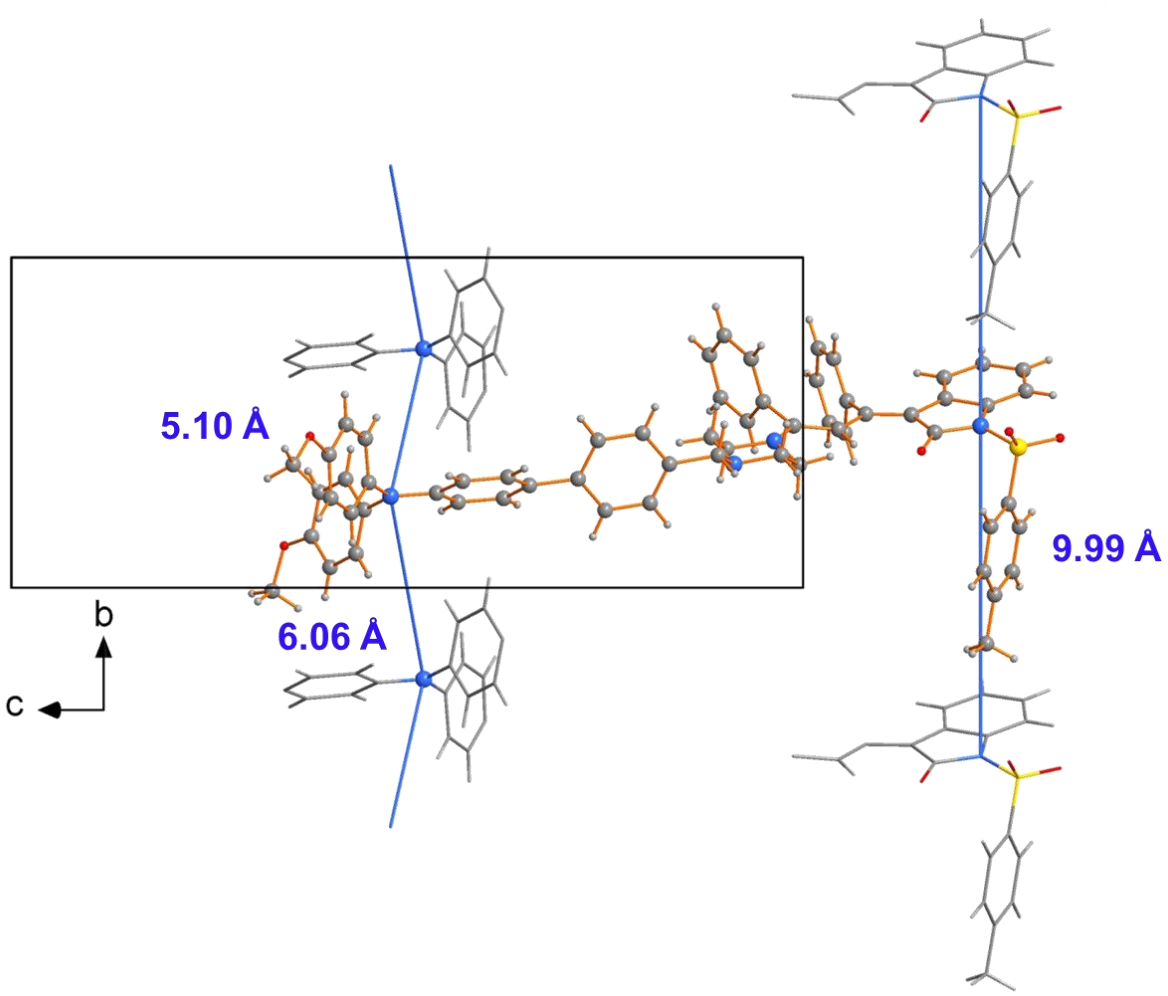

Figure SI-26. Cut of the crystal packing of bichromophore system **4e** showing intermolecular triarylamine-triarylamine (5.10 and 6.06 Å) and indolone-indolone distances (9.99 Å) (view along the *a*-axis).

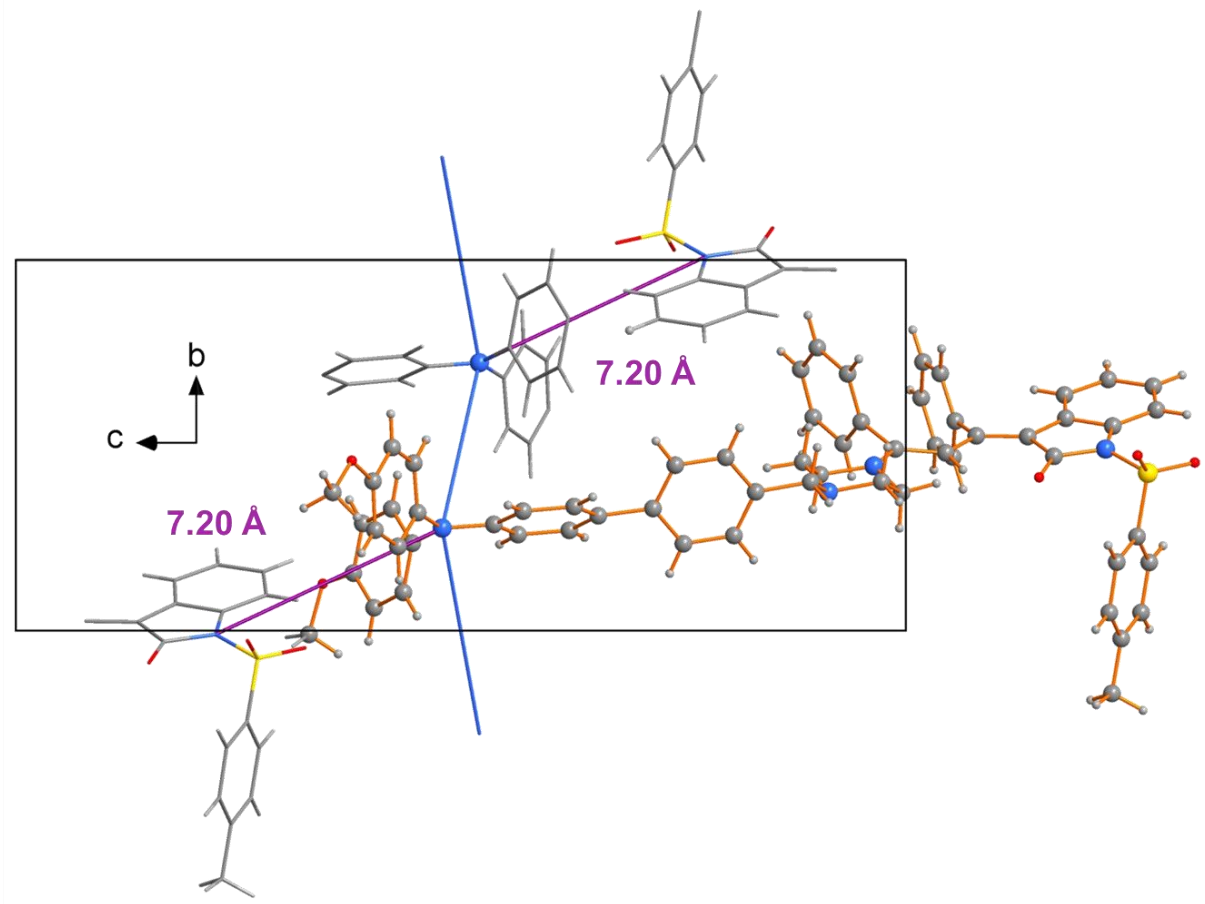

Figure SI-27. Cut of the crystal packing of bichromophore system **4e** showing intermolecular triarylamine-indolone distances (7.20 Å) (view along the *a*-axis).

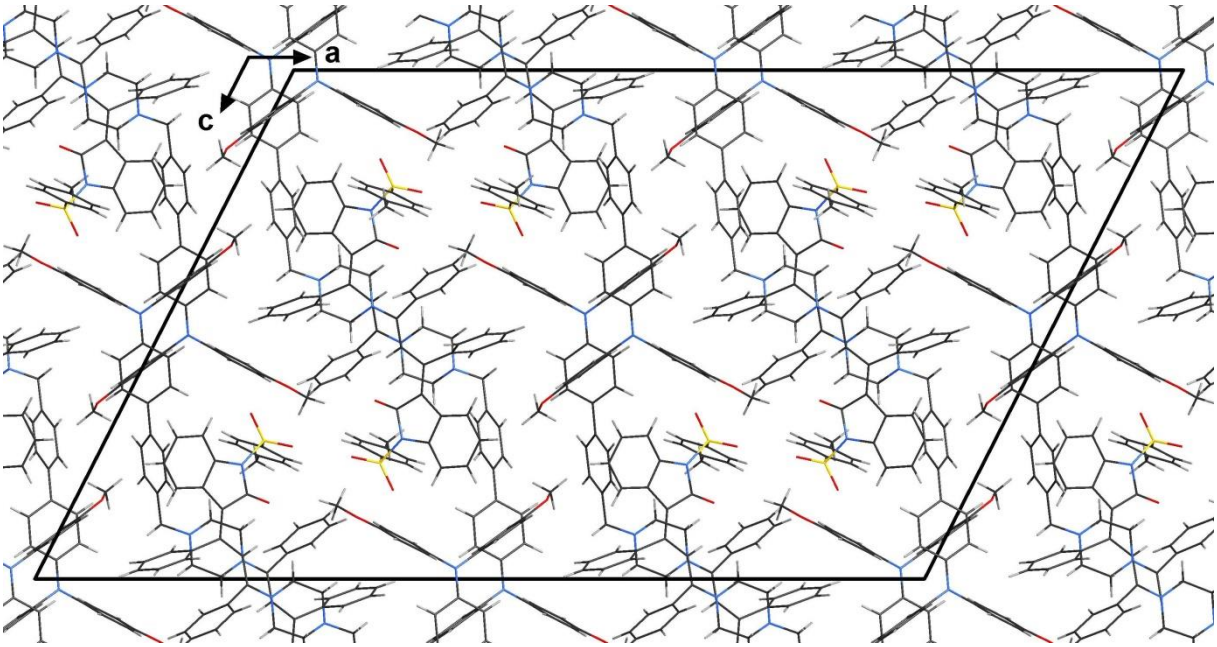

Figure SI-28. Crystal packing of bichromophore system **4e** (view along the *b*-axis).

9 References

[1] J. Glauder, *Speciality Chemicals Magazine*, **2004**, **24**, 30–31.

[2] The aryl propiolic acids were prepared according to literature: a) S. Tartaggia, O. De Lucchi and L. J. Gooßen, *Eur. J. Org. Chem.*, 2012, 1431–1438; b) K. Park, J.-M. You, S. Jeon and S. Lee, *Eur. J. Org. Chem.*, 2013, 1973–1978.

[3] S. A. Brunton and K. Jones, *J. Chem. Soc., Perkin Trans. 1*, 2000, 763–768.

[4] K. Sundaresan, S. N. Raikar, S. R. Sammeta, G. Prabhu, H. Subramanya and A. Bischoff, United States Patent, 2011, US 8,039,463 B2.

[5] Y. L. Chang and T. J. Chow, *Tetrahedron*, 2009, **65**, 9626–9632.

[6] K. Smith, D. Martin James, A. G. Mistry, M. R. Bye and D. John Faulkner, *Tetrahedron*, 1992, **48**, 7479–7488.

[7] M.-L. Louillat and F. W. Patureau, *Org. Lett.*, 2013, **15**, 164–167.

[8] J. Kwak, Y.-Y. Lyu, H. Lee, B. Choi, K. Char and C. Lee, *J. Mater. Chem.*, 2012, **22**, 6351–6355.

[9] M. Denißen, N. Nirmalananthan, T. Behnke, K. Hoffmann, U. Resch-Genger and T. J. J. Müller, *Mater. Chem. Front.*, 2017*,* **1***,* 2013–2026.

[10] A. Kokil, J. M. Chudomel, B. Yang, M. D. Barnes, P. M. Lahti and J. Kumar, *ChemPhysChem*, 2013, **14**, 3682–3686.

[11] N. O. Mcheldlov-Petrssyan, V. K. Klochkov, G. V. Andrievsky and A. A. Ishchenko, *Chem. Phys. Lett.*, 2001, **341**, 237–244.

[12] a) E. J. W. Verwey and J. T. G. Overbeek, *Theory of the Stability of Lyophobic Colloids* 1948, Elsevier Publishing Company Inc.; b) M. Boström, D. R. M. Williams and B. W. Ninham, *Phys. Rev. Lett.*, 2001, **87**, 168103; c) M. Hermansson, *Colloids Surf. B Biointerfaces*, 1999, **14**, 105–119.

[13] a) T. Behnke, C. Würth, K. Hoffmann, M. Hübner, U. Panne and U. Resch-Genger, *J. Fluoresc.*, 2011, **21**, 937–944; b) T. Behnke, C.Würth, E.-M. Laux, K. Hoffmann and U. Resch-Genger, *Dyes Pigm.*, 2012, **94**, 247–257.